INVESTIGATION OF MECHANICAL PROPERTIES OF SUGARCANE BAGASSE AND SISAL HYBRID FIBER POLYESTER COMPOSITE FOR TOYOTA RAUM INNER DOOR PANEL APPLICATION

BY

BIRHANU AWRARIS DEJEN

A Thesis Submitted as a Partial Fulfillment for the Degree of Master of Science in Mechanical Engineering (Automotive Engineering)

to

DEPARTMENT OF MECHANICAL ENGINEERING

ADDIS ABABA SCIENCE AND TECHNOLOGY UNIVERSITY

SEPTEMBER 2021

CERTIFICATE

This is to certify that the thesis prepared by **Mr. Birhanu Awraris Dejen** entitled "**Investigation of Mechanical Properties of Sugarcane Bagasse and Sisal Hybrid Fiber Polyester Composite for Toyota Raum Inner Door Panel Application**" and submitted as partial fulfillment for the Degree of Master of Science complies with the regulations of the University and meets the accepted standards concerning originality, content, and quality.

Singed by Examining Board:

External Examiner: Signature, Date:

Dr. Negash Alemu 13/10/2021

Internal Examiner: Signature, Date:

Samson Mekbib Atnaw (PhD) 13/10/21

Chairperson: Signature, Date:

Mezgebu A ....

DGC Chairperson: Signature, Date:

Elias Gebremicheal Habte
Head,Department of
Mechnical Engineering ....

College Dean/Associate Dean for GP: Signature, Date:

Muluneh Mekonnen Tufu (PhD)
Associate Dean for College of
Electrical and Mechanical
Engineering 15/10/21

College of Electrical & Mechanical Engineering
Science & Technology

DECLARATION

I hereby declare that this thesis entitled "**Investigation of Mechanical Properties of Sugarcane bagasse and Sisal Hybrid Fiber Polyester Composite for Toyota Raum Inner Door Panel Application**" was prepared by me, with the guidance of my advisor Dr. Bisrat Yoseph. The work contained herein is my own except where explicitly stated otherwise in the text, and that this work has not been submitted, in whole or in part, for any other degree or professional qualification.

Author Signature, Date

Birhanu Awraris 13/10/2021

Witnessed by;

Name of student advisor: Signature, Date

Dr. Bisrat Yoseph 13.10.2021

Name of student co-advisor Signature, Date

.....

ABSTRACT

Currently, composite materials are becoming popular in the automotive and aeronautics industries because of their high strength-to-weight ratio compared to traditional engineering materials. Bio-fiber composites are among natural fiber composites with carbon negative, bio degradable and renewable capabilities. In this research, the main aim was to investigate the mechanical and water-absorbing properties of sisal and sugarcane bagasse hybrid fiber polyester composite. During the manufacturing methods, extracting sisal fiber from the sisal plant, cutting of sugarcane bagasse fiber into chopped form and chemical treatment of the fibers with 5% NaOH solution for 24 hours were pre manufacturing process. Measuring the weight of these two constituent fibers in three different proportions as 10%Wt of sisal fiber with 20%Wt of sugarcane bagasse fiber (10S/20B), 15%Wt of sisal fiber with 15%Wt of sugarcane bagasse fiber (15S/15B) and 20%Wt of sisal fiber with 10%Wt of sugarcane bagasse fiber (the 20S/10B) to be manufactured in three different layering sequences of Sisal-Bagasse-Sisal (SBS), Uniform mixing (UNF) and Bagasse-Sisal-Bagasse (BSB) at two different curing temperatures (25°C and 60°C) was the next process. Hand layup these metered fibers with polyester resin and pressing with a hydraulic press machine in the confined steel molds was the second process. The manufactured samples were cut into the appropriate dimensions based on ASTM standards of 2017 for each test after they have been cured enough. As test results from Universal Testing Machine showed that both mechanical and water absorbing properties were highly dependent on the fiber loading proportions. When the sisal fiber increased from 10%Wt to 20%Wt tensile and flexural strengths increased from 27.98MPa to 37.89MPa and 78.53MPa to 102.55MPa which is increased by about 35% and 30% for the SBS layering sequence and 25°C curing temperature respectively. Water absorbing tendency is decreased from 15.07% to 6.37%. But the highest value of impact strength (29.46J/m2) was recorded at 10S/20B with uniform mixing and 25°C curing temperature. This is comparable with previous works of the same composites which was reported as 16.6MPa to 44.4MPa tensile strength, 2.5% to 11% water uptake tendency. From Taguchi method analysis the 20S/10B fiber loading with SBS layering sequence manufactured with 25°C has optimum mechanical and minimum water absorption properties. Based on this result Ansys simulation was made for manufactured composite material and has been compared with conventional automotive door materials.

Keywords: Biofiber composites; Sisal fiber; Sugarcane bagasse fiber; Water absorption; Taguchi method

ACKNOWLEDGEMENT

Throughout the working and writing of this thesis, I have received a great deal of support and assistance from many people and companies.

First of all, I would like to thank my advisor **Dr. Bisrat Yoseph**, whose expertise was more than everything in guiding, shaping, and supporting me for the methodology, for the focusing points, and for writing this thesis work. Your insightful and deep-hearted feedback and suggestion pushed me to sharpen my thinking and brought my work to a higher level.

Next, I would like to express my deep gratitude to my brothers, Mr. Tigabu Awraris and Mr. Natanim Awraris for their valuable ideas and for collecting research materials.

I also would like to thank all managing staff and laboratory assistances of Defence University College of Engineering especially Dr. Mezigebu Belay (HoD of Metallurgy department) and Tewodros Bundro for their permission and willingness to support me in the testing of my numerous test samples in their metallurgy laboratory.

The other deep appreciation goes to Mr. Samson Oryigi (Production Manager of African Bamboo plc) and Mr. Kiros Damtew (laboratory supervisor) and all laboratory machinists in African Bamboo plc for their technical and material support.

I would like also to extend my thanks to Mr. Yemanebihan Emiru Assistant of the Civil structural laboratory shop at AASTU for his kind support during the water absorption test.

My friends around me, Especially Mr. Sheleme Mosisa and Mr. Maru Sete, have also a great contribution to my work by supporting me with ideas and motivation. So, would like to thank all of them heartily.

Lastly, I would like to express my gratitude for the following institutes and companies' for every support during this work. Addis Ababa Science and Technology University, Defence University College of Engineering, Wonji Sugar Factory and Africa Bamboo plc.

TABLE OF CONTENTS

LIST OF TABLES

LIST OF FIGURES

ABBREVIATIONS AND ACRONYMS

SYMBOLS	DESCRIPTION
M_{bg}	Mass of sugar cane bagasse fiber
M_c	Mass of composite
M_f	Mass of fiber
M_s	Mass of sisal fiber
Mt	Mass at time t
M_m	Mass of matrix
V_c	Volume of composite
V_{bg}	Volume of sugar cane fiber
V_f	Volume of fiber
V_m	Volume of matrix
V_s	Volume sisal fiber
m_{fs}	Mass fraction of sisal fiber
m_{fbg}	Mass fraction of bagasse fiber
m_{fm}	Mass fraction of matrix
ρ_c	Density of composite
ρ_{bg}	Density of sugar cane bagasse
ρ_f	Density of fiber
ρ_m	Density of matrix
ρ_s	Density of sisal fiber
10S/20B	10%wt sisal and 20%wt bagasse
15S/15B	15%wt sisal and 15%wt bagasse
20S/10B	20%wt sisal and 10%wt bagasse
S	Sisal fiber
S/N	Signal to Moise ratio
SBS	Sisal- Bagasse-Sisal
SCB	Sugarcane bagasse fiber

TS	Tensile Strength
UNF	Uniform mix Layering
WA	Water Absorption
Wt	Weight
BSB	Bagasse-Sisal-Bagasse
CS	Compression Strength
CT	Curing temperature
FL	Fiber Loading
FS	Flexural Strength
IS	Impact Strength
LS	Layering Sequence

CHAPTER ONE

1. INTRODUCTION

1.1. Background

It is an ancient practice to use natural fibers in matrix material for composite development. People were using wheat straws as reinforcement in clay for increasing the strength of the material and built their houses. Natural fibers were recognized as a good application in the automotive sector since the year 1900[1]. Because of their lightweight, biodegradability, non-abrasiveness, environmentally friendly (Carbon negative), renewability, and high specific modulus, they are becoming a good alternative material of metals and synthetic fibers for automotive body manufacturing. The automotive industry is endlessly in the search of a good way to produce vehicles with a lighter weight, which will help to achieve low-carbon emission by reducing their fuel consumption [2-4].

Ultimately Ford motor company scientists observed that soybean can be used for the production of a good-quality paint enamel by extracting soy oil from soybean and molded it into a fiber-based plastic. From this, they found nearly ten times more shock resistance than steel. But much time requirement and molding difficulty were major shortcomings of this material. Later 1940s, which is the time of World War II, was the first time to use an actual natural fiber for the production of various aircraft parts such as fuselages, bearings, seat belts, and backrests, etc. to substitute the huge shortage of aluminum. At that time Gordon-Aerolite was an example of the fuselage made from unidirectional unbleached Flax Yarn reinforced Phenolic Resin composite [1].

In the later years between 1950 and 1990, the first car known as the Trabant car was made in East Germany from cotton fiber reinforced polyester composite material. Daimler Benz also started to use natural fibers for automotive body production in later 1991. The subsidiary of Daimler Chrysler Mercedes-Benz utilized natural fibers such as coconut fibers in their commercial vehicles for 9 years during headed a project namely “Beleem-Project” in South Africa’s Sao Paulo and again, in the late 1996 Daimler-Chrysler used Jute as natural fibers and used in making the door panels of their Mercedes E class vehicles[2,4,5]. Volvo also has started to use natural fibers like soya-based foil linings to produce seats and a cellulose-based cargo floor tray in its C70 and V70 models to improve

the quality of noise reduction. In Western Europe, up to 16 million vehicles equate to an including usage of 80 000 to 160 000 tons of natural fibers are produced annually[6]. Also, in the year 2000, Daimler Chrysler established their plant for the production of vehicles from natural fiber in East London and South Africa and transfers their technology from German Plants to South Africa. Here is also a piece of evidence that utilization of natural fibers in European countries has increased from 70,000 to 100,000 tons from the year 2005 to 2010 in their automobile industries[1,5]. Toyota also has developed an eco-plastic made from sugar cane lining of the interiors of the cars[6]. For the application of car instrument panels, biodegradable bark cloth reinforced green epoxy composites have been created. [7]. As A. Ticoalu et al. (2015) assessed on their review paper, the coir with polyester resin composites have been used to produce helmet and roof, mirror casing, mail-box, paper weights, voltage stabilizer cover, and projector cover. Natural fiber composites have been used to develop load-bearing elements such as beams and water tanks in structural and infrastructure applications, and green composites are suitable for developing load-bearing elements such as beams, multipurpose panels, roofs, pedestrian bridges, and water tanks, as well as for primary structural applications such as indoor elements in housing and temporary outdoor applications[8].

Netravali and Chabba (2003) reported that the rate of consumption of petroleum is unsustainable, which is about 100,000 times faster than what nature can create. Therefore, nowadays renewable and biodegradable with lower weight natural fibers are good alternatives to automotive body manufacturing. They are environmentally friendly, fully biodegradable, renewable cheap, and have low density. For a healthy ecosystem, the biodegradability of plant fibers is an essential attribute with their low cost and high performance to fulfill the economic interest of the industry [9].

In addition to being light-weighted, polymers are good corrosion-resistant and have good durability, self-lubricating properties over conventional metals and metal alloys. The use of polymer extremely reduces noise pollution and vibration, thereby maintaining driver's and passengers' comfort as well as ameliorating the resulting health hazards that can come from noise and vibration[10].

1.2. Bio Fibers

Bio fiber is a type of renewable source and a new generation of reinforcements and additions for polymer-based materials. Recently due to increasing awareness of environmental issues, bio fiber composites are becoming popular alternatives for automobile industries [11].

1.2.1. Application areas of natural fibers

Natural fibers are one such capable material that replaces the existing synthetic materials and their related products for energy conservation and fewer weight applications. Especially automotive and air crafts industries have been energetically developing different kinds of natural fibers, mainly on sisal, flax, hemp, and bio-resins systems for their interior components. Their high specific properties with lower prices, make them so attractive in various applications[11].

Plant-based natural fibers have a wide range of application areas in transportation industries, construction sectors, electric equipment, and our day-to-day life devices. We use them in building and construction industries to produce panels for partition and false ceiling, floor, window, wall and door frames, roof tiles, etc. and in the transportation areas to manufacture body parts for automobiles, trains, aero planes, and boats, etc. In addition to these areas they can be used for storage devices (grain storage silos, post-boxes, biogas containers, etc.), furniture like table, chair, shower, bath units, electric devices such as electrical appliances, pipes, and everyday applications like lampshades, suitcases, helmets, etc. [12]. As it is an emerging and rapidly growing potential substitute to the synthetic, metallic, and ceramic materials in the automotive, aerospace, marine, sporting goods, and electronic industries natural fiber composites need comprehensive research on their properties. Mostly natural fiber composites exhibit a good specific property, but there is high inconsistency in their properties across their sources and growing environments. This weakness can be overcome by using more advanced processing methods. In the 21st century "green" materials environment, their individual properties should be a solid base to generate new applications and opportunities of bio composites. It is a new avenue for researchers and manufacturing industries to set a sustainable module for future natural fiber composites applications[2]. Environmental awareness from all over the world pushes researchers and industrial manufacturers to focus on natural fibers composites to exploit

efficiently by improving their properties. Hybridizing is one of the most property improving methods which is accomplished by combining two or more different types of fibers to balance the deficiency of another fiber. At this time many natural fiber composites are being developed and marketed but very few of them met into their applications, and most of them are still in their research and development stages [13]. The main components of plant fibers or cellulosic fibers are cellulose, hemicellulose, and lignin. The amounts of cellulose, hemicellulose, and lignin differ in the plants owing to their maturity, location of growth, environment, and even species[14].

Table 1- 1. comparison between natural fiber and synthetic fiber[12]

Aspect	Property	Natural Fibers	Synthetic Fibers
Technical	Mechanical properties	Moderate	High
	Moisture sensitivity	High	Low
	Thermal sensitivity	High	Low
Environmental	Resource	Infinite	Limited
	Production	Low	High
	Recyclability	Good	Moderate

1.2.2. Automotive door panels

An automotive door is a panel which is typically hinged to the frame and situated in front of a vehicle's entrance or exit openings. It is usually made of aluminum alloy and steel, and it consists of two panels, inner and outer panel attached together. Most of the time automotive doors include numerous components, including a door handle, a door switch, a glass window, and several storage compartments [15].

In automotive body manufacturing the main concern is Weight reduction with sufficient strength to improve fuel efficiency and energy conservation. Among several automotive body parts, door panels serve as an interface between the interior of the car and the inner workings of the door, and between vehicle occupants and the door. They must adhere to several design requirements in terms of safety, aesthetics, and functionality[16]. Furthermore, they are expected to maintain the dashboard and pillars' material motif while concealing complex electrical and mechanical components for manipulating locks, windows, and other amenities. The door panel has progressed from a simple two-part latch and simple winding mechanism to a more complex enclosure[17]. In this thesis

investigation of mechanical properties of the hybrid composite of the two natural fibers (sisal fiber and sugarcane bagasse fiber) and check the ability to be an automotive door panel will be the central work. Among the three conventional strategies which are performed to reduce fuel consumption (vehicle redesign, lightweight material substitution, and vehicle downsizing), light weight material substitution is the focus of this study.

1.3. Sisal Plant and Sisal Fiber

The agave sisalana plant, which is originated from Mexico, is the source of sisal fiber that is extracted from the leaves. East African countries (like Ethiopia and Kenya), Brazil, Indonesia, India, and Haiti are the most cultivator countries of sisal plant in addition to Mexico [1]. The word "sisal" comes from a harbor town in Mexico meaning "cold water". This pant was cultivated by the Maya Indians before the arrival of Europeans. Sisal fiber is a strong and coarse fiber that is categorized as hard fiber. Sisal plant has an ability to grow in any environment and soil type except clay, unlike other many plants. It is also simple to cultivate this plant as it is resilient to diseases. After two years from planting the sisal plant can give strong fiber for about 12 years period and a single sisal plant can give 120 to 240 leaves in its lifetime depending on rainfall, altitude, and location. A single sisal leaf weighs nearly 600g and 3% of which is fiber weight and it can produce around 1000 to 1200 fiber bundles with 4% fiber, 8% dry matter, 0.75 cuticles, and 87.25% water. It has about 1.0m to 1.5m in length and (280±30) μm diameter[18]. Sisal fiber is one of the foremost broadly utilized characteristic strands in yarns, ropes, twines, linens, carpets, sleeping cushions, mats, and handcrafted articles.

1.4. Sugarcane Bagasse Fiber

Sugarcane is a grass family plant that is the main source of sugar juice and bagasse as a by-product. It is a representative of major crops in the large areas of tropical and subtropical regions of the world. As the demand for sugar increased in the last centuries large areas of the world were allotted for sugarcane crops. Easiness for maintenance and good productivity of sugarcane made the crop more attractive to the farmers of tropical regions. The second half of the 19^{th} century was the time for the development of sugarcane industries as steam power was available for agricultural machinery. Bagasse is considered

as the most important by-product in the sugarcane extraction process besides the main product, sugar juice[19].

It is essentially a waste product that needs to be disposed of by the mills with additional waste disposal costs. At this time researchers around the world are concerned to develop a new use of agricultural products to add value to forestry for better economic benefits. It is more than an option to use agricultural products in an environmentally responsible manner to recycle and utilize efficiently as alternative raw materials for many industries.

1.5. Resins

Nowadays three main types of resins are used in material science. These are polyester, epoxy, and vinyl ester with different characteristics and associated costs of each resin.

Table 1- 2. comparison between natural fiber and synthetic fiber[20]

Advantages	Disadvantages
Low densities	Low transverse strength
Good corrosion resistance	Low operational temperature
Low thermal conductivities	
Low electrical conductivities	
Translucence	
Aesthetic color effects	

1.6. Polyester

Polyester resins are the foremost widely used resins, especially within the sea and car businesses. Resins of this type are unsaturated and represent about 75% of the overall resin utilized within the composites industry. The unsaturated polyester resin may be a thermoset, able of being cured of the fluid or strong state when subjected to the correct conditions. Immersed polyester, on the other hand, cannot be cured this way. It is common to allude to unsaturated polyester resins as “polyester resins” or essentially “polyesters” [23-25].

Cost, cure time, shelf life, moisture resistance, odor, and toxicity are the most determining properties to identify polyester resin. It is brittle and prone to micro-cracking, has about 6 months to one year shelf life, slightly lower cost than epoxy. One can also vary the cure

time of polyester resin by adding more or less of Methyl Ethyl Ketone Peroxide (MEKP) catalyst and Polyester resin is UV resistant and doesn't degrade by sunlight.

1.7. Manufacturing Methods of Composites

Among several methods to manufacture automotive body parts from composite materials, Contact molding, compression molding, Vacuum bagging, filament winding, and pultrusion are the most common methods[23]. For this study, the compression curing process after hand lay-up is conducted to fabricate free void composite. For noncomplex structural composite, compression molding is a simple process[24].

1.8. Statement of the Problem

In the automotive body manufacturing industry, light-weight, strong enough, and easily machinable materials are chosen. But designing, composing, and manufacturing of such materials is highly dependent on the type, source, composition, chemical and heat treatment, and modification of raw materials. Conventional structural steel and aluminum alloy are the most common materials for automotive door panel manufacturing which are not renewable and obtained from environmental pollutant extracting process. Substituting these metallic materials with bio-fiber composite materials is growing from time to time. But composing and manufacturing process of natural fiber polymer composites needs to be studied for better performance and efficiency regarding with weight reduction, environmental protection, and mechanical abilities to substitute these conventional materials. During characterization of mechanical properties of sugarcane bagasse and sisal hybrid fiber polyester composite fiber loading, chemical treatment, layering sequence, and manufacturing temperature are the key factors to affect mechanical properties. But the extent of effect of these manufacturing parameters are not studied deeply for the hybrid fibers of sisal and sugarcane bagasse polyester composites. Therefore, studying mechanical water absorbing properties with different stacking sequences, varying the fiber loadings, and curing temperature of the composite is the concern of this study.

1.9. Objectives

1.9.1. General objective

The general objective of this thesis is to investigate the mechanical properties of sisal/sugarcane bagasse hybrid fiber polyester composite and study its suitability for Toyota Raum inner door panel applications.

1.9.2. Specific objectives

1. Fabricating a specimen made of sisal/SCB hybrid fiber polyester composite
2. Characterizing mechanical properties like tensile strength, flexural strength compression strength, and impact strength of the fabricated specimen.
3. Studying the effect of varying fiber loadings, layering sequences and curing temperature on the mechanical and water-absorbing properties of hybrid composite of sisal/SCB fiber with Polyester resin.
4. Selecting the best combination of manufacturing process parameters using Taguchi Method Analysis
5. Modeling an automotive inner door panel simulate mechanical strength with ANSYS 2020 R1 using test results of manufactured composite materials and compare with steel, aluminum, and E glass epoxy doors.

1.10. Scope of the Thesis

The scope of this thesis is characterizing only static mechanical and water absorption properties of sugarcane bagasse and sisal hybrid fiber reinforced polyester composite experimentally. It aims to study the ability of this hybrid composite material for low-strength automotive bodies by varying the proportion and layering sequence of the two constituent natural fibers with two different curing temperatures.

1.11. Limitation of the Study

In developing countries like Ethiopia, there are many issues and studying areas for engineering students. But the constraints which limit studies like the current study of composite materials are lack of suitable laboratory equipment and research centers that cooperate with researchers and students. For this study lack of suitable manufacturing equipment for natural fiber composites were the limitations to produce accurate and highly precise samples.

1.12. Significance and Beneficiaries

In the 21ts century, global warming is a big issue that is caused by the depletion of the ozone layer. This depletion is caused by excessive usage of materials that are environmentally pollutant and emission of carbon dioxide from vehicles and industries. Using eco-friendly and lightweight bio-composite materials for automotive body parts manufacturing is the significance of this research. Sugar factories, local farmers, and automotive industries are beneficiaries of this thesis.

1.13. Organization of the Thesis

This research Thesis is organized into five chapters. **Chapter 1 Introduction**: Introduces the background of natural fiber composite materials and their applications. This chapter also includes objectives, problem statement, scope, significance, beneficiaries, and limitations of the thesis research. **Chapter 2 Literature Review**: This chapter Reviewed all relevant research papers regarding natural fiber composite materials, ranging from polymer types, fiber types, and composite's chemical and mechanical properties. Recent researches on sisal, sugarcane bagasse fiber, and their hybrids compose with polymers is widely and deeply reviewed. **Chapter 3 Methods and Materials**: In this chapter Experimental procedures of the research and testing methods of mechanical properties of prepared specimens are discussed. Water absorption testing methods are also presented here**. Chapter 4 Result and Discussion**: In this chapter results from the test with their scientific reasons are discussed in detail using graphs and tables. Here the best design parameters are selected using Taguchi Method analysis. **Chapter 5 Conclusion and Recommendation**: Summary, conclusion, recommendation, and future works of this thesis are presented here.

CHAPTER TWO

2. LITERATURE REVIEW

2.1. Composite Material

Composite materials are a physical combination of a reinforcement (fiber) and a matrix (filler) to give a unique material from constituent materials. Scientists define composite materials in different ways.

D. Verma et al. (2018) stated four different statements about the definition of composite materials. ‘‘Composites are multifunctional material systems that provide characteristics not obtainable from any discrete material. They are cohesive structures made by physically combining two or more compatible materials, different in composition and characteristics and sometimes in form.’’

“Composites should not be thought of as a simple combination of two materials. In a broader sense, the combination has its own unique characteristics. It is better than any of the components alone or significantly different from each of them in terms of strength to heat resistance or some other desirable feature.”

‘‘Composites are composite materials that differ from alloys in that the individual components retain their properties but are blended into the composite in such a way that only their advantages, not their disadvantages, are used to generate superior materials.’’

‘‘Composite materials are heterogeneous materials consisting of two or more solid phases, which are in intimate contact with each other on a microscopic scale. They can be also considered as homogeneous materials on a microscopic scale in the sense that any portion of it will have the same physical property”[27,28].

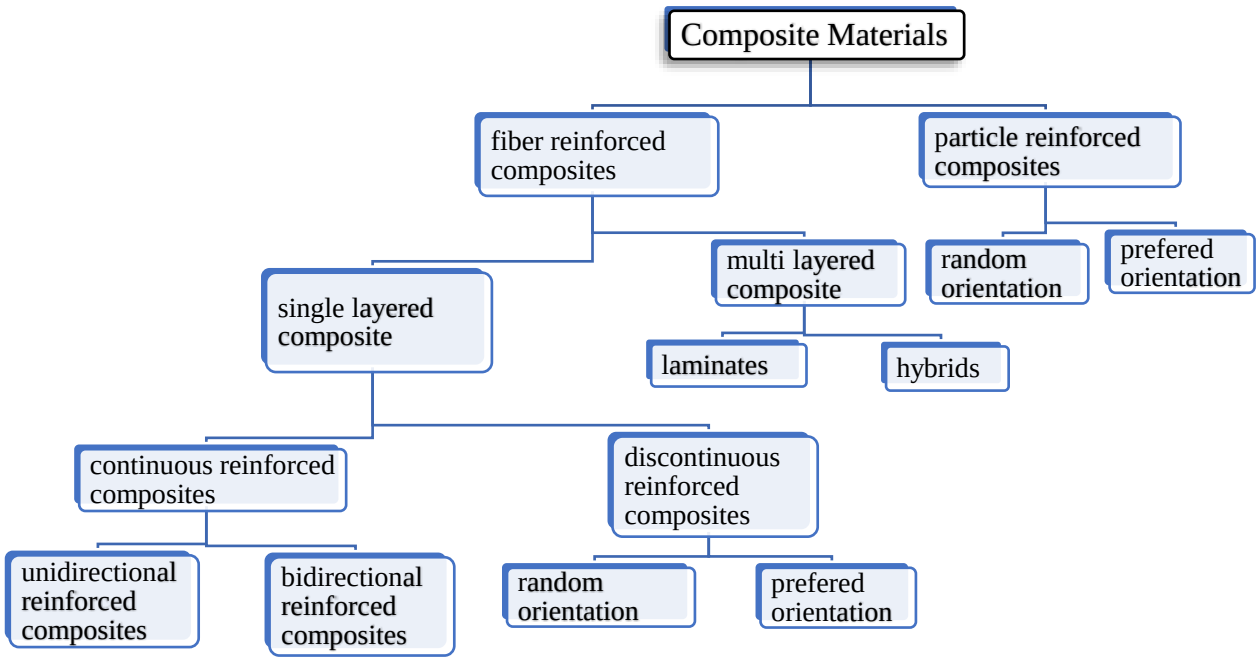

Figure 2- 1. classification of composites according to their composing technique with matrix

2.1.1. Natural Fiber Composite Materials and their Need

As demands for lightweight with high strength materials for specific applications are growing in the manufacturing sector and the market, composites that are composed of synthetic or natural fibers and polymer matrices are gaining more importance than other materials. These fiber-reinforced polymer composites enhance not only high strength to weight ratio, but also, gain exceptional properties like high stiffness, high durability, high damping ratio, and high flexural strength. In addition to these, they enhance resistance to wear, corrosion, impact, and fire.

The wide range of abilities of composites makes them be chosen in applications of mechanical, construction, automobile, marine, aerospace, biomedical, and many other manufacturing industries. The performance of natural fiber composites highly depends on constituent elements from which they are made and manufacturing methods. Therefore, functional properties of various fibers around the World need to be studied deeply their availability, functionality, classifications, and manufacturing methods to optimize their characteristics their desired application areas. Their exceptional performance in various application areas made composite materials the most promising alternatives over metals

and metal alloys. Researchers also intended to discover a new type of materials by hybridizing and modifying them for future applications [28,29].

Composite materials, plastics, and ceramics are the most dominant and emerging materials for the last thirty years. It is also steadily growing, penetrating, and conquering the market relentlessly with a high volume and number of applications. Modern composite materials substitute a significant proportion of the engineered materials market covering from everyday products to highly sophisticated applications. Apart from being weight-saving environmental positive materials, composite materials are challenged by cost-effectiveness. To overcome this challenge composite materials industries have begun to introduce to any commercial applications to get larger business opportunities[25].

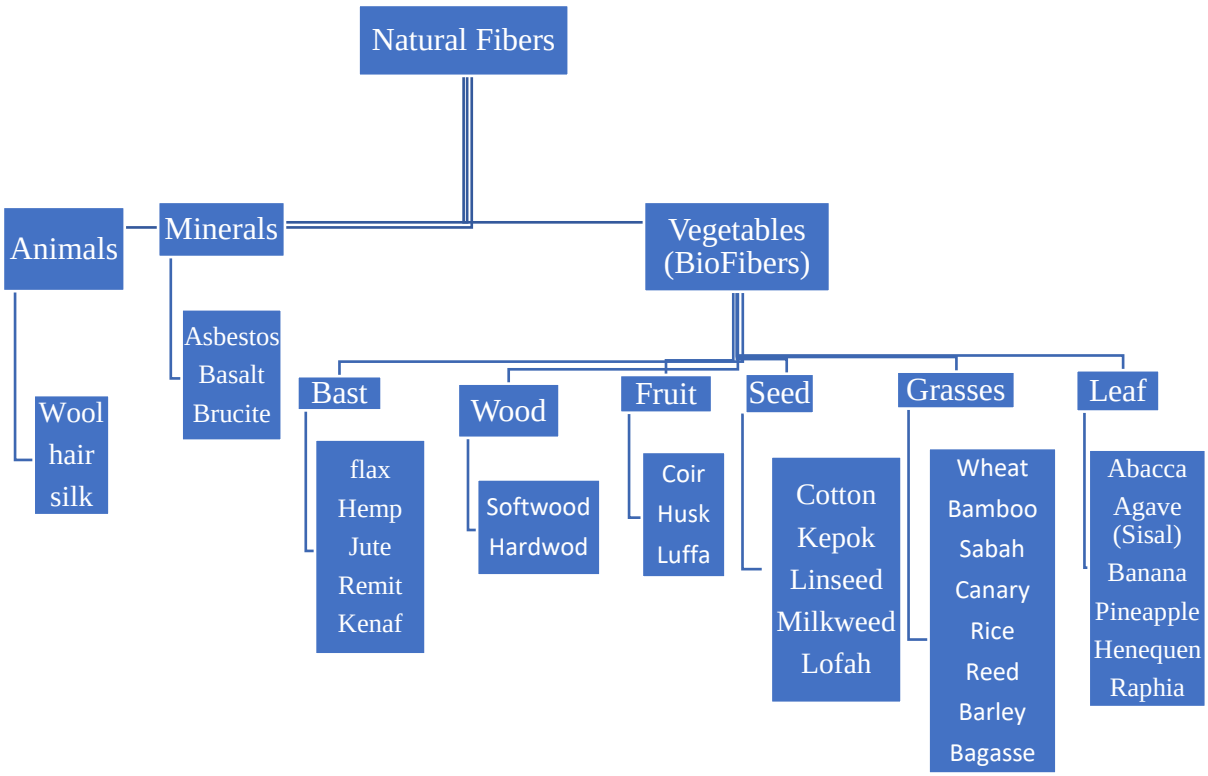

Figure 2- 2. Classification of Natural Fiber[7,14]

There are many species plants which are composed of above 50% cellulose and can be a source of fibers. Among these plants the following figure 2-3. shows the most common sources of bio fibers.

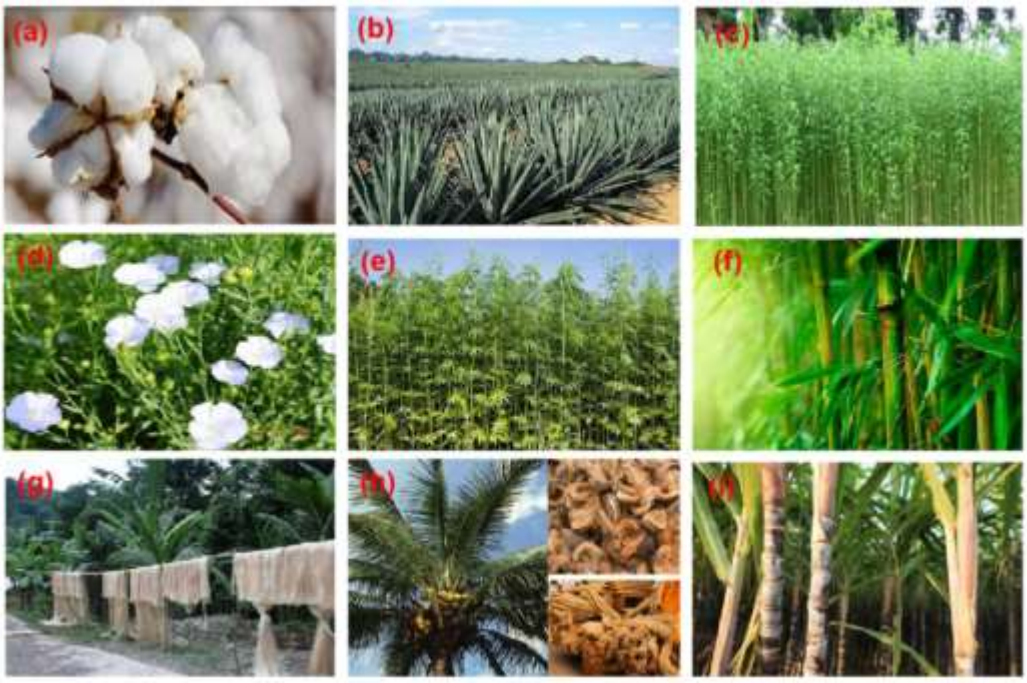

Figure 2- 3. Source of natural fiber plants :(a) cotton; (b) sisal; (c) jute; (d) flax; (e) hemp; (f) bamboo; (g) banana; (h) coir; (i) sugarcane. [16]

2.1.2. Properties of Natural Fibers

Advance synthetic composite materials are popular materials for many sectors. But they have many severe shortcomings related to environmental protection and health conditions. Advanced composites are difficult to recycle, which can cause serious environmental problems after disposal; advanced composites have a relatively high material cost for domestic products; and advanced composite structures can be over-strength, especially when carbon fiber reinforced polymer composites are used. To address these serious issues, it is critical to introduce research into the properties of bio-based fibers in order to manufacture similar products.[29].

Properties of composites are strongly affected by the properties of their constituent materials, their distribution, and the interaction between them and the matrix. Their properties may be the volume fraction sum of the properties of the constituents or it may

be improved to the better ability by enhancing the synergetic properties of the constituent materials. Composites are now widely being used for rehabilitation consolidating constituents. The concentration distribution, the orientation of the fiber, the geometry of the reinforcement (shape and size) influences the properties of the composite to a great extent. Figure 2-4 below shows the most common properties of Natural fiber that affect its mechanical properties.

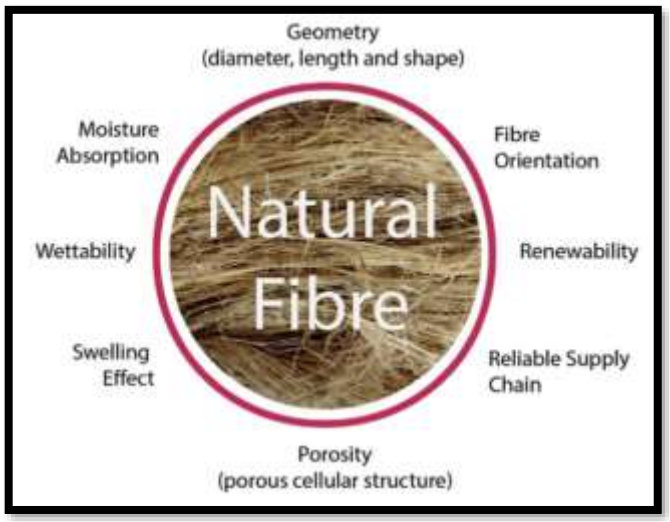

Figure 2- 4. Key factors that affect the mechanical properties of natural fiber composites[30]

Kin-Tak Lau et al. (2018) stated as many factors as they investigate during their research. These factors are high moisture content, inconsistency on their properties, poor bonding properties with polymeric resin (hydrophilic fiber and hydrophobic resin), flammability, uneven dispersion in products, in particular short fiber, and swelling effect. Knowing that these properties can be improved to better quality by modifying with chemical treatment and manufacturing techniques, hybridization of each other researchers devoting their time for current and future industrial applications[29].

2.1.3. Applications of natural fibers in automotive industry

Automotive and aircraft industries have been actively developing different kinds of natural fibers, mainly on hemp, flax, and sisal and bio-resins systems for their interior components. High specific properties with lower prices of natural fiber composites are making it attractive for various applications[1,2].

The natural fiber reinforced composites (NFRCs) are environmentally friendly, biodegradable, biocompatible, renewable, and cost-effective. For instance, there is a piece of evidence that composite materials have the potential to replace steel in the automobile industry, which can reduce the total weight of a vehicle by around 25% and then oil consumption by nearly 250 million barrels. The NFRCs can be used in the production of door and window frames, bicycle frames, columns, and ceilings [14]. Natural fiber composites are mostly being used for automobile parts such as dashboards, door panels, parcel shelves, seat cushions, backrests, and cabin linings whereas the use of natural fiber composite parts for exterior applications is very limited [30].

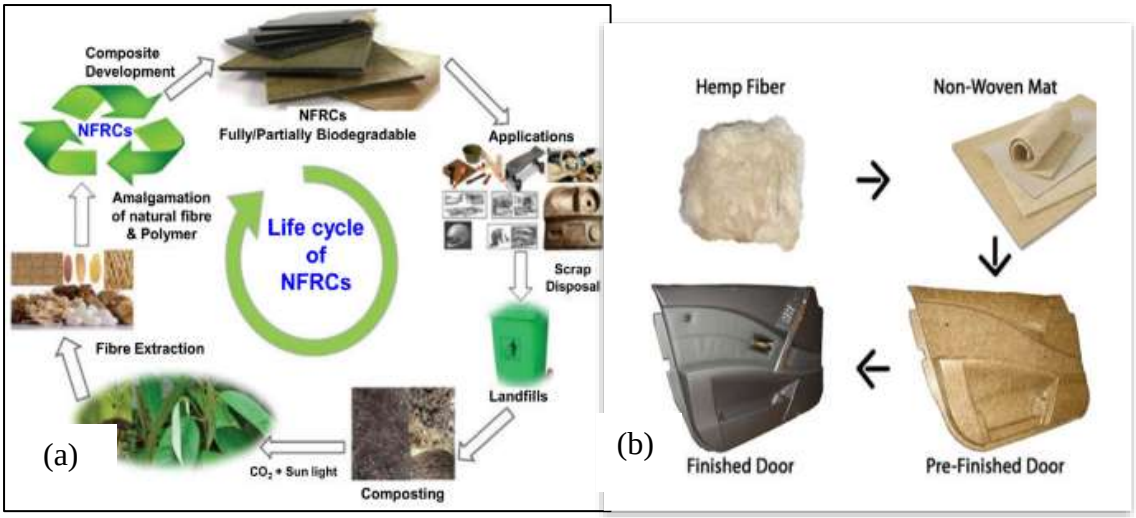

Figure 2- 5. (a)The life cycle of biodegradable, natural fiber-reinforced composites [16] and (b) Production of the door from hemp fiber [31]

After Henry Ford produced the first composite components in a car using hemp fiber in the 1940s, nowadays, many automotive manufacturers are engaged in producing many of their products from natural fibers, table 2-1 shows the summary of automotive manufacturers which used natural fibers.

Table 2- 1. Automotive manufacturers, models, and components using natural fiber–reinforced composite [18,32]

Manufacturers	Models	Components
Audi	A2, A3, A4, A4 Avant, A6, A8, Road star coupe	Seatback, side, and back door panel, spare tire lining, boot lining, hat rack.
Mercedes Benz	C, S, E, and A classes Trucks	Door panels (flax/sisal/wood fibers with epoxy resin/UP matrix), instrument panel support, insulation (cotton fiber), molding rod/apertures, seat backrest panel (cotton fiber), Internal engine cover, engine insulation, sun visor, bumper, wheel box, and roof cover
Citroew	C5	Interior door paneling
BMW	3,5,7 series	Door panel, noise insulation panels, headliner panels, boot lining, seatback, molded footwell lining
Saab	9S	Door panels
Fiat	Pento, Brava, Marea, Alfa, Romeo 146, 156	Door panel
Opel	Astra,Vectra, Zafira	Instrumental panel, headliner, door panels, pillar cover panel
Peugeot	406	Front and rear door panels
Rover	2000 and others	Insulation, rear storage shelf/panel
Toyota	Raum, Brevis, Harrier, Celsior	Door panels, seat backs, floor mats, spare tire cover
Volkswagen	Golf A4, Passat Variant Bora	Door panel, seatback, boot-lid finish panel, boot liner
Mitsubishi	Spare star, Colt	Cargo area floor, door panel, instrumental panels
Renault	Clio, Twingo	Rear parcel shelf
Honda	Pilot	Cargo area
Volvo	C70, V70	Seat padding, natural foams, cargo floor tray
General Motors	Cadillac Deville, Chevrolet Trail Blazer	Seat backs, cargo area floor
Saturn	L3000	Package tray and door panel
Ford	Mondeo CD 162, Focus, Freeze	Floor tray, door panels, B-pillar, boot liner
Lotus	Eco Elise	Body panel, spoiler, seats, interior carpets
VAUXHALL	Corsa, Astra, Vectra, Zafira	Headliner panel, pillar cover panel, interior door panels, and instrument panel

2.2. Sisal Fiber

At this time many types of research have been published on the property characterization and application of sisal fibers[18]. Amid the past two decades, sisal fiber has moreover been utilized as support in cement and polymer-based composites. Inside the leaf, there are three essential sorts of strands: mechanical or structural, arche, and xylem filaments. The

auxiliary filaments provide the sisal leaf its firmness and are found within the outskirts of the leaf. The comparable breadth of the filaments is around 200µm and the cross-section is rarely circular and ordinarily incorporates a ‘‘horseshoe” shape. The mechanical fibers are of awesome significance commercially since they nearly never part amid the method of extraction. The arch filaments develop in affiliation with the conducting tissues of the plant and are not found within the center of the leaf. These filaments run from the base to the tip of the plant and have great mechanical quality. The xylem strands develop inverse to the arche filaments and are associated with them through the conducting tissues[32].

Table 2- 2. physical properties and chemical composition of sisal fiber[2,19]

Properties	Sisal fiber
Density(g/cc)	1.33
Elongation at break (%)	2-2.5
Tensile strength (MPa)	511-700
Young’s modulus (MPa)	9.4-22
Cellulose (%)	65-78
Lignin (%)	8-10
Microfibrillar	22º
Wax (%)	2
Hemicellulose (%)	15-22
Pectin (%)	10-20
Ash (5)	0.6-1

J. Naveen et al. (2018) researched in their paper called “mechanical and physical properties of sisal and hybrid sisal fiber-reinforced polymer composites” decortication is the most effective and common process of extracting sisal fibers. Here also mentioned that surface modification by peroxide treatment (promotes grafting reaction), silane treatment, alkali, and permanganate treatment (improves surface contact) greatly affect mechanical and physical properties in addition to manufacturing methods, fiber length, fiber orientation, fiber volume, and fiber type. On the other hand fiber hybridization also improves mechanical properties up to 90% increment of strength with chemical treatment[32,33].

S Singh et al. (2017) reported in the "5th International Conference on Materials Processing and Characterization Effect" that dynamic mechanical properties are affected by the fiber length of sisal fiber [2] and Z . Alemayehu et al. (2020) showed in their research on sisal fiber epoxy composites that laminate sisal fiber with 0/90 degree orientation has a better static mechanical strength than other orientations[36]. Therefore, hybridizing fibers with both chopped and laminate helps to enhance both dynamic and static mechanical properties. The other research done by N. Uppal et al. (2019) on sisal fiber polyester composite ensured that sisal fiber composites can be comparable with synthetic fiber composites[37] and Hovorun T. P. et al (2017) conducted a research on the hybrid fiber composites of sisal and jute polyester composite and showed that hybridizing fibers for composites improves mechanical properties these fibers can be a recommended materials for modern automotive interior body applications [17]. But they did not go to show with simulation or in real application comparisons.

2.3. Sugarcane Bagasse Fiber

There is a shred of evidence that sugarcane/bagasse is a highly potent natural fiber for composite. Figure 1-5. shows process of changing sugarcane into bagasse and then into composite panels.

Figure 2- 6. Formation of Bagasse Bio-composite material [18,19]

Bagasse comprises water, filaments, and little sums of solvent solids. The percent commitment of each of these components change agreeing to the development assortment, collecting, and productivity of the pulverizing plant. For every 10 tons of sugarcane smashed, a sugar production line delivered about 3 tons of damp bagasse. Bagasse is primarily utilized as a burning crude fabric within the sugar cane process heaters. Bagasse

has moo caloric control, which makes this a low-efficiency handle. Around 9% of bagasse is utilized in liquor (ethanol) generation [19].

Table 2- 3. physico-mechanical properties of sugarcane bagasse fiber

Properties	Values
Tensile strength [MPa]	290
Young's Modulus [GPa]	17
Density [g/cc]	1.25

The approximate composition of sugarcane is 25% lignin, 25% hemicellulose, and the rest 50% cellulose. The large content of cellulose makes the sugarcane bagasse a reinforcement for composites and exhibits a crystalline structure. The chemical composition of bagasse is about 30% pentosanes, 2% ash, and 50% α- cellulose. This composition may vary with age, soil condition, source of fiber, and extraction method. To minimize this deficiency of natural fiber there are many modifying chemical treatments like alkali, silane treatment, acetylation, potassium permanganate, benzoylation, acylation, and acetone treatment[38]. When appropriate modifications with treatment and blending well with other materials are applied it enhances improved mechanical properties such as strength, modulus. It is also an ideal material to fulfill greening requirements by being biodegradability, recyclable, and reusable[39].

In the study of Subramonian et al. (2016), the correlation of composition fiber amount to the mechanical strength was presented. Bagasse was alkali-treated before being hot-pressed with polypropylene reinforcement. The fiber loading was set to range from 10% to 30% by weight. Tensile, hardness, and flexural testing were performed on composite samples. Composites with 30%wt of fiber loading registered maximum tensile strength while with 10%wt fiber loading registered the minimum. Hardness increases with the amount of fiber. Flexural strength and flexural modulus were found to be greater than original polypropylene[40].

A. Athijayamani et al. (2016), performed an ANOVA with the Taguchi method to analyze the effect of fiber length, fiber diameter, fiber loading, sodium hydroxide concentration, and sodium hydroxide treatment duration on the strength of sugarcane bagasse fiber reinforced vinyl ester composite. In this research, the optimum fiber content was around 30% to improve mechanical properties.[41]

Another study[42], on sugarcane bagasse fiber-reinforced polypropylene-based composites, were fabricated successfully and their tensile, bending, and water uptake behavior was studied. The composites were prepared by a compression molding process. The fiber composition in the composites was 30% by weight. Results revealed that due to reinforcement by fiber, composites achieved a 51% increase in tensile strength, 151% in tensile modulus, 109% in bending strength, and 68% in bending modulus over that of polypropylene.

M. K. Marichelvam et al. (2020) showed that sugarcane bagasse fiber reinforced polyester composite has a tensile strength of 19.80 ± 0.78 MPa, Young's Modulus of 0.953 ± 0.076 GPa, a flexural strength of 28.79 MPa, impact strength of 2 kJ/m^2 and the hardness value of 38.02 H [43]. A research called "Physical and Mechanical Behaviour of Sugarcane Bagasse Fibre-Reinforced Epoxy Bio-Composites" done by Lalta Prasad et al. (2020) proved that mechanical properties of sugarcane bagasse fiber composites highly affected by the species of the fiber plant and fiber length [44]. These researches tried to show the single fiber composite properties and did not go far to hybrid with other fibers.

2.4. Hybrid Composites of Sisal Fiber and Sugar Cane Bagasse Fiber

Hybridizing in general improves the mechanical properties of composite materials by enhancing synergetic properties of constituents. In addition to hybridizing layering sequence also affects the mechanical properties of composites. Jeffrey Daniel James et al. (2019) showed the variation in mechanical properties by changing the layering sequence of sugar cane bagasse and sisal fiber in an epoxy matrix [45]. Hybridizing aims at creating a new material that will preserve the benefits and reduce drawbacks of its constituents[46]. The addition of 20% SCB ash with 2% of sisal by volume fraction to the concrete material to substitute cement showed an improvement by 10% to mechanical properties compared to the reference concrete[42,43]. Prashant Dwivedi and Saurabh Kumar Shukla showed that hybridizing of sisal and SCB with chemical treatment improves impact strength, tensile modulus, and flexural modulus by 73.17%, 18.79%, and 54.89% respectively. Especially chemical treatment highly improves the water absorption properly by decreasing pectin and cellulose content which are primarily responsible for hydrophilicity. Alkali treatment dissolves the pectin and coats the -OH group of fibers thereby reducing their hydrophilic behavior[48].

2.5. Fiber Orientation

Fiber orientation is one of the factors that affect the mechanical properties of natural fiber composites positively or negatively. 0-degree unidirectional orientation is the best orientation to resist axial loads like tensile and compression loads[49]. Lasikun et al. (2019) researched the effect of fiber orientation on tensile and impact properties of Zalacca Midrib fiber by changing the fiber orientation from 0° to 90° with 15° difference and had investigated that the composite enhanced optimum value at 0° orientation. As the fiber orientation increased from 0° to 90° the strength of the fiber decreased gradually and attained its minimum value at 90° [50].

2.6. Fiber Loading

Fiber loading is the weight percentage proportion of fibers to the resin matrix in the composite. In natural fiber composites, the best working area of fiber weight proportion is between 20% to 40% for better enhancement of mechanical properties. As the fiber content decreased below 20% the property of the composite becomes dominated by the property of the resin and the advantages of fibers diminished. As the fiber content increased beyond 40% the composite starts to disintegrate and loses its compactness and so its mechanical properties start to deteriorate and it becomes weaker and brittle. Therefore, many types of research [2,36,43,] highly recommended making the fiber content around 30% to get the best mechanical properties. In addition to fiber orientation and fiber loading, composite materials can be positively affected by the fiber treatment[21,47,48] fiber hybridization[3, 34], and layering sequence[29,40].

The fiber loading for bio-fiber composite 30%Wt is the optimum proportion. If the proportion is increased beyond 30% the binding or stacking to each other by the matrix becomes weakened and it will disintegrate. This is because the nature of biofiber is highly liquid absorbent. For synthetic fibers like E-glass and carbon fiber, it is possible to make the fiber proportion above 30%Wt without disintegration of the composite.

2.7. Layering Sequence

During the hand layup phase of the manufacturing process, the sequence of the constituent fibers has an effect on the mechanical properties and water absorption properties of the composite material. A research conducted on the effect of stacking sequence by Subrata C.

Das et al. (2021) prevailed the influence of stacking sequence. They reported that for Jute and Glass hybrid fiber composite stacking with the two fibers in such a way Glass-Jute-Glass-Jute-Glass layering sequence enhances better mechanical properties than composing these fibers alone [55]. The effect of layering sequence on the mechanical properties and morphological behaviors of hybrid natural fiber composites is dominant next to fiber proportion and fiber orientations [56,57]. In this thesis examining the influence of stacking of the two fibers (sisal and bagasse) with three different sequences and select the best layering sequences which is not detailly studied before is the supplementary task. But it is expected that among the two natural fibers, sisal fiber is good to resist the water up taking as well as to resist mechanical loadings[45].

2.8. Curing Temperature

Curing temperature is one of the parameters that affect the mechanical properties of natural fiber composites. It is mostly the temperature given to the mold during pressing and sometimes it is a heat treatment which can be done in the post curing time. But there is no specific curing temperature to get maximum mechanical strength for all-natural fiber composites. Base on the research of Jai Inder Preet Singhs et al (2018) the optimum curing temperature for jute fiber epoxy composite was mentioned as 100°C. The curing temperature other than this harms the strength of the composite[58]. In the other accepted manuscript research done on the effect of curing temperature conclude that increasing post curing temperature above 150°C harms the mechanical properties of the composite as it approaches glass transition temperature and oxidation of resin probably begins [59].

Table 2- 4. A summary table for mechanical and water absorption properties of sisal fiber composites

Ref	Composite (Sisal+Resin)	Tensile strength (MPa)	Flexural strength (MPa)	Compression strength (MPa)	Impact strength (J/m^2)	Water uptake (Ms %)
[37]	Sisal+ polyester	41.35-49.65	91.82-116.88	---	27800-44900	---
[60]	Sisal +polyester	11.2-24.86	107-160	---	---	---
[61]	Sisal + epoxy	21.2	62.044	---	22.54	16.667
[35]	Sisal + epoxy	44.9-83.96	156-252.4	---	16.84-22.03	3.32-3.76
[13]	Sisal+ polyester	29.66-39.48	59.57-96.88	---	---	---

	Sisal + epoxy	---	221.7-237.2	62.53-98.53	---	5.0-15.6
[62]	Sisal+ polyester	42.7-73.55	71.5-85.6	---	14.8-80.3	4.24-12.49
[63]	Sisal/banana+ epoxy	49.5- 58	18.5-24	110-117	---	---
[36]	Sisal + epoxy	35-111	---	25.25-165.52	---	---

Table 2- 5. A summary table for mechanical and water absorption properties of SCB fiber composites

Ref	Composite (SCB + Resin)	Tensile strength (MPa)	Flexural strength (MPa)	Compression strength (MPa)	Impact strength (J/m^2)	Water up take (Ms %)
[44]	SCB + epoxy	17.49-29.23	---	---	2.1-4.5	7.12-16.14
[43]	SCB + epoxy	6.45-19.8	8.99-18.65	---	1.3-2.1	---
[26]	SCB+ polyester	10.3-12.73	---	1.079-2.315	---	27.66-48.238
[64]	SCB+polyester/epoxy	3.89-10.37	10.86-54.16	---	2094.84-10013.13	---

2.9. Automotive Inner Door Panel

During design of automotive doors, the main considerations taken into account are structural performance, cost, and weight of the door. Among these considerations weight reduction and cost minimization can be achieved by the substitution of new light weight and low-cost eco-friendly materials. Automotive manufacturers have paid their attention to biofiber composites to produce predominantly interion panels like door panels and dashboards. In 1941 Ford announced the “soyabean car” which incorporated flax and straw into soy-based panels. In 1999 the first commercial inner door panel made by Mercedes Benz from 35% S-Glass and 65% flax hemp and sisal fiber composites[65]. Researches showed that weight reduction of automotive door is in progress. From 1970s to 2014s the gross weight of automotive has been reduced from 29kg to 9.7kg by substituting steel materials with aluminum and composite materials [66]. Another research conducted by Vasile Gheorghe et al. (2021) achieved a weight reduction of an automotive door from 17.5kg to 5kg by substituting metallic materials with composite materials [67]. By optimizing shapes and size of components of the car door Xintao Cui et al. (2007) showed the reduction of weight by 48.3% and cost by 851.9%[65]. “A Numerical Study of

Automotive Doors" by Said Darwish et al. (2012) examined the structural analysis by applying a maximum of 200N at different edges and handlings of a door panel with thickness of 0.8mm to 1.2mm [68]. But these researches did not try to simulate the natural fiber materials in the door applications.

2.8. Summary of Literature Review

From the reviewed literature, understandably, introducing a new type of environmentally friendly and renewable with high strength-to-weight ratio materials is ultimately important. High cost and being a limited resource of metallic materials that are used in automotive body manufacturing drives the academic society to find and develop new renewable and lightweight biofiber materials. From the worked researches there are slight differences in test results because of growing environments of the plant and testing apparatus that the researcher used. The minimum tensile strength of sisal fiber resin composite is 11.2MPa [60] which is composed of sisal and polyester and the maximum value is 111MPa [59] which is composed of sisal with epoxy. The flexural strength of sisal fiber composed with resin has a minimum value of 18.5MPa[63] and a maximum value of 252.4MPa[35] which is composed of sisal and epoxy. The water absorption property of sisal fiber composed of resin varies from 3.32%[35] to 16.667%[61] weight gain. For the sugarcane bagasse fiber resin composites, the tensile strength varies from 3.89MPa[64] to 29.3MPa[44] and flexural strength varies from 8.99MPa[43] to 54.16MPa[64]. The water absorption property of SCB composed of resin also varies from 7.1%[44] to 48.24%[26]. These properties revealed that hybridizing and modifying these two bio fibers can be a good substitute for moderate-strength automotive body manufacturing materials.

2.9. Research Gap

The automotive industry is changing the trend of material usage from non-renewable and environmental pollutant metallic and synthetic materials to environmentally friendly lightweight natural composite materials. Lightweight eco-friendly hybrid bio-composite materials have comparable strength as synthetic polymer composites with low cost and renewability. Sisal fiber is a durable, comparatively strong, absorbent-which is easy to dye, abrasion-resistant, saltwater deterioration resistant, and can be made of up to 1200 cm long fiber. Sugarcane bagasse is a highly potent natural composite fiber, a good impact-resistant

fiber compared to the other natural fibers, and fully compostable natural fiber. Nowadays this huge amount of byproduct natural fiber has only a few applications. Sugar factories burn it to generate heat energy for their heater. But this process is not recommended as it emits smoke to the environment and it is also not efficient as sugarcane bagasse has a very low calorific value (17.4MJ/kg). And also, only about Nine percent of sugarcane bagasse is used for alcohol (ethanol) production. But due to the low level of sucrose left in bagasse the efficiency of ethanol production is quite low. Hence it is better to find other areas to use this plenty amount of natural fiber. Properties of hybrid composites are strongly dependent on the properties of their constituent materials, their distribution, and the interaction among them. Apart from the nature of the constituent materials, the geometry of the reinforcement (shape, size, and distribution) influences the properties of the composite to a great extent. The concentration distribution and orientation of the reinforcement also affect the properties. Therefore, hybridizing a chopped sugarcane bagasse fiber, which has a good shock absorption property with low density, and sisal fiber, which has better durability, strength, and water absorption property will enhance a synergetic property of the two fibers. Automotive body materials are mostly required to be lightweight, strong, environmentally friendly, easy to manufacture, and low cost. This hybrid composite of sisal and sugarcane bagasse has low density, moderately high strength, fully biodegradability, availability, renewability, and ease of manufacturability is a good substitute material for scarce conventional steels and synthetic polymer materials. Therefore, the investigation of mechanical and physical properties of the hybrid composites of these natural fibers is the aim of this thesis research.

CHAPTER THREE

3. MATERIALS AND METHODS

3.1. MATERIALS

In this research sisal fiber, which is extracted from the sisal plant, sugar cane bagasse fiber, polyester matrix, Sodium Hydroxide for treatment, Hardener #2060 as a catalyst are used.

3.1.1. Sisal Fiber

During material collection time 20kg of sisal plant has been collected from the high lands of Woldia town and it has been abraded using a sharp piece of wood to extract and get 0.7kg of dried fiber. The figure below shows the naturally cultivated sisal plant, manual fiber extraction process, and sisal fiber.

Figure 3- 1. Sisal plant and fiber extraction process (a) sisal plant , (b) extraction process, (c) sisal fiber

3.1.2. Sugar Cane Bagasse

The sugar cane bagasse was brought from Wonji sugar Factory with the permission of the general manager. A 10kg of a newly extracted and dried bagasse was taken not to lose the mechanical properties due to decomposition.

Figure 3- 2. Sugar Cane Bagasse from Wonji Sugar Factory

3.1.3. General-purpose Polyester Resin

The general-purpose polyester resin is a quick curing unsaturated polyester resin. It is suitable for both hand-lay-up and gun spray-up. The resin offers excellent mechanical properties, impact, and water resistance. Composite materials made with this resin have excellent mechanical strength, good rigidity, and outstanding durability[65,66].

Usage

The general-purpose polyester resins perform best if the laminate is completely post cured. The quantity of catalyst and accelerator can be adjusted to get a shorter or longer gel time.

Post curing

It is recommended to mature the products for 24 hours and post-curing should be done for a minimum of three hours at 800°C or 2-3 weeks at room temperature. This is essential for getting the optimum properties.

Storage/ Handling

The polyester resin remains stable for 3 months at 300°C in the dark and 4 months at 250°C. The resin stability deteriorates markedly at elevated temperatures, especially when exposed to direct sunlight. It has a flashpoint of 340°C and is classified as flammable. "NO SMOKING " rules should be strictly followed. In case of spillage, use sand or earth to

absorb and shovel off for disposal as per local regulations. In case of fire, use dry chemical foam, Carbon dioxide, or water spray to extinguish the flame.

Health and safety

Never add metal salts (Accelerator) or Pre-Accelerator resin to Peroxides when adding peroxides to a resin solution, mix thoroughly the resulting product do not add organic peroxides to a hot diluent or process. Prevent contamination of Accelerator, a promoter from materials like (Iron Copper, Cobalt) salts, storing acids and sanding dust. Suggested containers are glass, polypropylene, Teflon, Poly-ethylene, or stainless steel to prevent contamination of material during its handling.

Figure 3- 3. General-purpose Polyester Resin

3.1.4. Hardener (Catalyst)

Polyester resin is cured by adding a catalyst, which causes a chemical reaction without changing its composition. The catalyst initiates the chemical reaction of the polyester resin and monomer ingredient from liquid to a solid-state. The curing agent applied in this liquid polyester resin is a hardener with the brand name SYSTEM #2060 HARDENER purchased from the local market (world glass fiber) in Addis Ababa Ethiopia.

3.1.5. Sodium Hydroxide (NaOH) pellets (Eka Pellets)

Sodium hydroxide, popularly known as caustic soda, is a very caustic metallic base and alkali salt with the chemical formula NaOH. Pure sodium hydroxide is a white solid that comes as pellets, flakes, granules, and as a 50% saturated solution. Water, ethanol, and methanol are all soluble in sodium hydroxide. This alkali is deliquescent, absorbing moisture and carbon dioxide from the air quickly. Although the characteristics of molten

sodium hydroxide are comparable to those of the other forms, its high temperature comparatively limits its applications. In this work, NaOH was used in pellets form, purchased from local suppliers with the brand name and code of LABKEMICAL, 04897 respectively, and performed chemical treatment of both sisal and sugarcane bagasse fibers.

3.1.6. Honey Wax® 250 (RAYPLEX) for mold release

The honey wax was used to polish the mold to the surface smooth enough and help the demolding process. The roughness on the mold surface can be smoothed with careful polishing of the wax and covering with aluminum foil or polyethylene sheet shown in Figure 3- 5. below.

Figure 3- 4. Sodium Hydroxide Pellets(a) and Wax for demolding(b)

3.1.7. Home smart Aluminum Foil (REYNOLDS WRAP) and Polyethylene Sheet (BRAXX)

Aluminum foil and polyethylene sheet are used to cover the steel mold for a good surface finish. Aluminum foil was used for hot pressing and polyethylene was for cold pressing.

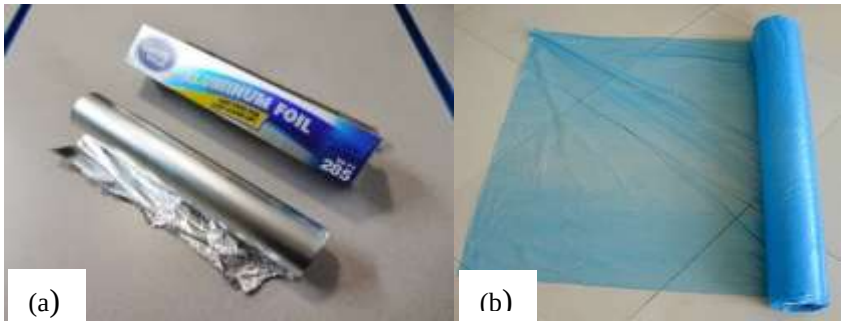

Figure 3- 5. Aluminum foil (a) and polyethylene sheet(b)

3.2. Sample Preparation and Testing Method Flow Chart

Samples for this Thesis were prepared according to the following flow chart. After the required amount of the two fibers (sisal and sugarcane) are collected a proper chemical treatment process is performed. Then the molding of the fibers by hybridizing with selected proportion and polyester resin is accomplished. After demolding the samples, curing and cutting them into appropriate dimensions is accomplished. Testing Universal Testing Machine, impact test machine, and water media; their respective samples is the last process that should be done before result analysis. After all results are obtained as required, the results are discussed with the help of charts and tabular data. Therefore, the selection of optimum manufacturing parameters Taguchi method analysis is applied. The last task of this thesis is modeling an automotive inner door panel and compare its strength with three other conventional materials (steel, aluminum, and E glass epoxy UD).

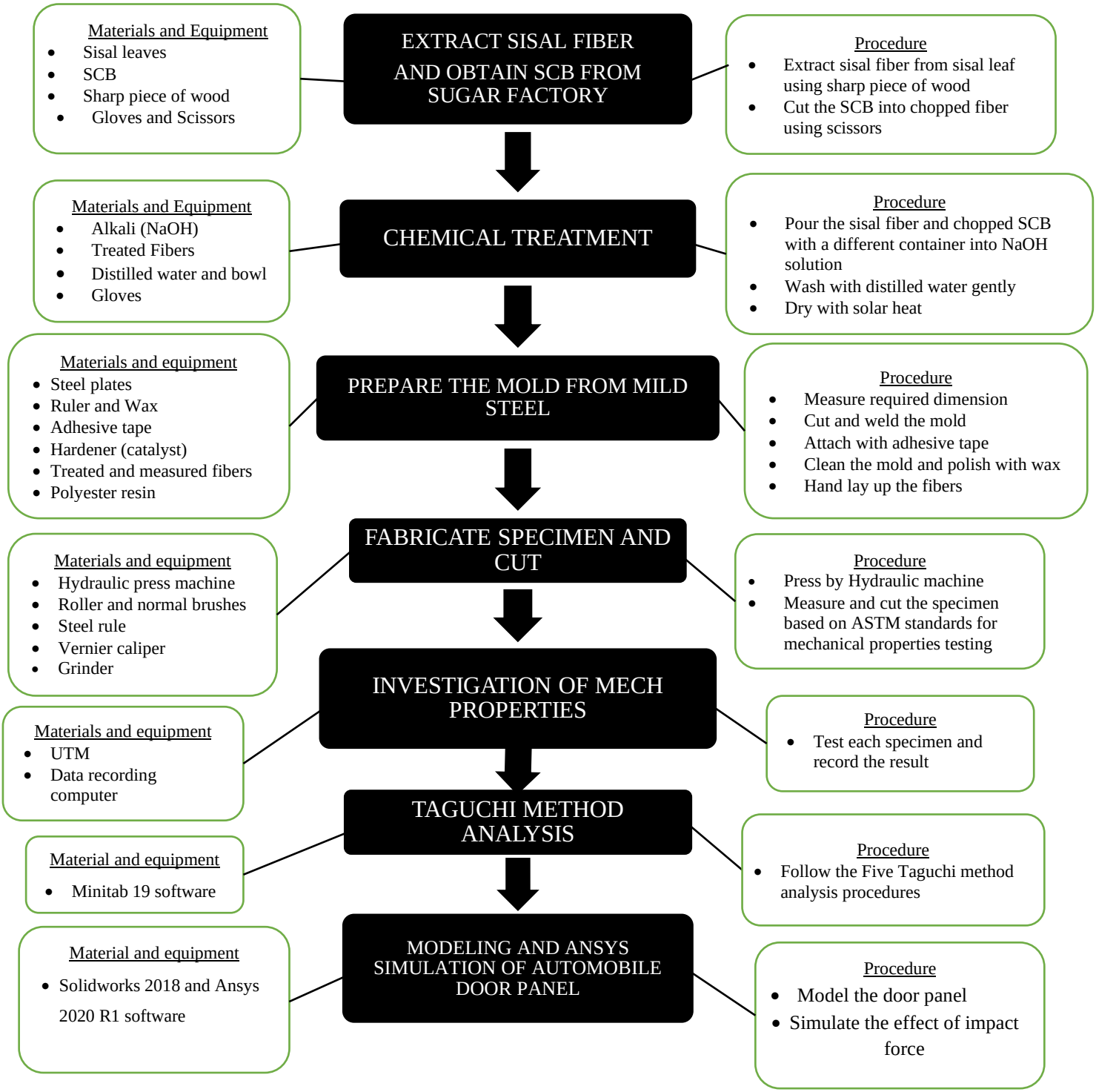

Figure 3- 6. Sample preparation Methodology procedures

3.3. Alkali Treatment of Sisal Fiber

Alkali treatment is the simplest method of chemical treatment of fibers; it leads to an increase in the amount of amorphous cellulose at the expense of crystalline cellulose. The important modification occurring here is the removal of hydrogen bonding in the network structure. The following reaction takes place as a result of Alkali treatment

Sisal Fiber-OH +NaOH → Sisal Fiber-O-Na+ + H_2O

According to the literature, alkali solution has a good effect on treating natural fibers. In this study, a 5% NaOH solution was used to treat the raw Sisal fibers, to modify their fiber structures. During this process Dried and laminate sisal fibers were taken into a tray that contains 5% NaOH solution. The fiber is soaked in for 24 hours, to remove fatty impurities and followed by washing gently with distilled water to neutralize the alkali content. Lastly, the fiber was allowed to dry in solar heat for Four days.

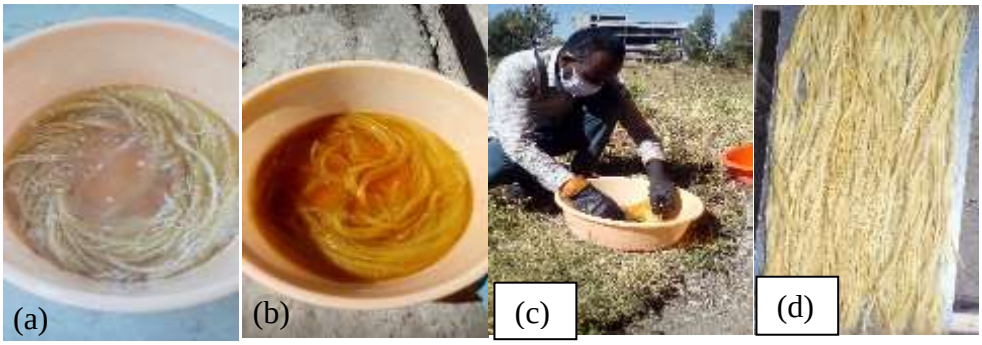

Figure 3- 7. Sisal Fiber Alkali Treatment Process (a) pouring sisal fiber to 5% NaOH solution, (b) sisal fiber treatment for 24 hours, (c) washing the fiber with distilled water, (d) drying the fiber with sun heat

3.4. Cutting and Alkali Treatment of Sugarcane Bagasse

Before treating with Alkali solution, the sugar cane bagasse was chopped into the average length of two millimeters to increase contact surface area with the matrix, polyester. Then the chopped sugarcane Bagasse fiber was poured into a total of 5% NaOH solution and it was kept for 24 hours. Then Alkali solution was drained out from the fiber and was rinsed with distilled water several times until getting rid of excess alkali. Lastly, the fiber was allowed to dry in solar heat and for Four days. The chemical reaction takes place as follow

Sugarcane Bagasse Fiber -OH + NaOH→ Sugarcane Bagasse Fiber Fiber-O-Na+ + H2O

Figure 3- 8. sugar cane bagasse fiber alkali treatment process (a)cutting the SCB fiber into the chopped fiber, (b) pour the chopped SCB fiber into NaOH solution, (c) washing the treated SCB fiber, (e) drying the treated fiber with sun heat.

3.5. Experimental Design

The total number of specimens is decided and calculated based on how the experiments are intended to be performed. Here the sisal fiber orientation is decided to be 0º. Because, as indicated in the literature review section 2.5, almost all researchers proved and showed that this orientation is the best type for better mechanical strength. The fiber to matrix mass proportion for this research is 30% to 70% (30% fiber and 70% matrix). Because according to researchers, for biofiber composite materials 30%wt is the optimum proportion to get better mechanical properties. But the main aim of this research is to characterize mechanical properties and check the effect of different proportions of sisal fiber and sugar cane bagasse fiber with three different proportions, that is (10S/20B, 15S/15B, 20S/10B) with three trials for each sample. In addition, in this research, there are three different layering sequences. (Uniform mixing, Bagasse-sisal-bagasse, sisal-bagasse-sisal). Five

tests will be performed (Tensile test, flexural test, compression test, impact test, and water absorption test)

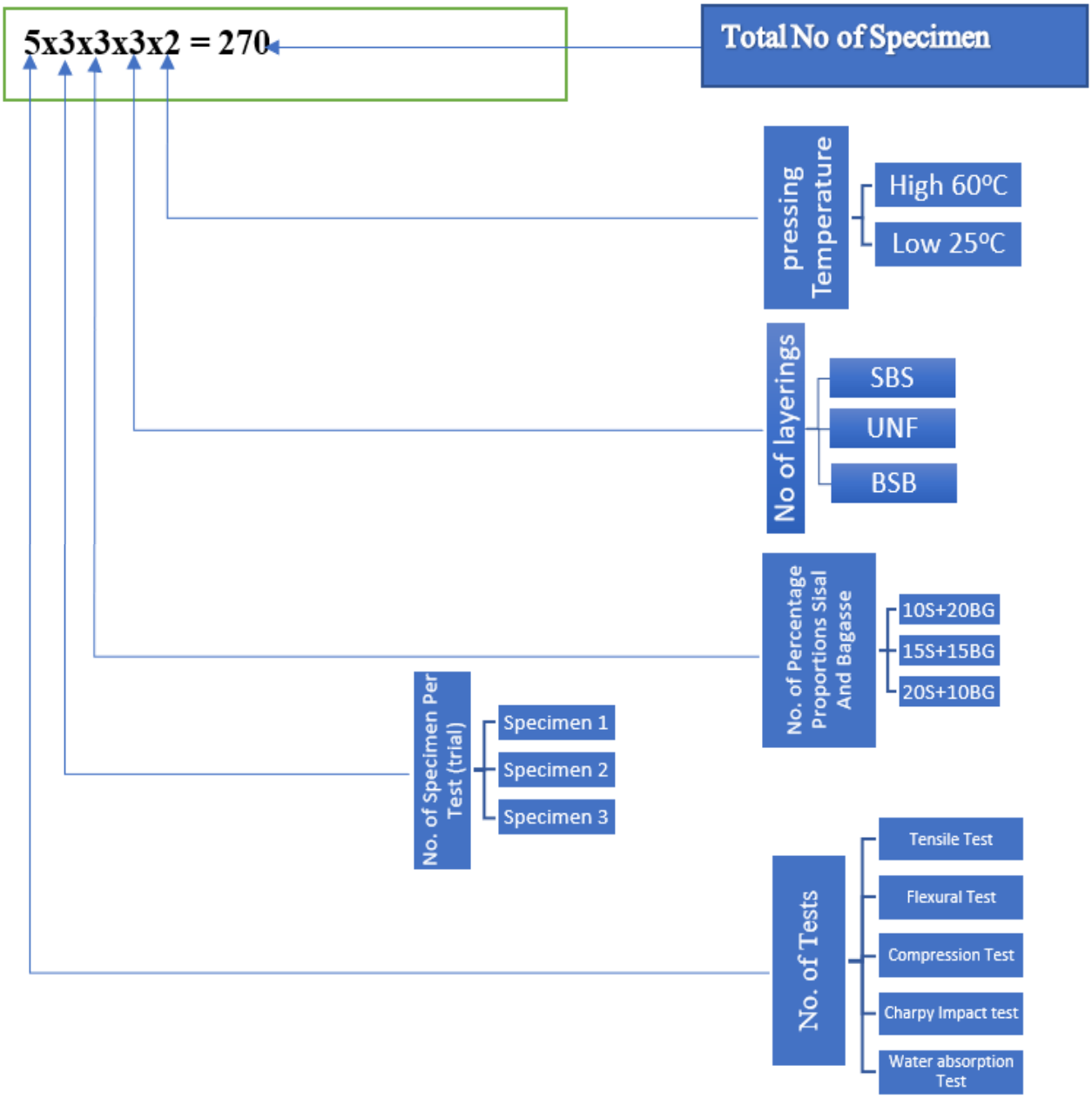

Total volume calculation

According to ASTM standards, the specimen for each test is specified as follows.

1. Tensile test specimen (according to ASTM D3039, 220x25x3mm^3)

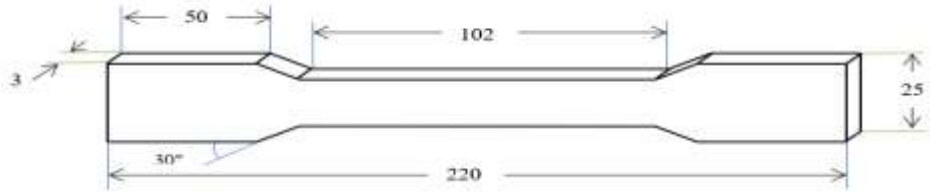

2. Flexural test specimen (according to ASTM D790 180x12.5x3 mm^3)

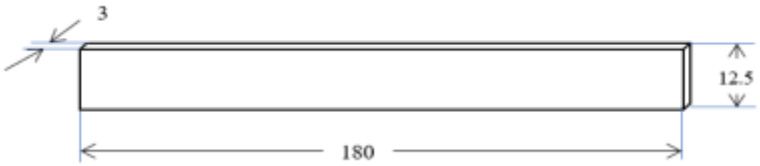

3. Compression test specimen (according to ASTM D3410,155x25x3mm^3)

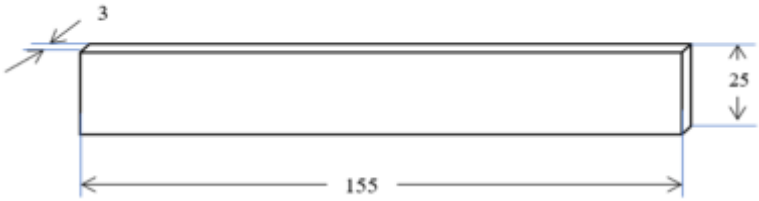

4. Impact test specimen (according to ASTM A370, 65x10x3mm^3)

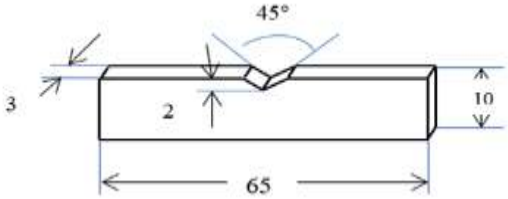

5. Water absorption test specimen (according to ASTM D570, 20x20x3mm3)

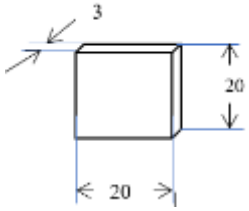

Mold volume calculation

The area of the five specimens for a single trial is given by

$220\text{x}25 + 180\text{x}12.5 + 155\text{x}25 + 20\text{x}20 + 65\text{x}10 = 12675\text{mm}^2$ and for three trials of each test, the total area becomes $12675\text{x}3 = 38025\text{mm}^2$

But, by considering the maximum specimen length for the tensile test which is 220mm, and with the allowance for the cutting, trimming, and edge finishing the area of all specimens for one proportion should be

$$250\text{x}250 = 62500\text{mm}^2$$

The volume is $62500\text{x}3 = 187500\text{mm}^3 = 187.5\text{cc}$

Required Mass Calculation (using the rule of mixture)

The volume of the composite (Vc)=volume of the fiber (Vf) + volume of the matrix (Vm)

$V_c = V_f + V_m$, and $V_f = V_{sisal} + V_{bagasse}$ (3-1)

$V_c = V_s + V_{bg} + V_m$, and volume $=$ mass /density

$V_c = M_c/\rho_c = M_s/\rho_s + M_{bg}/\rho_{bg} + M_m/\rho_m$ (3-2)

divided this equation by mass of the composite Mc, it becomes

$$1/\rho_c = m_{fs}/\rho_s + m_{fbg}/\rho_{bg} + m_{fm}/\rho_m \quad (3\text{-}3)$$

where m_f is stand for mass fraction given by the mass of constituent/ mass of composite

Therefore, taking the reciprocal of this equation gives

$$\rho_c = \frac{1}{m_{fs}/\rho_s + m_{fbg}/\rho_{bg} + m_{fm}/\rho_m} \quad (3\text{-}4)$$

Densities of constituent materials

The density of sisal $(\rho_s) = 1.33\text{g/cc}$

Density of sugar cane bagasse $(\rho_{bg})\text{min} = 0.12\text{g/cc}$

$$(\rho_{bg})\text{max} = 1.25\text{g/cc}$$

$$\left(\rho_{bg}\right)\text{ave} = 0.69\text{g/cc}$$

Density of polyester matrix $(\rho_m) = 1.35\text{g/cc}$

As it has been reviewed above most researchers show that 20 to 40 weight percent of fiber content is the optimum loading for good binding of natural fiber and polymer resin. For this research 30%Wt of fiber is selected for better binding.

Table 3- 1. Calculated mass proportions of each constituents

Parameter	10S/20B	15S/15B	20S/10B
Volume of composite (V_c in cc)	187.5	187.5	187.5
Density of composite (ρ_c in g/cc)	1.13	1.18	1.23
Mass of composite (M_c in g)	211.88	221.25	230.63
Mass of sisal (M_s in g)	21.19	33.19	46.13
Mass of sugarcane bagasse (M_{bg} in g)	42.38	33.19	23.06
Mass of matrix (M_m in g)	148.31	154.88	161.44

- ***Cutting fibers and measuring the mass with electronic balance***

The sisal fiber is cut into 250mm length and weighted according to the calculation in Table 3-1 for all samples as 46.13g, 33.19g, and 21.19g. The chopped SCB fiber was also weighted according to the proportions depicted in Table 3-1. as 23.06g, 33.19g, and 42.38g.

Figure 3- 9. Measuring of Fibers and Resin

- Mold preparation

  Required materials

- Mold (flat plate and frame)
- Brush
- Mold release (wax)
- Aluminum foil
- Polyethylene plastic

Mold (flat plate and frame) the mold pattern is prepared from steel plate and rectangular frame.
Aluminum foil and polyethylene plastic for the covering of the mold for a good surface finish of the composite.

Mold release (wax) is for coating on the surface of the aluminum foil and polyethylene plastic for the easy removal of the mold.

The mold was prepared with the volume 250x250x3 mm^3 as calculated above. The hydraulic press machine in the laboratory has three plates with an area of 600x400 mm^2 and has the capacity of pressing Two layers at Once with this area. Therefore, the mold was prepared with sections in 250x250 mm^2 areas and a Three-millimeter height frame. The frames were attached to the upper surface of lower and middle plates firmly with adhesive tape as shown in Figure 3-10. Then the mold was shielded with a polyethylene sheet for cold press and shielded with aluminum foil for the hot press.

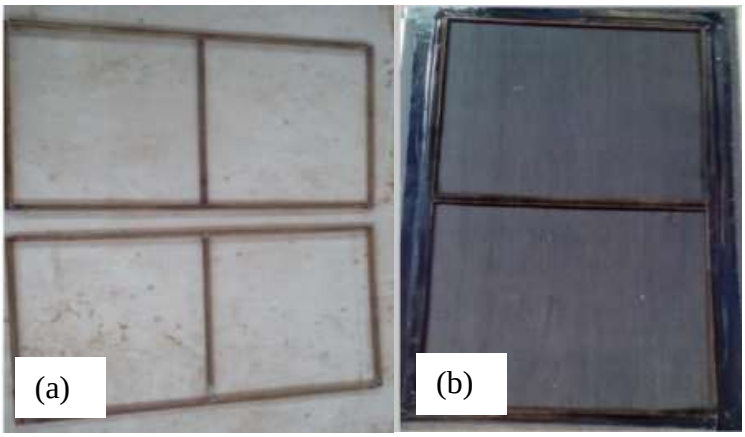

Figure 3- 10. Prepared Mold(a) pairs of molds, (b) waxed mold

- ***Hand-laying-up***

In this work, a hand-lay-up method is preferred for the preparation of three different proportions of sisal and sugarcane bagasse fiber hybrid composite with 30%Wt and three different layering sequences. According to reviewed articles above the orientation of sisal fiber was selected to be horizontal which is a longitudinal direction to the test specimens to maintain a good mechanical property. But the bagasse fiber was uniformly distributed in a random direction because it was chopped at an average length of two millimeters. First, the mold was covered with polyethylene plastic for the cold press and aluminum foil for the hot press to get a good surface finish. Then honey wax was polished on the polyethylene plastic and aluminum foil for ease of mold removal for each pressing. Then the amount of polyester resin which is mixed with 5% catalyst (hardener) was added to the prepared step-by-step with calculated respective amounts of sisal and SCB fibers. This was performed for different layering sequences and uniform fiber mixtures. The next procedure was pressing with 5MPa hydraulic press machine tightly to make resin distribution uniform and to remove air gaps created between the fiber and the resin. Then it was kept for 24 hours for complete curing. Here the fiber layering sequence, fiber hybridizing proportions, and curing temperature were the three important factors that affect the mechanical properties of the composite. The layering sequences were sisal-bagasse-sisal (SBS), bagasse-sisal-bagasse (BSB), and uniform mixture. The hybridizing proportions were 10% sisal and 20% bagasse (10S/20%), 15% sisal and 15% bagasse (15%S/15%B), and 20% sisal and 10% bagasse (20S%/10B%) by weight. But the fiber to resin proportion was kept constant at 30% fiber and 70% resin which is the optimum proportion for natural fiber composites. The curing temperature was kept at 25 degrees Celsius (room temperature) and 60 degrees Celsius.

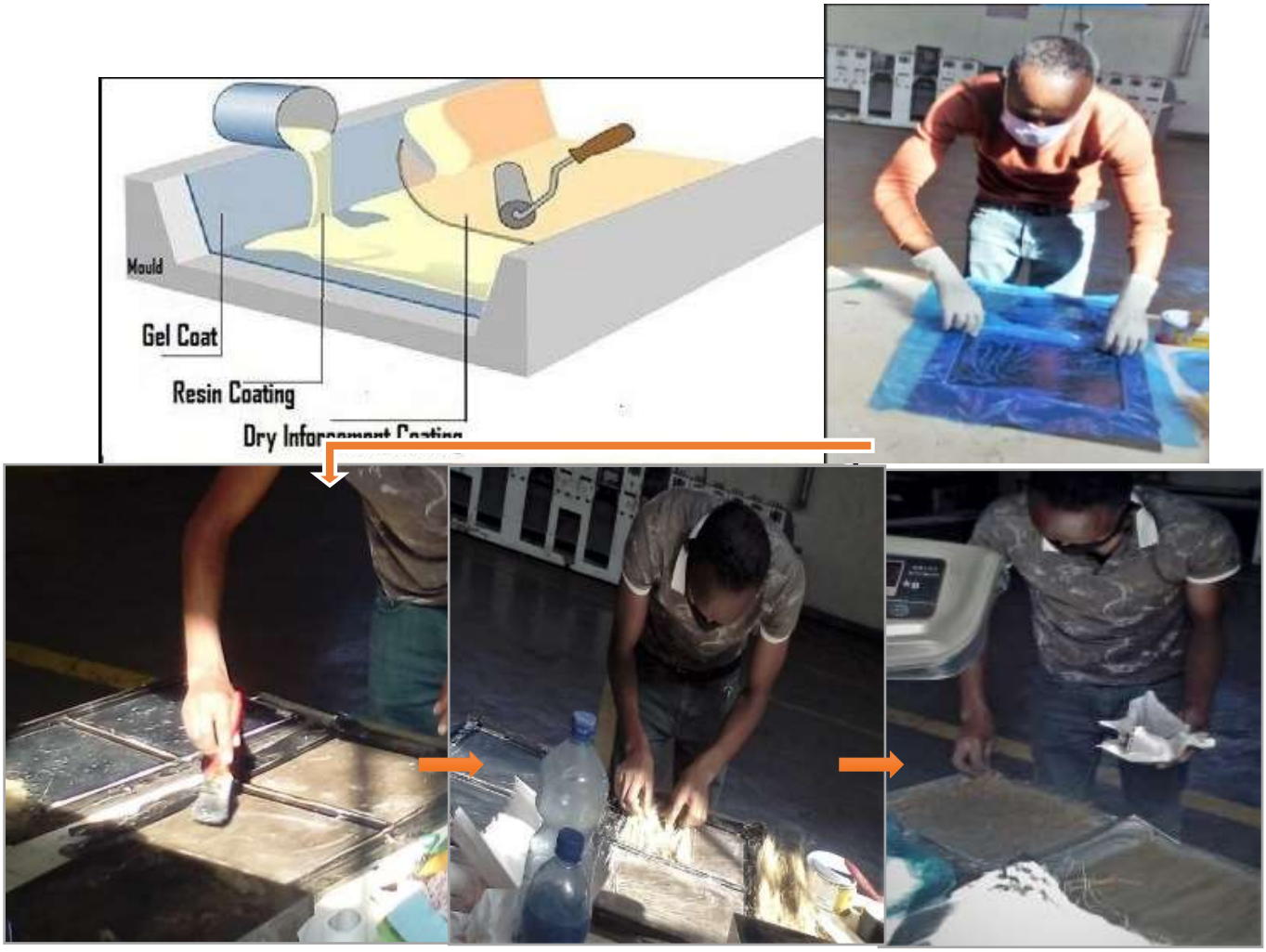

Figure 3- 11. Hand laying up

- ***Compression and Curing***

After the mold preparation and the hand-lay-up process is finished the compression was followed. The compression process was performed at the African Bamboo PLC workshop laboratory with 5MPa pressure and three steel plate hydraulic press machines. The steel plates have a uniform upper and lower surface. The first mold frame was installed on the upper surface of the lower plate. The second mold frame was installed on the upper surface of the middle plate. Then as the hand-laying-up process was performed on both molds (double sandwiched), they were pressed at Once in such a way the middle plate was situated to covers the bottom mold, and the uppermost plate can cover the middle one. After placing

the two molds and uppermost plate on the lower jaw of the press machine properly the machine was allowed to press until 5MPa pressure is attained and self-lock is activated. Then it was allowed to cure for 24 hours before demolding. After the cured samples were removed from the mold, post cured for 20 days at standard laboratory atmosphere was followed prior to cutting to standard specimens and mechanical property test.

Figure 3- 12. Pressing Machine Captured at African Bamboo plc

- ***Mold Release***

The mold release process is a simple process which is separating the upper and lower jaw of the pressing machine. Then move the molds from the machine and place them on the table. After that, molded samples were removed from the mold the polyethylene plastic was peeled from the samples.

Figure 3- 13. Manufactured Samples

3.6. Experimental Procedures and Setups

3.6.1. Specimen sampling procedures

In this research, three mechanical testing and one physical test is performed. A total of 270 sample specimens are prepared for the test. According to ASTM standards, samples are cut into their respective dimensions as shown in Figure 3-16. The cutting to a standard dimension is performed in two steps, first trimming at African Bamboo PLC workshop with 3000RPM grinder and secondly with a high speed (11,400RPM) hand grinder for cutting and finished the job.

Figure 3- 14. High-Speed Hand Grinder

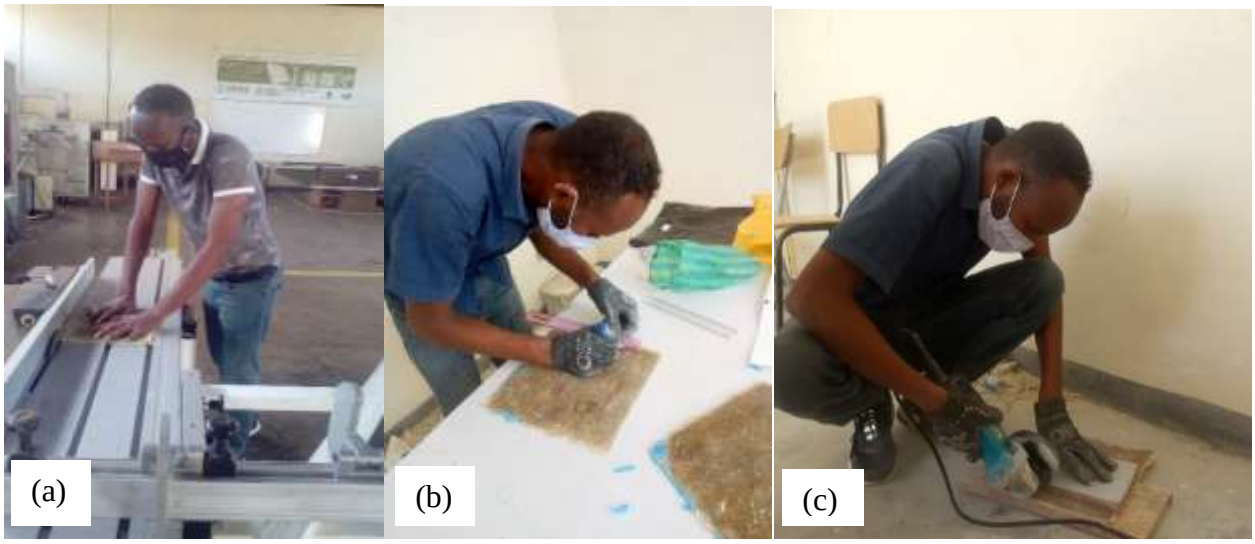

Figure 3- 15. Cutting of specimens (a) Trimming, (b) measuring, and (c) cutting process

Figure 3- 16. final produced sample specimens which are ready for mechanical test

3.7. Introduction of Testing Apparatus

Universal Testing Machine or commonly called UTM is a general-purpose machine used to check tension load and compression load applied via different fixtures to test materials. Any test material that has elongation or compression properties can be tested in a UTM machine. The test sample can be any material, component, or structure. In different industries or sectors, universal Testing Machine is referred differently but it serves a similar purpose. For example, it is referred to as 'tensile strength tester', 'tensile testing machine', 'compression testing machine, 'compression strength tester', etc. UTM Testing Systems are highly integrated testing packages that can be configured to meet different testing needs. Each includes a load unit with an integrally mounted actuator and servo valves, the control system, and the hydraulic power unit as presented in Figure 3-17. The control system has three major parts: the system software running on a digital controller, the personal computer, and a remote station control panel. These functions work together to provide fully automated test control.

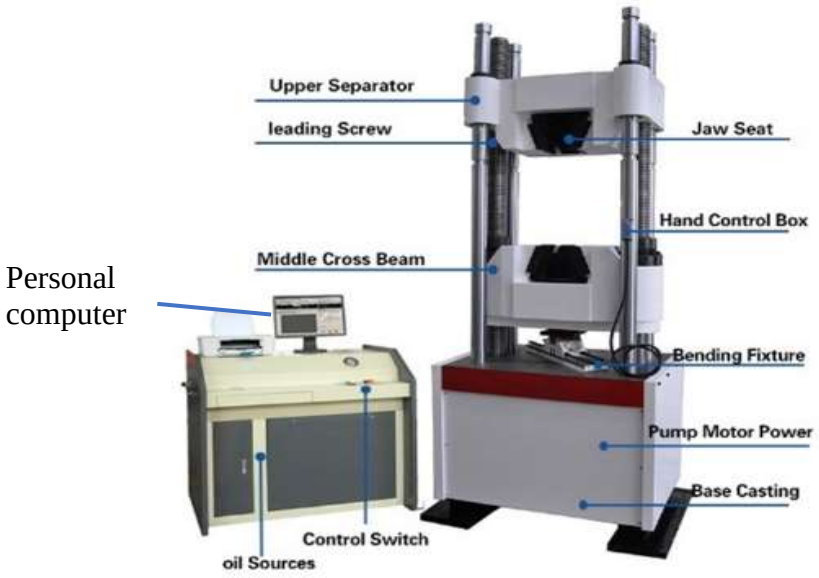

Figure 3- 17. Universal Testing Machine

Tensile Strength Test (ASTM D3039/D3039M):

The primary objective of this test was to evaluate the in-plane tensile properties of sisal/sugarcane bagasse fiber composites. For each sample, 3 specimens were tested. Each specimen was 25 by 220 mm. During the test, the specimens were placed in the grips of UTM and axial load is applied through both ends of the specimen. Typical points of interest when testing a material include: ultimate tensile strength (UTS) or peak stress; The cross-head speed used was 0.5 mm/min, and gauge length was 120 mm. The testing procedure is shown in Figure 3-18.

The Modulus of Elasticity (Young's Modulus) is calculated by taking two random points on the steep line of the graph and divide the differential of stress (MPa) by the differential of strain(mm/mm).

$$Modulus(MPa) = \frac{\Delta stress(MPa)}{\Delta strain(\frac{mm}{mm})} \quad (3\text{-}5)$$

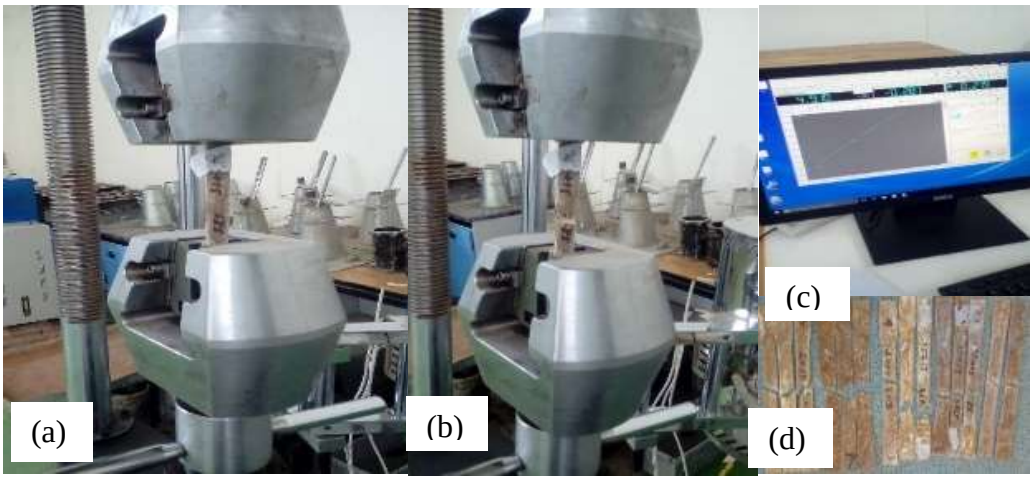

Figure 3- 18. Tensile test setups (a) before fracture, (b) after fracture, (c) digital computer reading, and (d) broken specimens

Flexural Strength Test

The bending (Flexural strength) is The ability of a substance to withstand deformation when subjected to a load. The inter-laminar shear strength of sisal/sugarcane bagasse hybrid fiber-reinforced composites samples is evaluated using short beam shear tests (ILSS). It's a three-point bend test that usually leads to inter-laminar shear failure. This test is performed using UTM in accordance with the (ASTM D790) standard. Figure 3-19 depicts the loading arrangement. The dimension of the specimen is (180x12.5x3) mm with a support span length of 152.4 mm rate of crosshead motion 0.5mm/min.

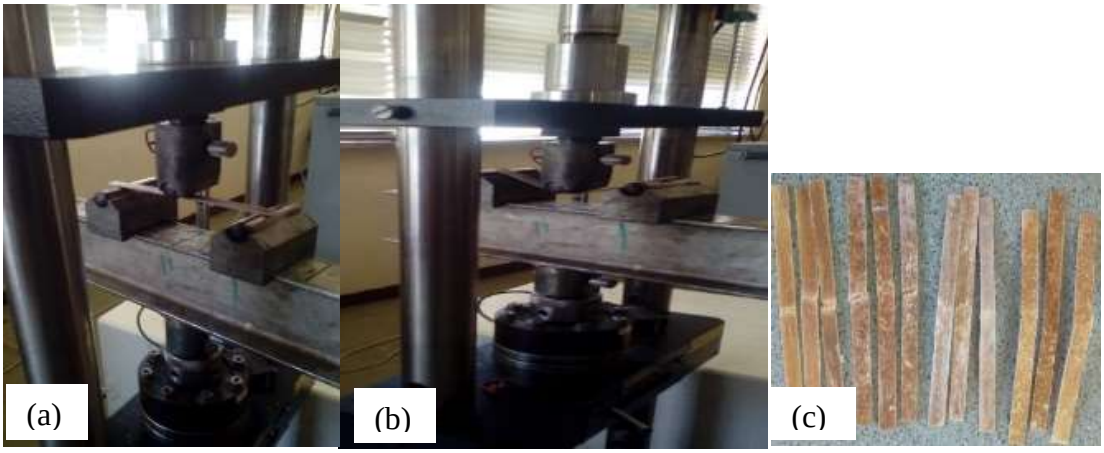

Figure 3- 19. Flexural test setups (a) before loading, (b) during loading, and (d) broken specimens

The three-point bending test was conducted using Universal Testing Machine according to ASTM D790 to measure the stress to resist bending at the center of the span. Considering

the composite as a homogeneous mixture along the length, this test can be calculated analytically as follow.

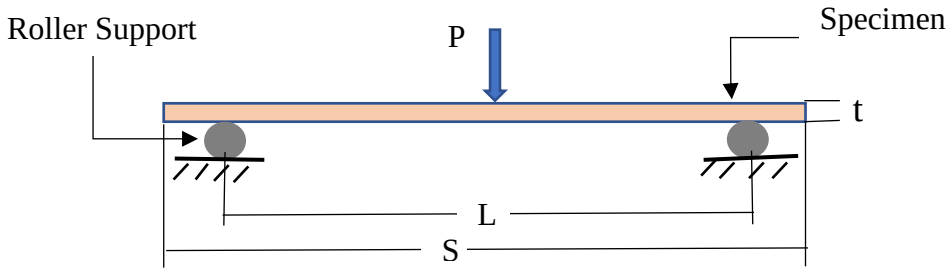

Figure 3- 20. Diagram for bending test set up

Where P: applied to bend load, L: span length, S: length of the specimen, t: the thickness of the specimen

The maximum flexural (bending) strength is given by

$$\boldsymbol{\sigma_{bmax}} = \frac{\mathbf{M_{bmax}}}{W_b} \qquad (3\text{-}6)$$

The maximum bending moment (M_{bmax}) can be calculated as follow

$$\mathbf{M_{bmax}} = \frac{\mathbf{F_{bmax} * L}}{\mathbf{4}} \qquad (3\text{-}7)$$

The moment of (inertia) resistance corresponding to bending with the region of elastic deformations are calculated as

$$\mathbf{W_b} = \frac{\mathbf{b * h^2}}{\mathbf{6}} \qquad (3\text{-}8)$$

Where, $\boldsymbol{\sigma_{bmax}}$ = maximum bending stress, $\mathbf{M_{bmax}}$ = maximum bending moment, $\mathbf{W_b}$ = section modulus, L =Span length of the specimen b = width of the specimen and h = (height) thickness of the specimen

The maximum flexural test results for all samples are given in the discussion part bar graph shown in Figure 4-5. These results are the average results of the three trials.

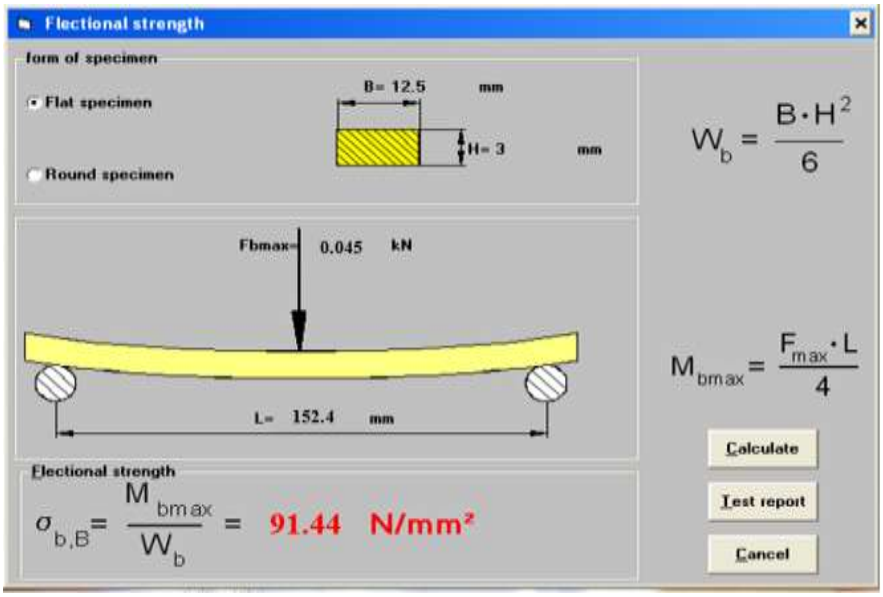

Figure 3- 21. Flexural test result from testing software

Compressive Strength Test

The compression strength testing was performed on sisal/sugarcane bagasse hybrid fiber-reinforced composite in laboratory experiments. In this section, the prepared specimen was involved in axial compression loading using the UTM. The dimension of the specimen is prepared according to ASTM D3410 (155x25x3) mm with 25 mm gauge length. To obtain compression test results the specimen is inserted into the test fixture which is placed between the plates of the testing machine and loaded in compression. The maximum load attained was recorded by the UTM testing system after the specimen failed. A typical specimen failure is shown in Figure 3- 22.

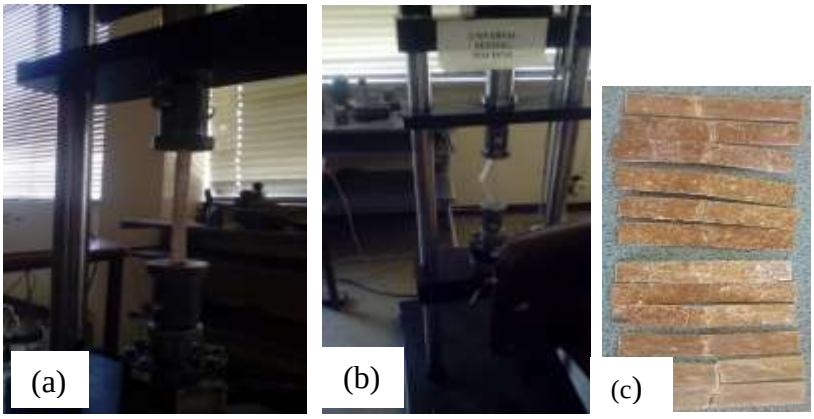

Figure 3- 22 .Compression testing setups (a) before loading, (b) during loading, and (c) broken specimens

Charpy Impact Test

The Charpy impact test is performed based on ASTM A370 on the impact testing machine. The purpose of an impact test is to determine the ability of the material to absorb energy during a collision. In the Charpy impact test, (sometimes referred to as the V-notch Charpy impact test), the sample lies flat on the testbed as a simple beam. Both ends of the specimen get secured before the moment of impact as shown in Figures 3-23. The impact toughness of a specimen is determined by measuring the energy absorbed in the fracture of the specimen. This is simply obtained by noting the height at which the pendulum is released and the height at which the pendulum swings after it has struck the specimen. In this test, notches are commonly used in material impact tests where a morphological crack of a controlled origin is necessary to achieve standardized characterization of fracture resistance of the material. The most common is the Charpy impact test, which uses a pendulum hammer (striker) to strike a horizontal notched specimen. The Charpy impact value (kJ/m2) is calculated by dividing the fracture energy by the cross-section area of the specimen.

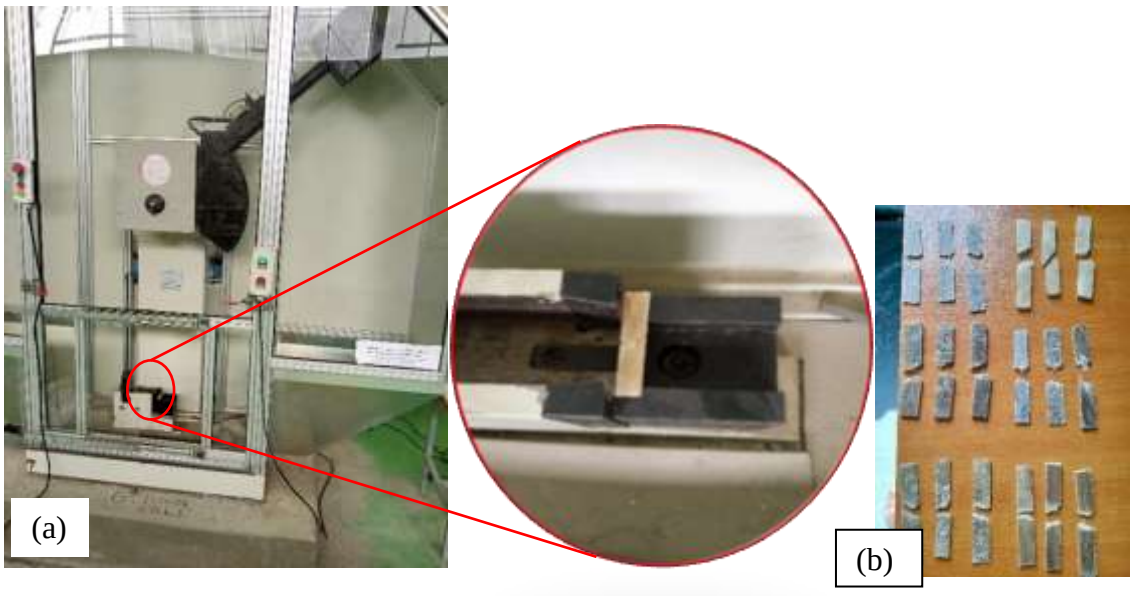

Figure 3- 23. Impact test setups (a) specimen placing and (b) specimen after fracture

Water absorption test

The water absorption test was tested at AASTU civil structural engineering laboratory for 19 days at an average temperature of 25°C. Specimens were prepared based on ASTM D570-98 standards (20mm×20mm×3mm) and the samples were dried with an oven drier for 24 hours at 80°C. After the samples were kept at room temperature for three hours, measuring with electronic balance was followed and recorded as the initial weight of samples. After recording the initial weight of samples, they were immersed completely in distilled water for 432 hours with 24 hours intervals for measuring and recordings. During measuring, samples were cleaned with a towel to remove the water on the surface and immerse immediately into distilled water to prevent water evaporation to the environment. At the final record thickness of the samples was recorded to evaluate the thickness swelling.

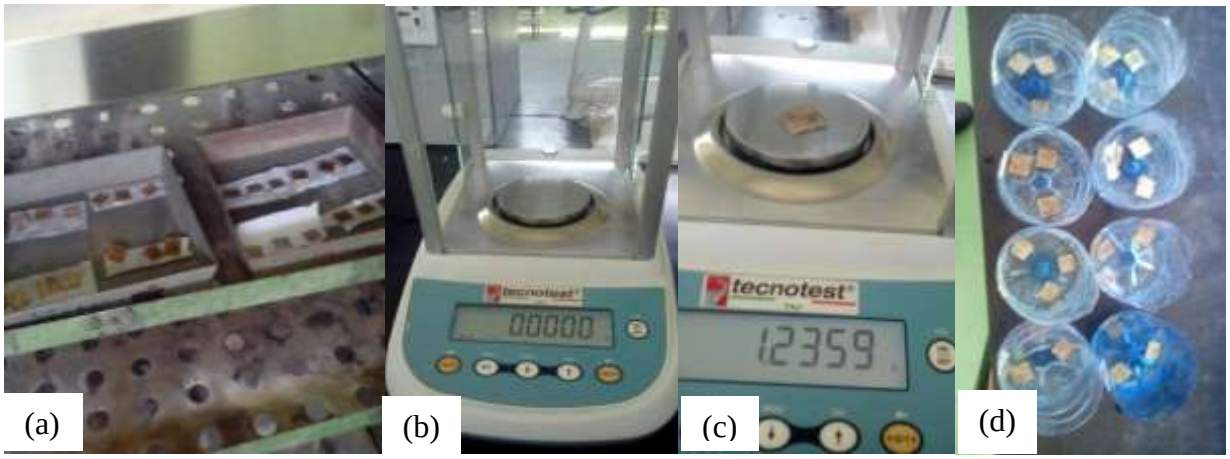

Figure 3- 24. Water absorption test setups (a) drying with oven, (b) setting up measuring electronic balance, (c) measuring a specimen, and (d) immersed specimens in distilled water

The weight gain is calculated for different immersion time as follow.

$$M_t(\%) = \frac{W_t - W_o}{W_o} * 100 \qquad (3\text{-}9)$$

Where, $M_t(\%)$ is percentage weight gain, W_t weight at any time, W_o initial weight

Diffusion Coefficient (D)

The diffusion coefficient (D) is a physical constant dependent on molecule size and other properties of the diffusing substance, in this case, water through the composite material.

For the calculation of the diffusion coefficient, the Fickian First law of diffusion was applied. The criteria whether the diffusion obeys the Fickian diffusion equation or not is based on the fitting of the experimental data to the Boltzmann equation and check that n is between 0.5 and 1[61-63].

$$M_t = kt^n => logM_t = logk + nlogt \quad (3\text{-}10)$$

Where, M_t is the gain at time t, t is immersion time, k and n are constants determined from the fitting of experimental data. The criteria to categorize the diffusion as Fickian or non-Fickian diffusion is the constant n from the above equation. If $0.5 < n < 1$ then the diffusion follows the Fickian diffusion equation, and if $n = 1$ then, the diffusion follows the non-Fickian diffusion equation[70]. In this research, the constant n values are determined from fitting of experimental data to the above equation (3-10) using Microsoft excel as shown in figure 4-14. and all values of n are found to be around 0.5 as shown in table 4-1 below in the discussion section.

The k values are obtained from the inverse of logarithmic function (ln) of the constant term of the fitting equation and n values are the coefficients of time-containing the term. The graphs depicted that the experimental data plot and the approximate line fit to the data graph.

Thickness swelling

The thickness swelling is a phenomenon of an increment in the thickness of the samples that happened when the water flows into the fiber during immersion. This increment of the thickness is evaluated by measuring the thickness of the samples before the immersion and after the saturation. The percentage increase of the samples by thickness can be calculated as follow.

$$TS(\%) = \frac{T_s - T_o}{T_o} * 100 \quad (3\text{-}11)$$

Where; TS is Thickness swelling, T_s is the thickness at saturation, T_o is the initial thickness of the specimen

3.8. Taguchi Method of Experiment

Taguchi method is started after Second World War by Japanese engineer Dr. Genichi Taguchi to develop new methods to optimize the process of engineering experimentation and he believed, that the best way to improve the quality was to design and build it into a product. Dr. Taguchi developed the technique which was known as the Taguchi method. His main contribution does not lie in the mathematical formulation of the design of experiments, but rather in the accompanying philosophy. Besides that, his concept produced a unique and powerful improvement technique that differs from traditional practices. His ideas can be summarized in three core points as follow[71].

1. **Quality should be designed into a product, not inspected into it**. Quality "inspected into" a product means that the product is produced at random quality levels and those too far from the mean are simply thrown out.

2. **Quality is best achieved by minimizing the deviation from a target**. The product should be designed so that it is immune to uncontrollable environmental factors. In other words, the signal (product quality) to noise (uncontrollable factors) ratio should be high.

3. **The cost of quality should be measured as a function of deviation from the standard and the losses should be measured system-wide**. This is the concept of the loss function, or the overall loss incurred upon the customer and society from a product of poor quality. Because the producer is also a member of society and because customer dissatisfaction will discourage future patronage, this cost to the customer and society will come back to the producer.

3.8.1. Taguchi Design of Experiment

Taguchi experimental design is a popular design and is a set of fractional factorial designs concentrated on the estimation of the main effect. Among experimental design, the Taguchi experimental design is the appropriate design as it is used for various product quality control, product development, process optimization and use a minimum number of runs. According to the Taguchi design approach, the impact of uncontrollable factors on product characteristics is very minimum. Generally, this method depends on the quality

loss function. In other ways, the product quality (signal) to uncontrollable factors (noise) should be high.

The general steps involved in the Taguchi Method are as follows[72]:

Brainstorm the quality characteristics and design parameters important to the product/process (Define the Problem and Noise Factors);

Here the objective of the design of the experimental method is to analyze the influence of fiber loading, layering sequence, and pressing temperature on mechanical properties (tensile strength, flexural strength, compression strength, and impact strength) and water absorption property of sisal and sugarcane bagasse hybrid fiber polyester composite material.

1. ***Identify Design Parameters That Influence Product Properties.***

The performance of composite materials is mostly depending on the types of fiber, fiber loading proportions, continuity of microstructure, and manufacturing technique. Hence, in this research fiber loading proportions, layering sequence, and curing temperatures are considered as design factors that affect the performance of the hybrid composite material.

2. ***Determine Control Parameters, Response Variables, and Their Levels***

Control parameters are the variables that influence the output of the process or the product. These parameters are listed in table 3-2 with their levels. Tensile strength, flexural strength, compression strength, impact strength, and water absorption are response variables chosen to be investigated.

Table 3- 2. Process Parameters for Taguchi Method

levels	Fiber loadings	Layering sequence	Curing Temperature
1	10S/20B	SBS	Low (25°C)
2	15S/15B	UNF	High (60°C)
3	20S/10B	BSB	

3. ***Select Orthogonal Array***

Selecting orthogonal array in the Taguchi method is based on the convention $L_N(S^K)$,

where N: Total number of runs during experimentation

S: Total number of levels for each factor

K: Maximum number of factors whose effect can be estimated without any interaction

In this research three levels of fiber loading, three levels of layering sequence, and two levels of curing temperature have been considered as the influential parameters to investigate composite response variables. For these two with three-level and one with two-level parameters, the convention for orthogonal array selection from the standard orthogonal array table has been used as follows. The selected array is highlighted in a thick border in the table below based on the calculation L18 = (2^1 x3^2).

Table 3- 3. Standard Orthogonal Array Table

Array	Experimental runs	Max # of factors	Max # of factors that can be considered at various levels of factors			
			Level 2	Level 3	Level 4	Level 5
$\mathbf{L_4}$	4	3	3		1	
$\mathbf{L_8}$	8	5	4			
$\mathbf{L_8}$	8	7	7			
$\mathbf{L_9}$	9	4				
$\mathbf{L_{12}}$	12	11	11			
$\mathbf{L_{16}}$	16	15	15			
$\mathbf{L_{16}}$	16	5			5	
$\mathbf{L_{18}}$	18	8	1	7		
$\mathbf{L_{25}}$	25	6				6
$\mathbf{L_{27}}$	27	13	1	13		
$\mathbf{L_{32}}$	32	31	31			
$\mathbf{L_{32}}$	32	10	1		9	
$\mathbf{L_{36}}$	36	23	11	12		
$\mathbf{L_{36}}$	36	16	3	13		
$\mathbf{L_{50}}$	50	12	1			14
$\mathbf{L_{54}}$	54	26	1	25		
$\mathbf{L_{64}}$	64	63	63		21	
$\mathbf{L_{64}}$	64	21		40		
$\mathbf{L_{81}}$	81	40				

Therefore, for the combination of one with two-level and two three-level parameters L_{18}-orthogonal array is tabulated below.

Table 3- 4. Orthogonal Array for L18 (2^1 x3^2)

Exp Runs	**Curing Temp**	**Fiber loading**	**Layering sequence**
1	25	10S/20B	UNF
2	25	10S/20B	SBS
3	25	10S/20B	BSB
4	25	15S/15B	UNF
5	25	15S/15B	SBS
6	25	15S/15B	BSB
7	25	20S/10B	UNF
8	25	20S/10B	SBS
9	25	20S/10B	BSB
10	60	10S/20B	UNF
11	60	10S/20B	SBS
12	60	10S/20B	BSB
13	60	15S/15B	UNF
14	60	15S/15B	SBS
15	60	15S/15B	BSB
16	60	20S/10B	UNF
17	60	20S/10B	SBS
18	60	20S/10B	BSB

4. Conduct experiment

After recording all the results from experimental tests Taguchi method optimization has been conducted using Minitab 19.0 software

5. Analysis of the final results and predicts the optimum level

The optimum combination of parameters and their levels are predicted based on the calculation of signal-to-noise ratio by the three Taguchi method scenarios defined below[73].

1) **Larger-the Better**: when the maximum value of the product is necessary Larger-the better scenario is applied. Signal to noise ratio is given by:

$$[S/N]_L = -10\log_{10}[MSD] = -10\log_{10}\frac{\sum\frac{1}{\mu^2}}{n} \quad (3\text{-}12)$$

where MSD is the mean standard deviation, μ is the signal mean and n is the number of trials/ sample size.

2) **Smaller-the Better**; when the minimum value of the product is necessary Smaller-the better scenario is applied. the signal to noise ratio is given by:

$$[S/N]_S = -10\log_{10}[MSD] = -10\log_{10}\frac{\sum\mu^2}{n} \quad (3\text{-}13)$$

where MSD is the mean standard deviation, μ is the signal mean and n is the number of trials/ sample size.

3) **Nominal- the Best;** when the specified value is MOST desired (Neither smaller nor Larger value is desirable) the Nominal- the best scenario is applied. The signal to noise ratio is given by;

$$[S/N]_N = -10\log_{10}\frac{\mu^2}{\sigma^2} \quad (3\text{-}14)$$

where μ is the signal mean and σ is the standard deviation.

For this research Larger- the Better principle is applied. Because maximum values of mechanical properties (tensile strength, flexural strength, compression strength, and impact strength) of this sisal and SCB hybrid fiber composite material is desirable. But for the water absorption property minimum water gain up to saturation is desirable. therefore, the Smaller-the Better principle is applied.

3.9. Toyota Raum Inner Door Panel Modeling and Ansys Simulation

Based on the test results of the natural fiber composite static structural analysis simulation with ANSYS 2020 R1 is executed for the conformation of applicability in automotive body manufacturing. For this validation process, Toyota Raum inner door panel has been selected for its simple features among several types of automotive doors. The biofiber composite material developed in this research is less viable for water absorption and has moderate strength. Inner door panels are door parts designed for the installation of inside door accessories and to absorb external impact from the outer door panel. Therefore,

applying it to automotive bodies, which, should have moderate strength and less environmental interaction become suitable. For the modeling of the inner door panel SolidWorks 2018 software was used. The measured overall dimensions of the inner door panel were 920mm×960mm with 1.5mm thickness. The comparison analysis was made between manufactured SCB and sisal hybrid fiber polyester composite and three common materials used in automotive inner door panel manufacturing namely structural steel, aluminum alloy, and E-glass epoxy UD composite material.

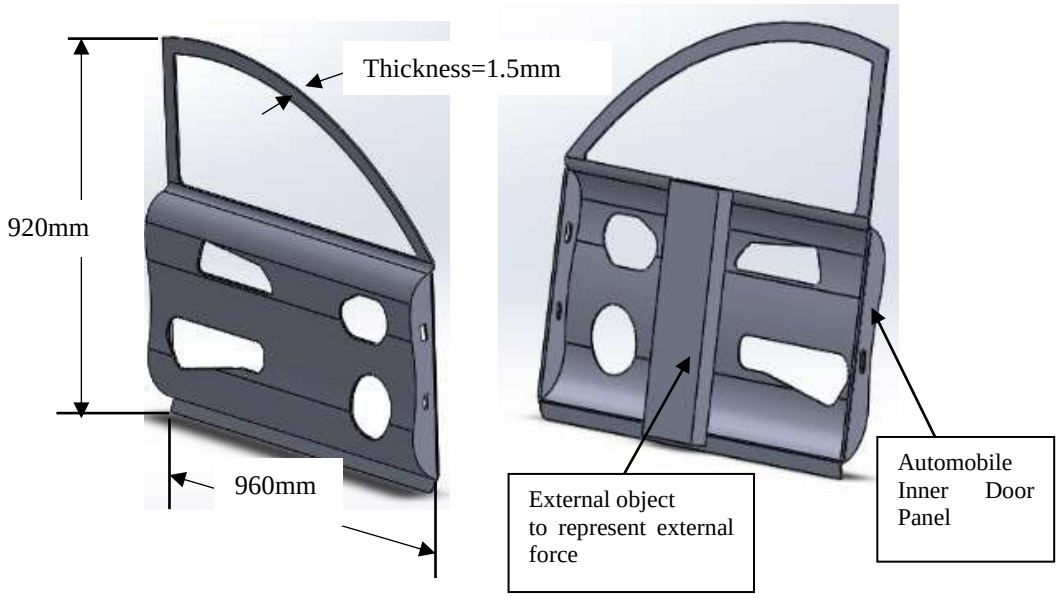

Figure 3- 25. Inner Door SolidWorks 2018 models

For the Ansys simulation analysis test results of the current sisal and SCB hybrid fiber composite are used in the Ansys engineering data. The optimum mechanical property values were recorded from Taguchi method analysis at the combination of 20S/10B fiber loading and SBS layering sequence with 25°C curing temperature. These recorded values are 37.89MPa tensile strength, 102.55MPa flexural strength, 18.78MPa compression strength, and 20.29J/m2 impact strength. The water absorption tendency is also minimum at this combination of the composite with 6.37%. The Young's Modulus for the maximum tensile strength is 789.4MPa. The Poisson's ratio was taken as the weighted average of the three constituents. Their values of 0.44, 0.32, and 0.22 polyester resin, sisal fiber, and sugarcane fiber respectively, and the weighted average is 0.39. After filling in these engineering data the analysis continued to examine the strength and the weight reduction

with other conventional materials. The force applied was selected to be 600N for the safe working stress. This magnitude was applied with a factor of safety not less than one. The strength comparison is done based on the safety factor (FoS) and is done by Ansys stress tool for structural steel and aluminum alloy or analytically using equation (3-15) which are ductile materials. But Since natural fiber composite materials are considered as brittle materials, they have no yield stress to calculate the factor of safety in the Ansys workbench. Therefore, the safety factor for epoxy E-glass UD composite and sisal/sugarcane bagasse hybrid fiber polyester composite was calculated analytically by the equation (3-16).

$$\text{Factor of Safety for Ductile Materials (FoS)} = \frac{\text{Yield Point Stress}}{\text{Working Stress}} \quad (3\text{-}15)$$

$$\text{Factor of Safety for Brittle Materials (FoS)} = \frac{\text{Ultimate Stress}}{\text{Working Stress}} \quad (3\text{-}16)$$

The directional and total deformation of these materials is calculated by the Ansys workbench structural static analysis. Strain energy is a type of potential energy that is stored in a structural member as a result of elastic deformation. It can be calculated by the software and the following equation.

$$\text{Strain Energy } (U) = \frac{\sigma^2 * V}{2E} \quad (3\text{-}17)$$

Where σ is stress, V is volume and E is Young's modulus

The other comparison is done by the mass of the inner door panel made of these materials. The mass for each material was calculated using their density and the total volume of the door panel.

Table 3- 5. Candidate Materials Density

Material	Density (ρ in kg/m^3)
Structural steel	7850
Aluminum alloy	2000
Epoxy E-glass UD	2770
Sisal/sugarcane bagasse polyester	1230

The volume and mass of these materials are calculated by the software and they are discussed in the result and discussion section below.

CHAPTER FOUR

4. RESULTS AND DISCUSSION

4.1. Tensile Test Results

For tensile strength test specimens were prepared from 30%wt of fiber (sisal and SCB) and 70%wt resin (general purpose polyester) at 0^o sisal fiber orientation and chopped SCB fiber with different fiber proportions (10S/20SCB, 15S/15SCB, and 20S/10SCB) and with three different layering sequences (uniform mixing, SBS, and BSB) at two different curing temperatures (25^oC and 60^oC). The total number of specimens for the tensile test was 54 samples with three testing trials for each fiber proportion and layering sequence. The results for these tests are depicted in figures 4-1, 4-2, and 4-3 below. On the graph, the relatively steep slope of initial records represents the elastic behavior of the material and the slope defines the elastic modulus.

These graphs are plotted on an excel worksheet by using values taken from test results for each sample. Figure 4-1 shows engineering stress versus engineering strain for the 10S/20B fiber loading for different layering sequences (UNF, SBS, and BSB) manufactured at two different pressing temperatures (25°C and 60°C).

Observation from Tensile Strength Test Result

In this research, fiber loading was varied from 10% to 15% and 20% for sisal fiber and conversely, SCB fiber decreased from 20% to 15% and 10% with the combination of (10S/20B, 15S/15B, and 20S/10B). Here tensile test values showed an increment from 26.87MPa to 34.96MPa as sisal fiber increases from 10%wt to 20% in the composite for uniform mixing and cold pressing. For all samples manufactured at elevated temperature, there is a negative effect on the tensile strength of the composite. The only advantage of hot pressing is to lower the curing time from 24 hours to 3 hours. By considering only the cold pressing technique on the graph SBS layering maintains the largest tensile strength (27.98MPa for 10S/20B, 30.44MPa for 15S/15B, and 37.89MPa for the 20S/10B) of the three layering. This is because of placing sisal fiber which has a relatively better tensile strength at the skin of the composite on both sides that can resist crack initiations on the composite. This is also the reason for the uniform mixing samples to have moderate tensile

strength (26.87MPa for 10S/20B, 29.67MPa for 15S/15B, and 34.96MPa for 20B/10S) for cold pressing conditions.

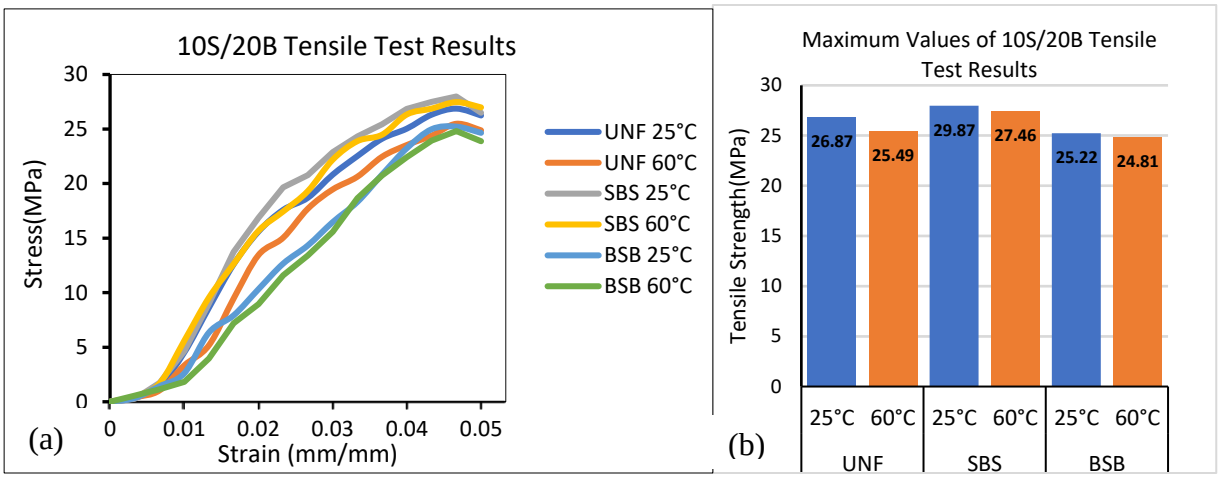

Figure 4- 1. Engineering stress vs Engineering strain for Tensile testing (a)and Maximum stress(b) values for 10S/20B

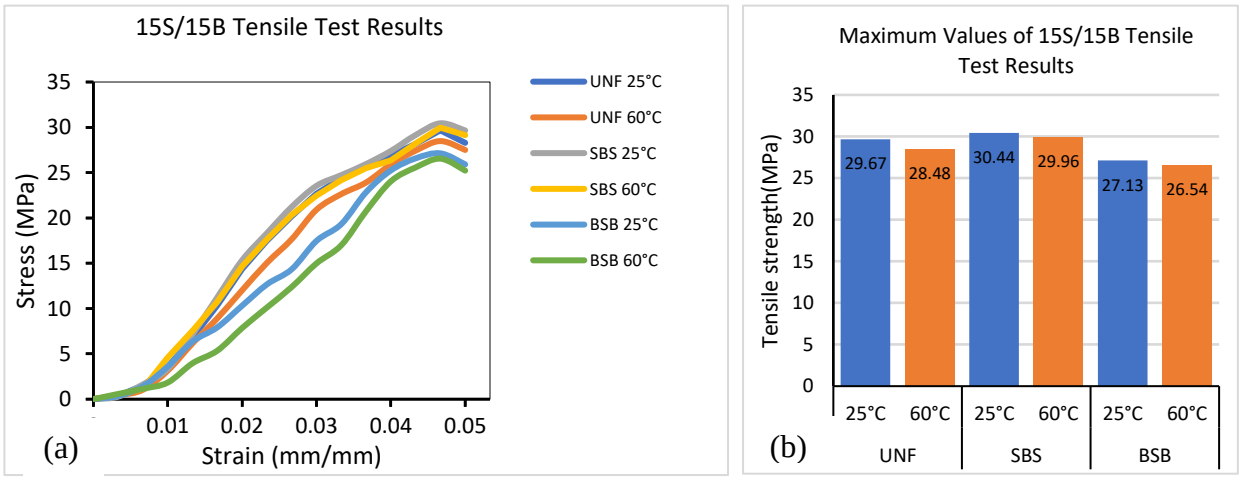

Figure 4- 2. Engineering stress vs Engineering strain for Tensile testing (a) and Maximum stress(b) values for 15S/15B

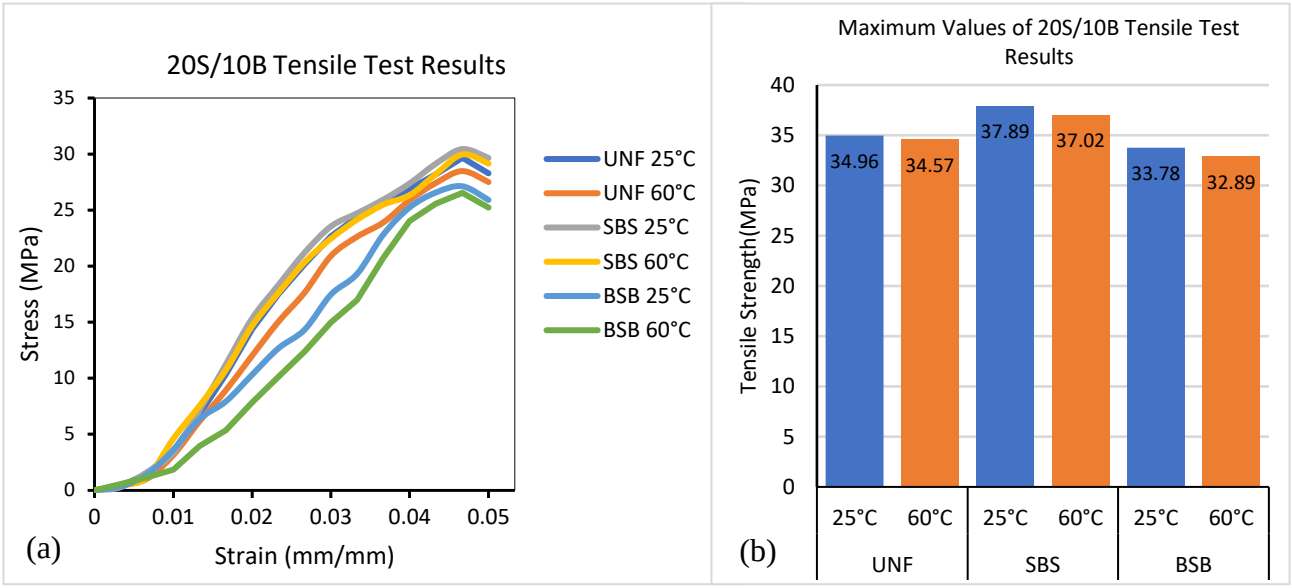

Figure 4- 3. Engineering stress vs Engineering strain for Tensile testing (a) and Maximum stress(b) values for 20S/10B

Tensile modulus which can be calculated by equation (3-5) is presented in Figure 4-4 These bar graphs show that elevated pressing temperature has a negative effect on the tensile strength. For example, for the uniformly mixed samples, cold pressing values of tensile modulus are bigger by 5.5% for 10S/20B, 4.2% for 15S/15B, and 1.1% for 20S/10B than hot pressing samples respectively. The SBS layering still has the highest tensile modulus as that of tensile strength. This is because of the higher rigidity property of cold-pressed samples. This higher rigidity is the result of compact molecular interaction due to cold pressing temperature.

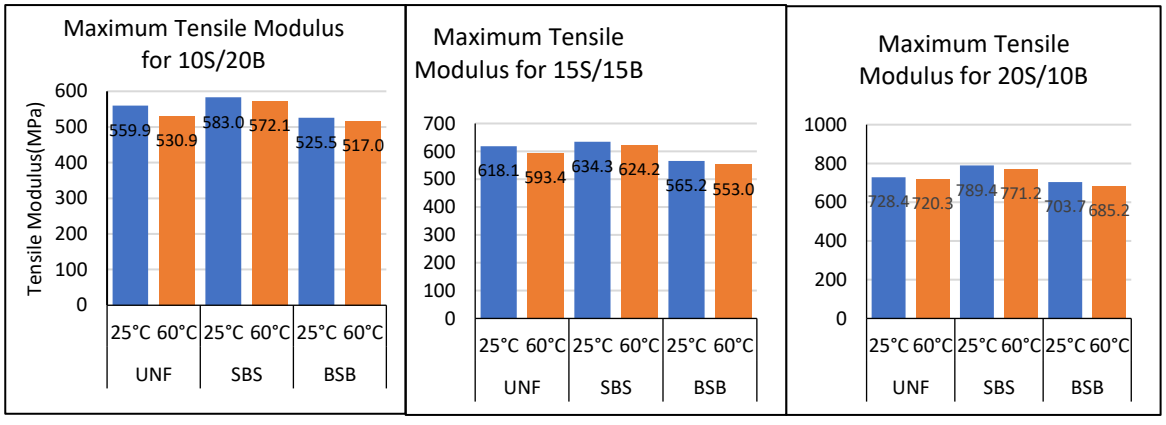

Figure 4- 4. Tensile modulus for all samples

4.2. Flexural (Three-Point Bending) Test Results

The three-point bending test was conducted using Universal Testing Machine according to ASTM D790 to measure the stress to resist bending at the center of the span. The bending stress values were calculated by the equation 3-6 which were discussed in the methodology section above.

Observation from Flexural Test Results

As one can observe from the bar graph below in Figure 4- 5, the flexural strength is highly influenced by the fiber loading proportions of hybrid constituents. When the amount of sisal fiber increased from 10% to 15% and 20% keeping the amount of matrix and decreasing amount of SCB fiber from 20% to 15% then 10%, the flexural strength increases from 72.94MPa to 84.63MPa and 96.83MPa for the uniformly mixing composite which manufactured at 25°C. This is because of the relatively higher strand strength of sisal fiber which is about (400-700MPa). On the other hand, SCB fiber strand has about (170 - 350MPa)[4,33]. Manufacturing in cold conditions (25°C) maintains higher strength than manufacturing in hot conditions (60°C). This is because of fast curing time which causes pores and cracks on the specimen. Layering sequence is the other factor that affects the strength of the composite. It is clear to observe from the graph that SBS layering has the highest flexural strength(102.55MPa). This is because placing sisal fiber at the skin of the composite can give better strength during flexure.

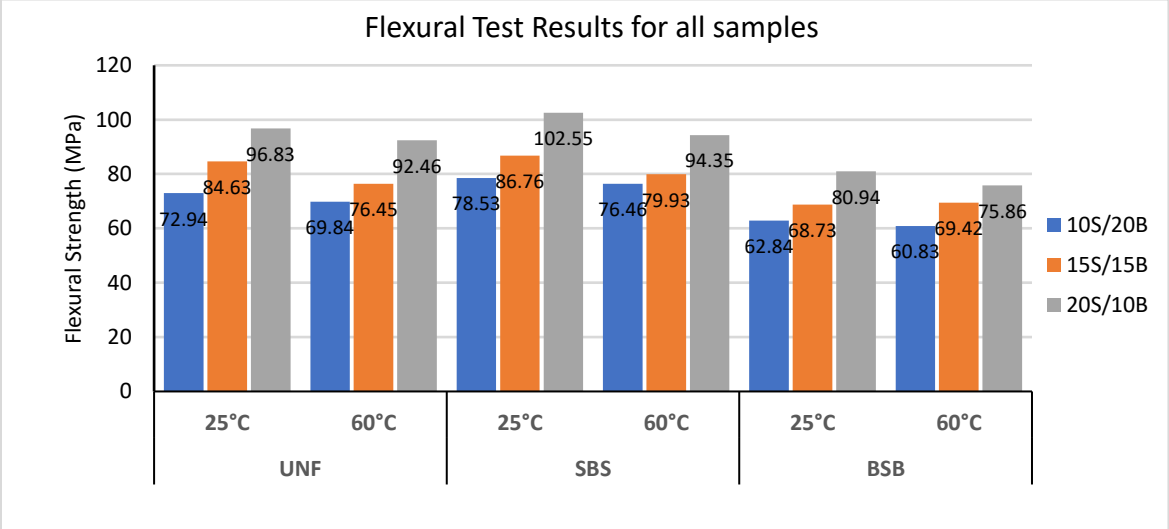

Figure 4- 5. Flexural Test Results for Maximum Values of Each Sample

4.3. Compression Test Results

The compression test in this research was accomplished by preparing specimens according to ASTM D3410 on the Universal Testing Machine. The computer software integrated into the UTM records the maximum stress at the breakage of the sample during buckling. This shows the ability of the composite to resist the buckling force. From the graph, the compression force increases uniformly from the starting up to breakage and falls gradually to zero. This is because the breakage of fibers stands has no specific point. The strands break down one after the other. Here also the compression strength differs not only by altering hybrid proportions it also differs as the layering sequence differs. From the graph, BSB layering maintains the highest compression strength with the values 19.54MPa, 22.56MPa, and 21.62MPa for 10S/20B, 15S/15B, and 20S/10B consecutively. It is for the cold pressing condition.

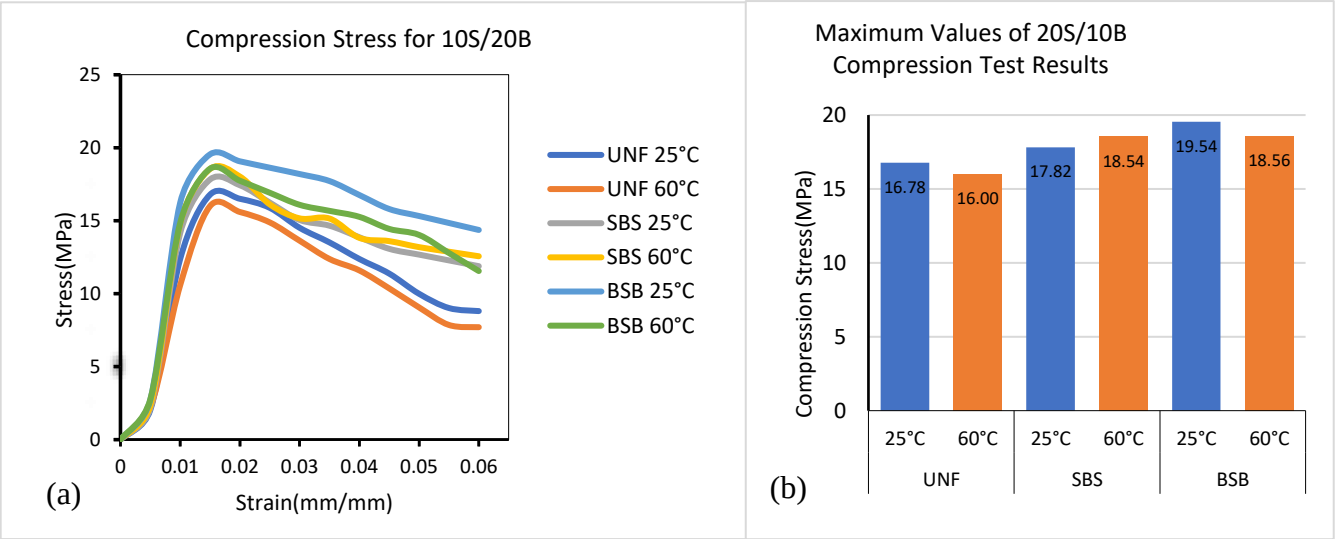

Figure 4- 6. Engineering Stress Vs Engineering Strain (a) and Maximum Stress of Compression Test Results(b) for 10S/20B

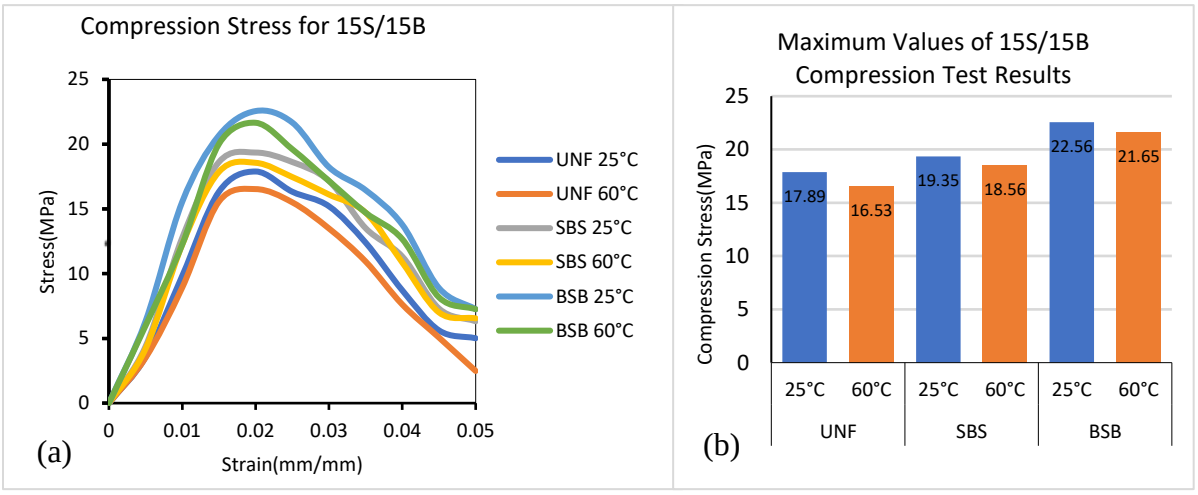

Figure 4- 7. Engineering Stress Vs Engineering Strain(a) Maximum Stress(b) of Compression Test Results for 15S/15B

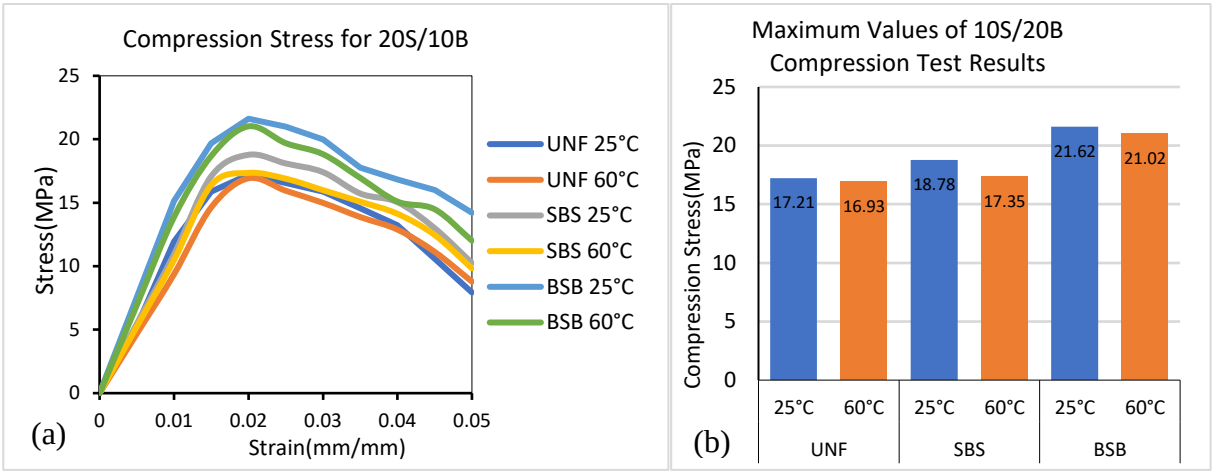

Figure 4- 8. Engineering Stress Vs Engineering Strain (a) Maximum Stress(b) of Compression Test Results for 20S/10B

4.4. Impact Test Results

The Charpy impact test is performed based on ASTM A370 on the impact testing machine. The test results recorded by the computer are shown in Figure 4-9 and test results from testing of Charpy impact test machine for all samples are depicted on the bar graph in Figure 4-12. Unlike other mechanical properties, the result of impact strength is better for the composites which have a higher proportion of SCB fiber. The impact (energy

absorbing) ability is increasing with the addition of SCB fiber for all cases. The spongy property of SCB fiber makes the composite with a higher proportion of SCB fiber better to absorb higher impact energy. The highest value of absorbed impact energy is recorded at 10S/20B uniformly mixed and cold pressing manufactured composite samples with the value of 29.46kJ/m^2 Whereas the lowest value is recorded at 20S/10B SBS layered and hot-pressing manufactured composite with the value of 19.54kJ/mm^2

Figure 4- 9. computer records of impact strength test

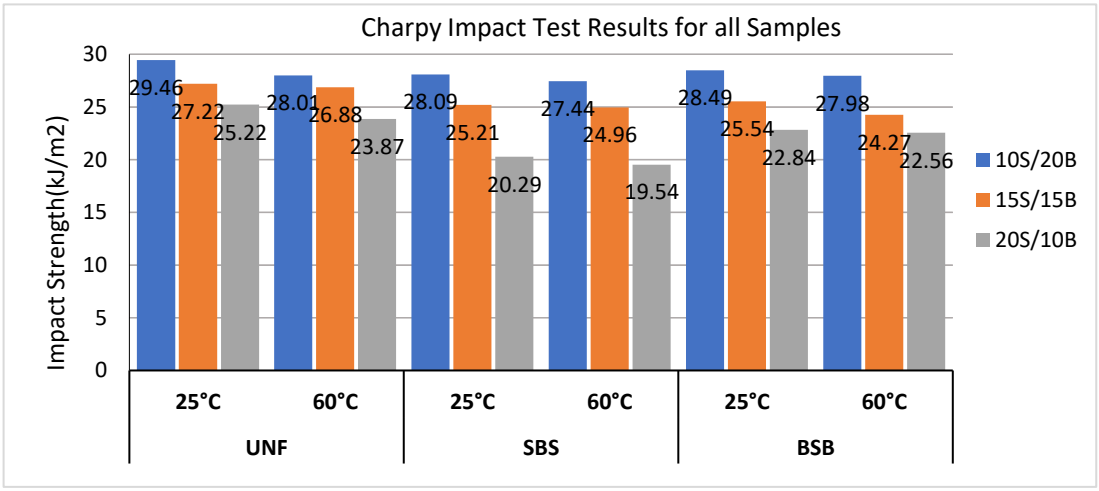

Figure 4- 10. Impact Strength Test Results for all specimens

Generally, test results of mechanical properties of natural fiber composites are highly dependent on the stick-slip phenomenon, like pinning (slip/slow) and depinning (slip/fast) dislocations of granular materials and the arrangement of particles, particle groups, and associated pore spaces. Changes in the internal structure due to large deformation may cause changes in mechanical behavior. These changes may include particles sliding, rolling and interaction, shear band formation; and fabric anisotropy. During compression or extension changes, stick-slip behavior may take place between the granular particles. Because of the non-linearity of the curve, this stick-slip effect makes it challenging to interpret test findings. The stick-slip between the granules of sisal and sugarcane bagasse fibers caused the load oscillation[74]. To support the imparted load, these granules form chains of particles within the polyester. Some granules will slip out of the chain as it gets unstable, causing the load to drop. This decrease generates a sharp decrease in stresses during compression and bending. When particles in anisotropic materials begin to slide and roll over each other, this stick-slip phenomenon happens. Due to the 'stick-slip' nature of frictional stress transfer, relative lipping of the fractured interface is normally expected from relative displacement of the matrix and fiber elements at the interface[75]. Stick-slip is characterized by crack propagation and crack arrest, indicating unstable crack growth. This jerky (stick-slip) behavior is related to the well-known physical mechanism of dislocation motions, particularly the pinning (stick/slow) and depinning (slip/fast) of dislocations. The arrangement of particles, particle groups, and associated pore spaces has a significant impact on the mechanical behavior of granular materials. Mechanical behavior may be affected by changes in the internal structure as a result of substantial deformation. Particles sliding, rolling, and interacting, shear band development, and fabric anisotropy are examples of these changes. The stick-slip behavior of the bonds appears to vanish at high strain rates, and it is sensitive to rapid variations in deviator stress forcing it to vanish. Furthermore, slick-slip disappears in relatively large specimens with high loading rates, implying that strain variations are largely influenced by the stick-slip behavior of the bonds[76,77].

4.5. Water Absorption Test Results

As we can see in the following graph the water absorption rate increased as we increase the amount of SCB fiber in general. As the amount of SCB fiber for uniform mixing and 25°C pressing temperature increases from 10% to 20% the water gain increases from 7.31% to 17.09%. The fiber layering sequence also affects water-absorbing property. Among the three layering sequences, the BSB layering has the highest absorption rate for 15S/15B (13.48%) and 20S/10B (20.43%). The graph in figures 4-10, 4-11, and 4-12 clearly shows SCB fiber has a relatively higher water absorption tendency. This is because of the lower density and pores formation property of SCB fiber.

The other interesting result that depicted in figures 4-10, 4-11, and 4-12 is that the steepest portion of the graph which shows the water absorption rate is highest in the first 24 hours of immersion time. After the 24th hour immersion time, the absorption rate gradually decreases up to saturation attains. About 60% of the total water gain takes place in the first immersion date for all proportion and layering sequences.

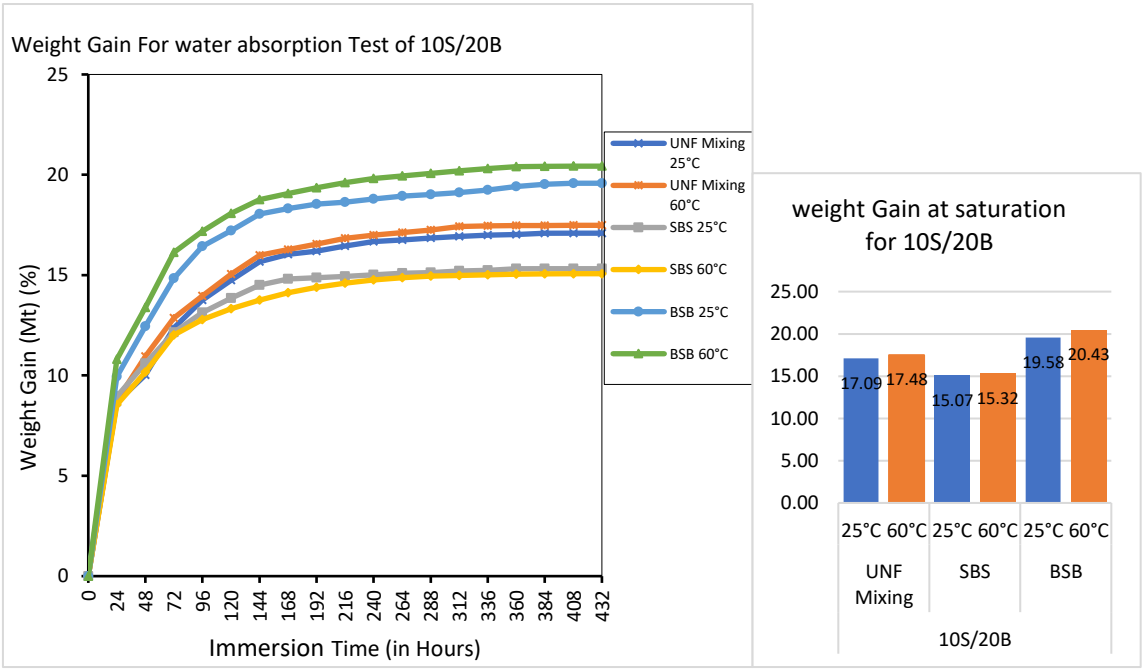

Figure 4- 11. Water Absorption Test For 10S/20B

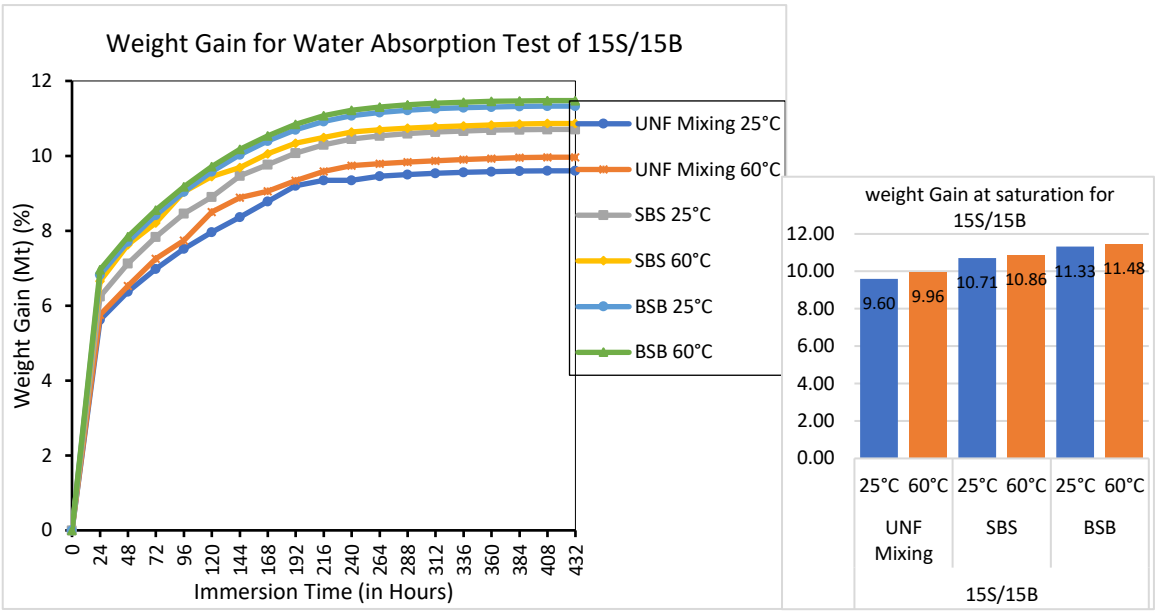

Figure 4- 12. Water Absorption Test For 15S/15B

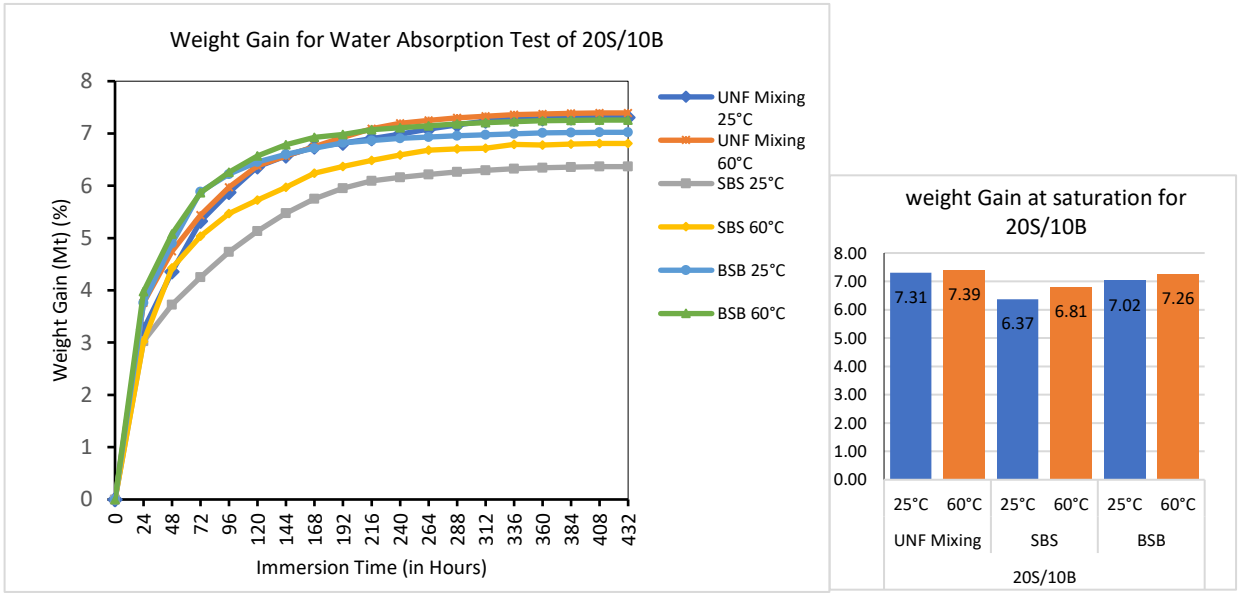

Figure 4- 13. Water Absorption Test Results for 20S/10B

4.6. Diffusion Coefficient (D)

To determine the diffusion coefficient, sorption coefficient, and permeability coefficient, the Fickian First law of diffusion was applied. The criteria whether the diffusion obeys the Fickian diffusion equation or not is based on the fitting of the experimental data to the Boltzmann equation and check that n is between 0.5 and 1 [64,65].

$$M_t = kt^n => logM_t = logk + nlogt \quad (4\text{-}1)$$

Where, M_t is the gain at time t, t is immersion time, k and n are constants determined from the fitting of experimental data. The criteria to categorize the diffusion as Fickian or non-Fickian diffusion is the constant n from the above equation. If $0.5 < n < 1$ then the diffusion follows the Fickian diffusion equation, and if $n = 1$ then, the diffusion follows the non-Fickian diffusion equation[70]. In this research, the constant n values are determined from fitting of experimental data to the above equation using Microsoft excel as shown in Figure 4-14 and all values of n are found to be around 0.5 as shown in table 4-14 below. The k values are obtained from the inverse of logarithmic function (ln) of the constant term of the fitting equation and n values are the coefficients of the time-containing term. The graphs depicted that the experimental data plot and the approximate line fit to the data graph.

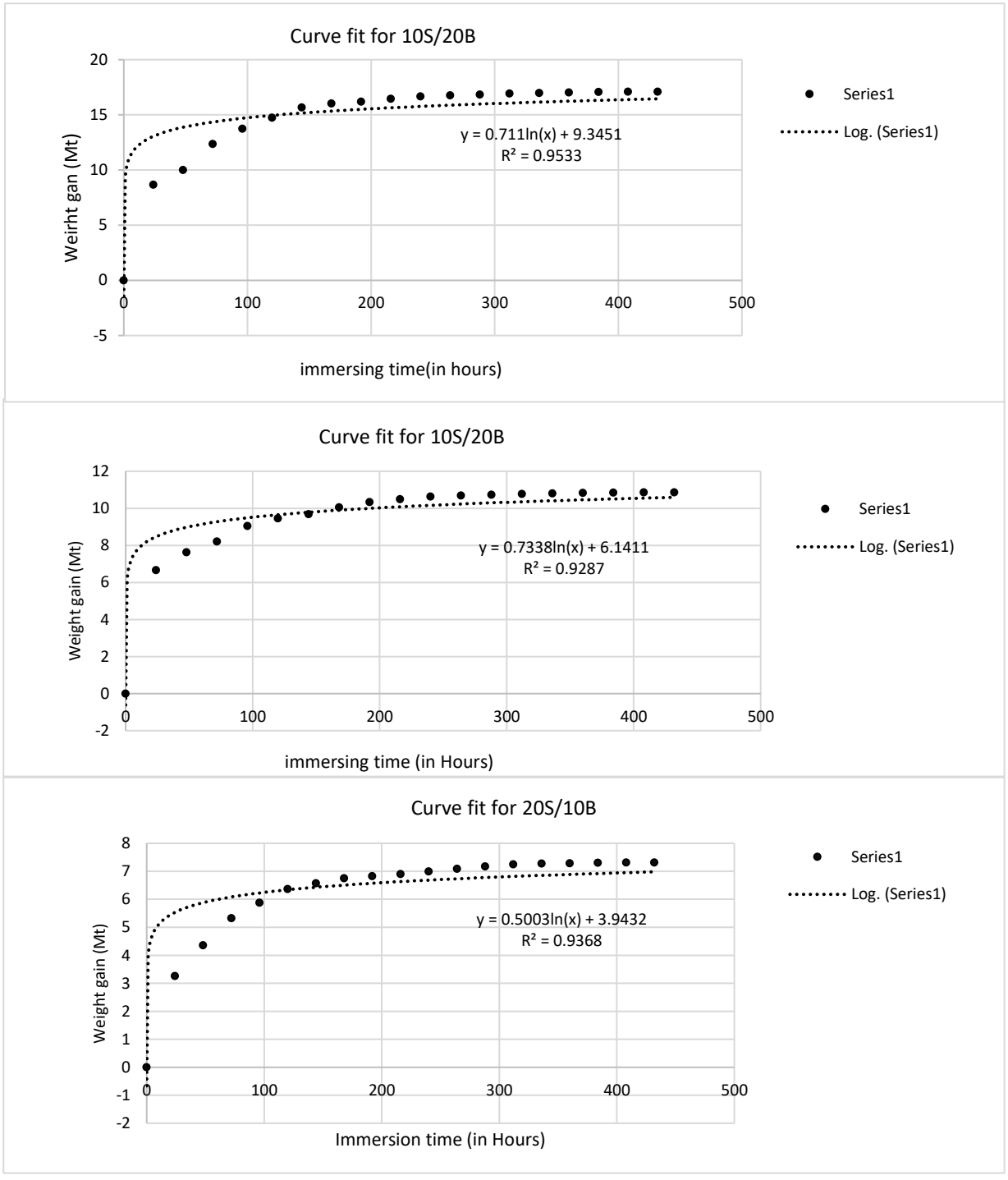

Figure 4- 14. Curve fit for randomly selected data from the three proportions

Table 4- 1. Values of k and n determined from Curve Fit

Fiber loading	Layering sequence	Pressing temperature	water content at Saturated (Ms %)	k	n
10S/20B	UNF	25°C	17.0900	1.14E4	0.711
		60°C	17.4820	1.47E4	0.916
	SBS	25°C	15.0706	5.02E3	0.612
		60°C	15.3200	6.41E3	0.541
	BSB	25°C	19.5800	4.96E4	0.923
		60°C	20.4300	9.10E4	0.931
15S/15B	UNF	25°C	9.6004	204.17	0.650
		60°C	9.9637	244.69	0.674
	SBS	25°C	10.7061	376.86	0.724
		60°C	10.8637	464.56	0.734
	BSB	25°C	11.3278	615.15	0.766
		60°C	11.4756	561.15	0.775
20S/10B	UNF	25°C	7.3060	51.58	0.50
		60°C	7.3928	57.82	0.504
	SBS	25°C	6.3658	29.32	0.484
		60°C	6.8089	40.11	0.466
	BSB	25°C	7.0222	55.89	0.481
		60°C	7.2561	62.44	0.496

For the relation of weight gain (M_t) and the square root of immersion time ($\sqrt{t}$) the Fick's First Law is simplified as follows.

$$\frac{M_t}{M_s} = \frac{4}{\sqrt{\pi}}\sqrt{\frac{tD}{h^2}} \qquad (4\text{-}2)$$

Where, M_t is the moisture content in time t,

M_s is the saturated water content of the sample,

t is immersion time *and* h is the sample thickness

D is the moisture diffusion coefficient,

The diffusion coefficient, D, can be determined from the following equation

$$D = \pi\left[\frac{hk}{4M_s}\right]^2 \qquad (4\text{-}3)$$

Where, h is sample thickness, and k is slope determined from the graph of weight gain versus time.

$$k = \frac{M_2 - M_1}{\sqrt{t_2} - \sqrt{t_1}} \qquad (4\text{-}4)$$

4.7. Thickness Swelling

In addition to mass increment, there was also size increment after immersion in the distilled water for 432 hours. But the size change along width and length specimen was negligible due to the resistance of fiber extension lengthwise which is caused by water absorption. In the thickness direction, there was a significant change as it has been measured with the Vernier caliper. The result has been depicted in table 4-2. The thickness increment can be calculated using equation(4-4) as following with the same fashion as weight increment[39,77].

$$TS(\%) = \frac{T_s - T_o}{T_o} * 100 \qquad (4\text{-}5)$$

where TS is Thickness swelling, T_s is the thickness at saturation, T_o is the initial thickness of the specimen

Table 4- 2. Average Thickness Swelling and diffusion coefficient (D) values for all Samples

Fiber loading	Layering sequence	Pressing temperature	Initial thickness (T_o)	Thickness at saturation (T_s)	water content at Saturated (Ms%)	(slope*thickness)^2 = (kh)^2	Diffusion Coefficient (D in mm^2/s)	$\mathbf{TS}(\%) = \frac{\mathbf{T_s - T_o}}{\mathbf{T_o}} * \mathbf{100}$
10S/20B	UNF	25°C	2.98	3.12	17.09	0.0085	4.02E-04	4.70
		60°C	2.97	3.13	17.48	0.0087	4.07E-04	5.39
	SBS	25°C	2.99	3.13	15.07	0.0083	4.18E-04	4.68
		60°C	2.96	3.11	15.32	0.0090	4.51E-04	5.07
	BSB	25°C	3.02	3.16	19.58	0.0114	5.07E-04	4.64
		60°C	3.03	3.18	20.43	0.0137	5.93E-04	4.95
15S/15B	UNF	25°C	2.96	3.09	9.60	0.0035	2.21E-04	4.40
		60°C	3.00	3.14	9.96	0.0038	2.36E-04	4.67
	SBS	25°C	3.02	3.13	10.71	0.0044	2.65E-04	3.64
		60°C	3.01	3.12	10.86	0.0050	2.98E-04	3.65
	BSB	25°C	2.97	3.08	11.33	0.0051	2.99E-04	3.70
		60°C	2.99	3.08	11.48	0.0053	3.08E04	3.01
20S/10B	UNF	25°C	3.00	3.11	7.31	0.0012	8.6E-05	3.37
		60°C	3.00	3.09	7.39	0.0016	1.13E-04	3.00
	SBS	25°C	3.01	3.08	6.37	0.0010	7.82E-05	2.33
		60°C	3.02	3.11	6.81	0.0010	7.68E-05	2.98
	BSB	25°C	3.03	3.13	7.02	0.0016	1.19E-04	3.30
		60°C	3.02	3.13	7.26	0.0018	1.31E-04	3.64

4.8. Taguchi Method Analysis

Genichi Taguchi used a loss function to determine a difference of experimental values which is again target values into the S/N ratio. S/N ratio is defined as the ratio of mean to standard deviation. Taguchi used the terms signal and noise which represent wanted value (mean) and unwanted value (standard deviation) for the response. Based on the requirements of responses, Taguchi categorizes the S/N ratio into three categories namely Smaller-the Better, Larger-the Better, and Nominal-the Best. For this study, Larger-the Better for mechanical properties (tensile strength, flexural strength, compression strength, and impact strength) is selected to maximize their values. For the water absorption properties Smaller- the Better principle is applied to get a sample with minimum water absorption property. Hence equations have been used to calculate the S/N ratio and the results are depicted in table 4-3. For the Taguchi analysis, Minitab 19.0 tool was used to plot means of mean, means of S/N ratio, and analysis of variance (ANOVA) which are presented in the upcoming discussions.

S/N ratio for the Larger-the Better: $[S/N]_L = -10\log_{10}\frac{\sum\frac{1}{\mu^2}}{n}$, (4-6)

S/N ratio for the Smaller-the Better: $[S/N]_S = -10\log_{10}\frac{\sum\mu^2}{n}$, (4-7)

Where, μ is the signal mean, and n is the number of trials/ sample size.

4.9. Effect of manufacturing process parameters on mechanical characteristics

Effect of manufacturing process parameters on Tensile and flexural strength

As the figure 4-15. (a), (b), (c), and (d) depicted, the effects of the three parameters on the tensile and flexural strength is changed as their value and types of incorporation change. The value of tensile and flexural strength is increased with the increment of sisal fiber from 10%wt to 20%wt and slightly decreases with the increment of curing temperature of 25°C to 60°C. Tensile and flexural strengths are highest for the SBS layering sequence due to the good tensile property enhanced by the sisal fiber strand is placed at the outer layer of the composite which is better resistant of the crack propagation than SCB fiber during breakage.

Table 4- 3. Experimental plan, experimental results, and their calculated S/N ratio

Exp. Runs	Controllable Process Parameters			Experimental Results					S/N Ratio of Results				
	CT	FL	LS	TS (MPa)	FS (MPa)	CS (MPa)	IS (kJ/m^2)	WA (Mt%)	TS (dB)	FS (dB)	CS (dB)	IS (dB)	WA (dB)
1	25	10S/20B	UNF	26.874	72.94	16.78	29.46	17.09	28.5866	37.2593	24.4958	**29.3847**	-24.655
2	25	10S/20B	SBS	27.982	78.94	17.82	28.09	15.07	28.9376	37.9459	25.0182	28.971	-23.562
3	25	10S/20B	BSB	25.223	62.84	19.542	28.49	19.58	28.0359	35.9647	25.8194	29.0938	-25.836
4	25	15S/15B	UNF	29.667	84.63	17.888	27.22	9.6	29.4455	38.5505	25.0512	28.6978	-19.645
5	25	15S/15B	SBS	30.444	86.76	19.35	25.21	10.71	29.67	38.7664	25.7338	28.0315	-20.596
6	25	15S/15B	BSB	27.129	68.73	22.559	25.54	11.33	28.6687	36.7429	**27.0664**	28.1444	-21.085
7	25	20S/10B	UNF	34.963	96.83	17.212	25.22	7.31	30.8722	39.7202	24.7166	28.0349	-17.278
8	25	20S/10B	SBS	37.889	102.55	18.779	20.29	6.37	**31.5703**	**40.2187**	25.4734	26.1456	**-16.083**
9	25	20S/10B	BSB	33.778	80.94	21.619	22.84	7.02	30.5727	38.1633	26.6967	27.1739	-16.927
10	60	10S/20B	UNF	25.976	69.84	15.998	28.01	17.48	28.2914	36.8821	24.0813	28.9463	-24.851
11	60	10S/20B	SBS	27.463	76.46	18.54	27.44	15.32	28.775	37.6687	25.3622	28.7677	-23.705
12	60	10S/20B	BSB	24.814	60.83	18.558	27.98	20.34	27.8939	35.6824	25.3706	28.937	-26.168
13	60	15S/15B	UNF	28.481	76.45	16.53	26.88	9.96	29.0911	37.6675	24.3655	28.5886	-19.965
14	60	15S/15B	SBS	29.939	79.93	18.561	24.96	10.86	29.5247	38.0542	25.372	27.9449	-20.717
15	60	15S/15B	BSB	26.542	69.42	21.651	24.27	11.48	28.4787	36.8297	26.7096	27.7014	-21.199
16	60	20S/10B	UNF	34.574	92.46	16.931	23.87	7.39	30.775	39.3191	24.5737	27.557	-17.373
17	60	20S/10B	SBS	37.018	94.35	17.351	19.54	6.81	31.3683	39.4948	24.7865	25.8185	-16.663
18	60	20S/10B	BSB	32.889	75.86	21.021	22.56	7.26	30.341	37.6003	26.4531	27.0668	-17.219

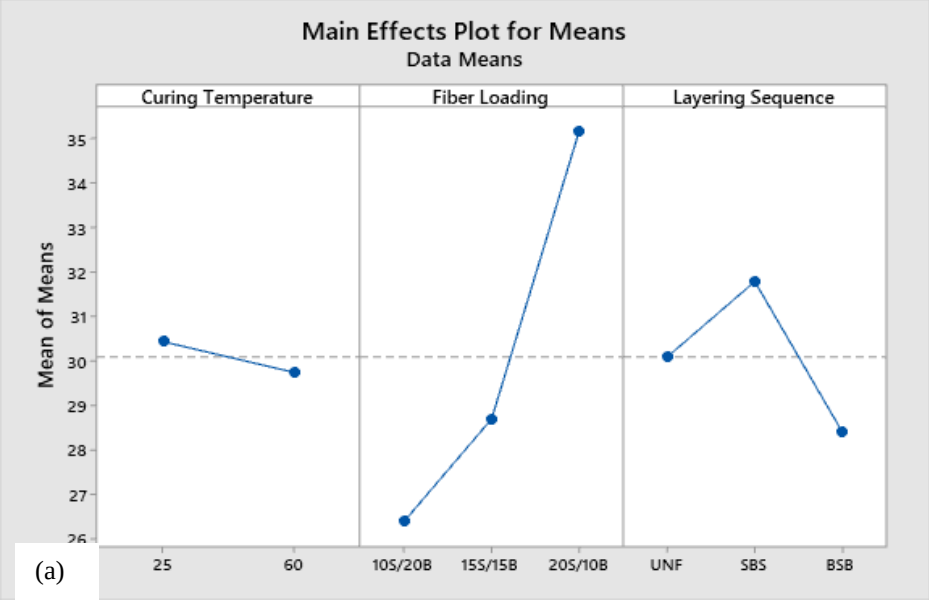

(a)

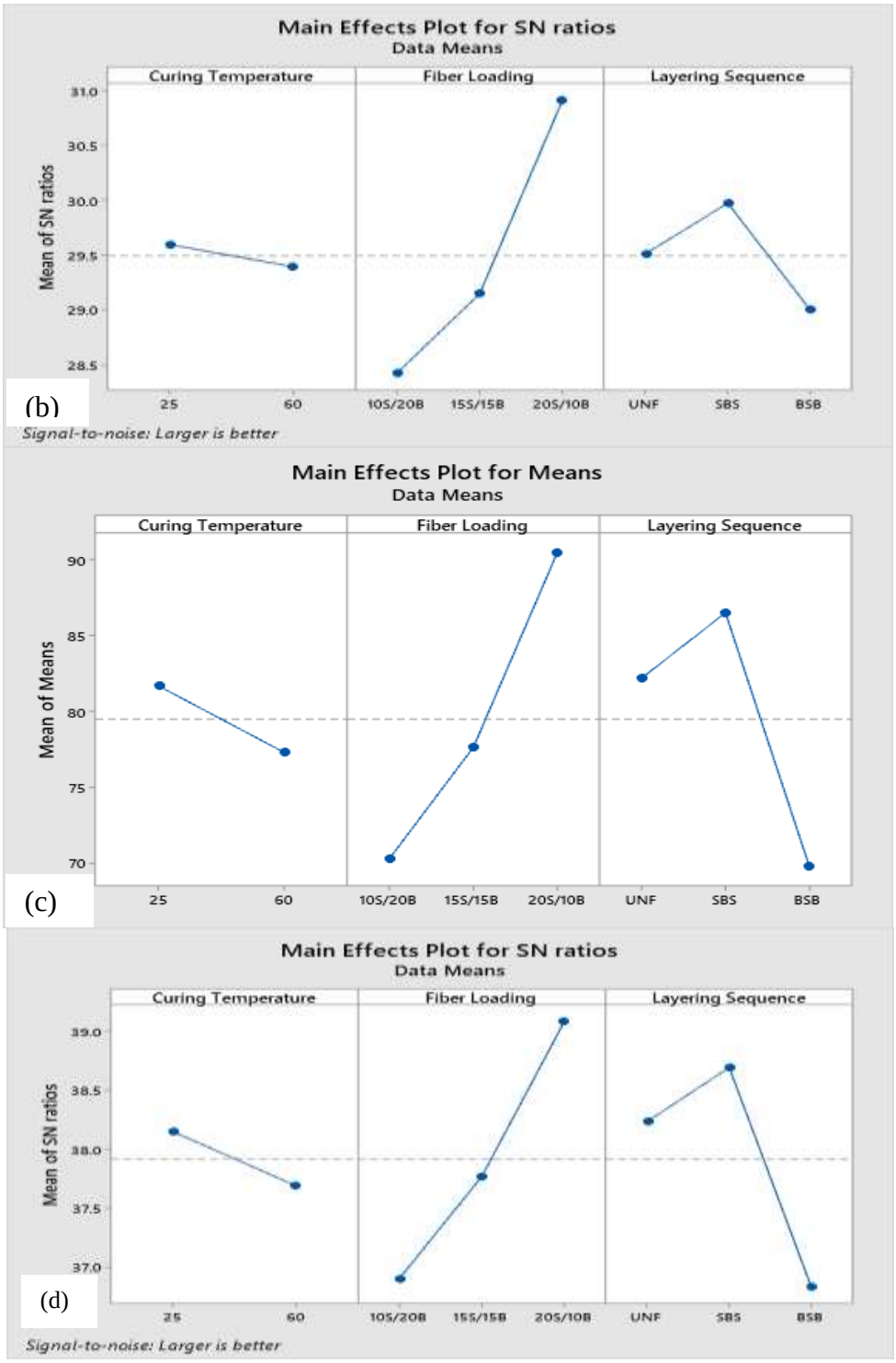

Figure 4- 15. Effect of manufacturing process parameters (a) Mean of Means (b) S/N ratio for Tensile strength and (c) Mean of means (d) S/N ratio for Flexural strength

Effect of Manufacturing process parameters on Compression Strength

The influence of these parameters on compression strength is displayed in Figure 4-16 below. The compression strength is highly influenced by the layering sequence which is depicted in fig 4-16 (b) which is the mean of means. This is because laying up the SCB fiber in the outside of the composite gives more compressive strength than sisal fiber as SCB fiber is chopped. The fiber loading moderately affects compression strength and composite which is built from equal weight of the two fibers has the highest compressive strength. The curing temperature has the least influence of the three parameters.

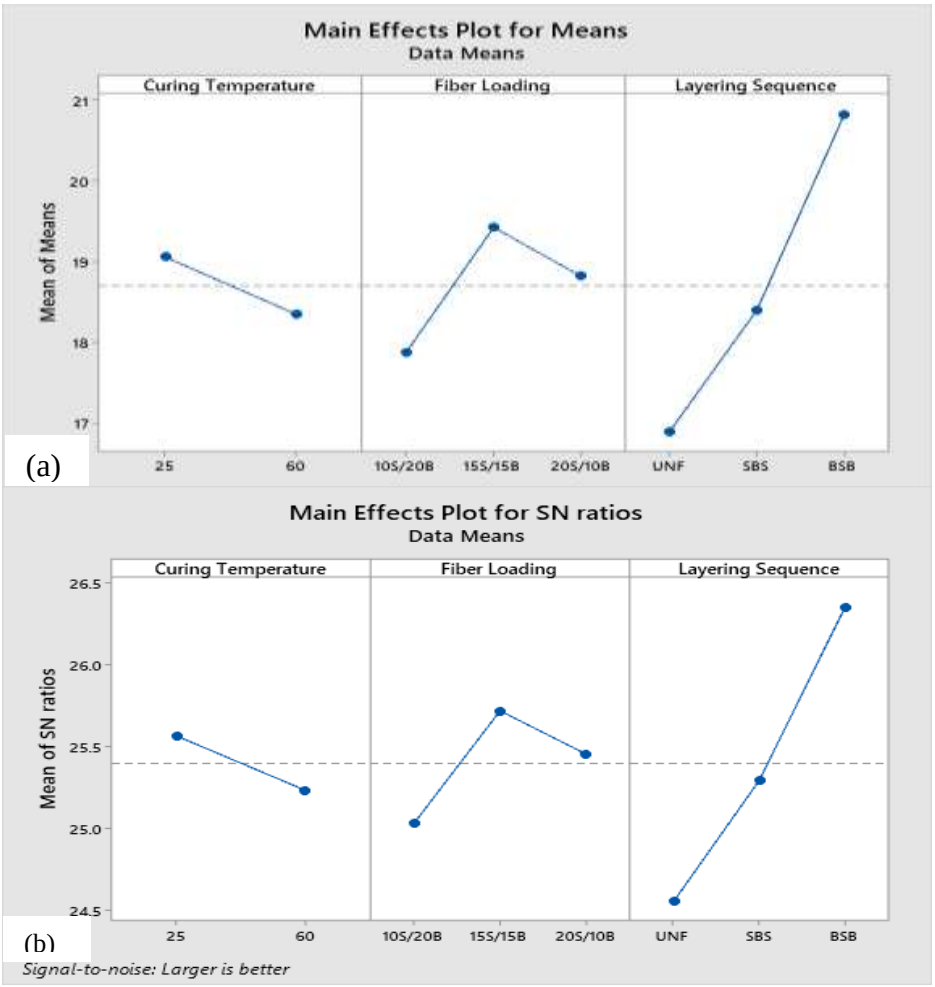

Figure 4- 16. Effect of manufacturing process parameters for compression strength (a) mean of means and (b) mean S/N ratio

Effect of Manufacturing process parameters on Impact Strength

Figure 4-19 depicted that impact strength highly influenced by the fiber loading and proportion with high SCB fiber enhanced the highest energy-absorbing ability. The spongy property of SCB fiber gives a better energy-absorbing ability than the rigid sisal fiber. Uniform mixing of the two fibers is the case to have the highest impact strength as shown in figure 4-17 below. But as the other responses impact strength is slightly affected by the curing temperature with the cold pressing enhances better impact absorption property[33, 36, 47].

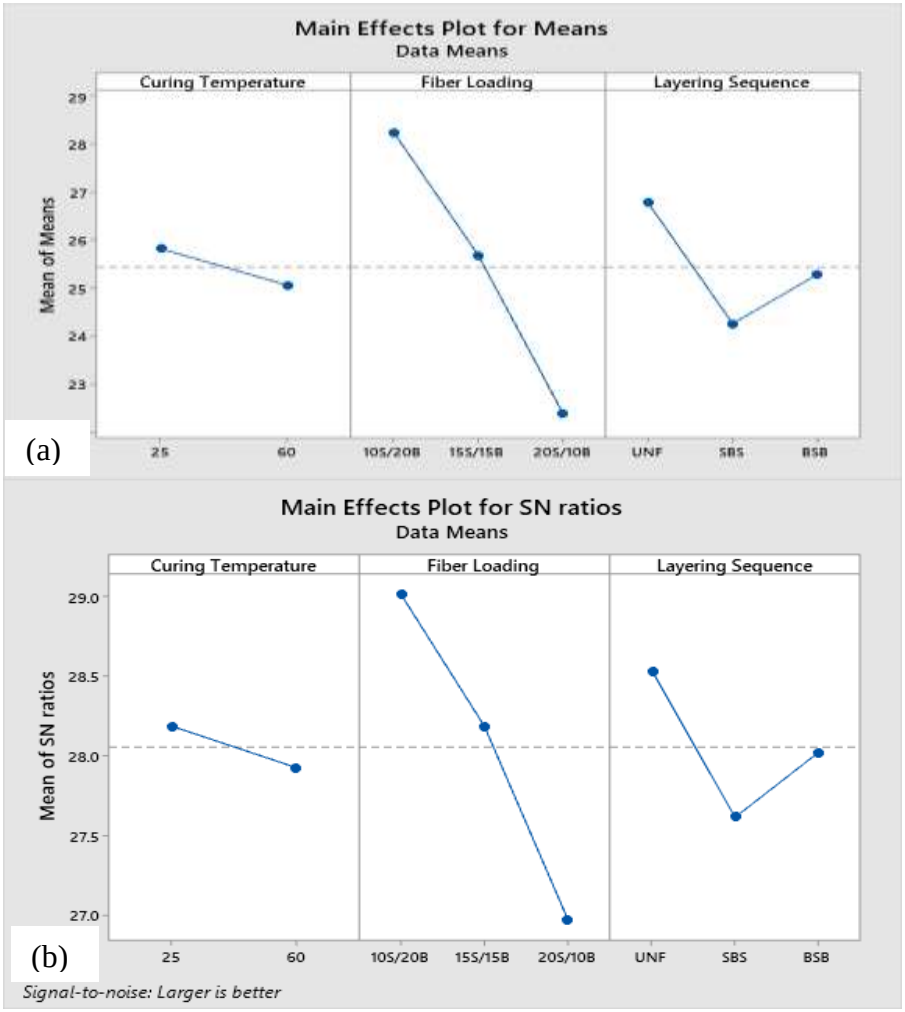

Figure 4- 17. Effect of manufacturing process parameters for Impact Strength(a) mean of means (b) mean of S/N ratio

Effect of Manufacturing process parameters on Water Absorption property

In the water absorption case, the S/N ratio calculation based on the Smaller-the Better principle because the lower value of water uptake is better to be for composite materials. From figure 4-18 below, the lower magnitude of water uptake is recorded at the 25°C curing temperature, 20S/10B fiber proportion, and SBS layering sequence. Like other responses, the water absorption property is highly affected by the fiber loading. When the proportion of sisal fiber increases, the water absorption decreases averagely from 17.48% to 7.027% which is about 10%. The SBS layering also minimizes the water uptake property of the composite. But the curing temperature has no significant influence as shown in Figure 4-18.

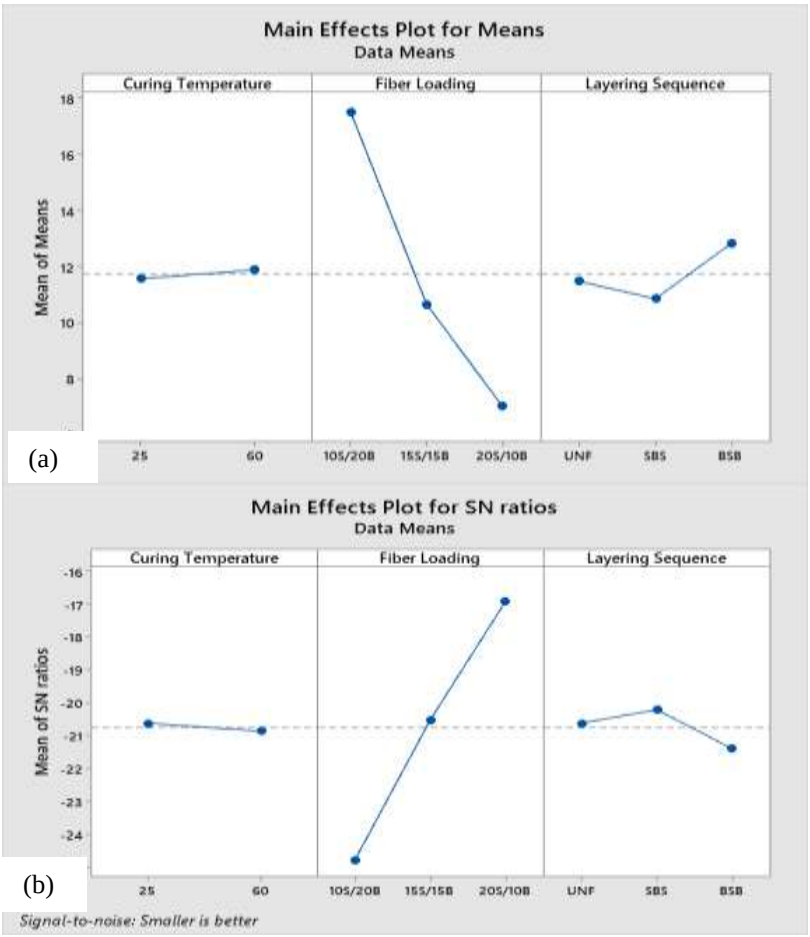

Figure 4- 18. Effect of manufacturing process parameters for water absorption test (a) mean of means (b) mean of S/N ratio

4.10. Selection of Optimum Manufacturing Conditions for all Responses Parameters

As shown in Table 4-4 below the optimum S/N ratio values of all response parameters are written in bold font for better visualizing. The optimum manufacturing process parameters are the highest S/N ratio values which represent the minimum variation difference between the desired output and measured output. For the tensile strength**,** the optimum value is obtained at 25°C curing temperature (CT), 20S/10B fiber loading (FL), and SBS layering sequence (LS). It can be represented as $CT_1 - FL_3 - LS_2$ respectively and also for the flexural strength, the optimum value is represented as $CT_1 - FL_3 - LS_2$. For the compression strength, the optimum value is in the $CT_1 - FL_2 - LS_3$ combinations but for the Impact strength the optimum value is obtained at $CT_1 - FL_1 - LS_1$. For the water absorption, the S/N ratio is calculated based on the Smaller-the Better formula and the optimum values are obtained at the lowest magnitude of S/N ratio values. Here the subscript numbers represent the levels of parameters. Therefore, it can be represented as $CT_1 - FL_3 - LS_2$.

Table 4- 4. Response table for all parameters which are corresponding with their respective graphs

Response Parameters	Signal Parameters	Symbols	Mean S/N ratio(dB)			Max-Min	Rank
			Level 1	Level 2	Level 3		
Tensile Strength	Curing Temp(°C)	CT	**29.60**	29.39		0.21	3
	Fiber Loading	FL	28.42	29.15	**30.92**	2.5	1
	Layering Sequence	LS	29.51	**29.97**	29	0.98	2
Flexural Strength	Curing Temp(°C)	CT	**38.15**	37.69		0.46	3
	Fiber Loading	FL	36.9	37.77	**39.09**	2.19	1
	Layering Sequence	LS	38.23	**38.69**	36.83	1.86	2
Compression Strength	Curing Temp(°C)	CT	**25.56**	25.23		0.33	3
	Fiber Loading	FL	25.02	**25.72**	25.45	0.69	2
	Layering Sequence	LS	24.55	25.29	**26.35**	1.81	1
Impact Strength	Curing Temp(°C)	CT	**28.19**	27.93		0.26	3
	Fiber Loading	FL	**29.02**	28.18	26.97	2.05	1
	Layering Sequence	LS	**28.53**	27.61	28.02	0.92	2
Water Absorption	Curing Temp(°C)	CT	**-20.63**	-20.87		0.24	3
	Fiber Loading	FL	-24.8	-20.53	**-16.92**	7.87	1
	Layering Sequence	LS	-20.63	**-20.22**	-21.41	1.18	2

4.11. Analysis of variance (ANOVA) for all the response parameters

ANOVA gives the manufacturing process parameter that mostly affects the performance characteristics

Table 4- 5. ANOVA for Tensile Strength

Source	Degree of freedom	Sum of Squares	Mean Squares	Contribution (%)
CT	1	0.1841	0.18409	0.80
FL	2	19.7866	9.89332	86.27
LS	2	2.8590	1.42948	12.47
Residual error	12	0.1062	0.00885	0.46
Total	17	22.9359		100.00

Table 4- 6. ANOVA for Flexural Strength

Source	Degree of freedom	Sum of Squares	Mean Squares	Contribution (%)
CT	1	0.9491	0.94909	3.48
FL	2	14.5318	7.26590	53.23
LS	2	11.2807	5.64035	41.32
Residual error	12	0.5398	0.04498	1.98
Total	17	27.3014		100.00

Table 4- 7. ANOVA for Compression Strength

Source	Degree of freedom	Sum of Squares	Mean Squares	Contribution (%)
CT	1	0.4991	0.49905	3.84
FL	2	1.4611	0.73057	11.24
LS	2	9.8781	4.93904	76.00
Residual error	12	1.1600	0.09666	8.92
Total	17	12.9982		100.00

Table 4- 8. ANOVA for Impact Strength

Source	Degree of freedom	Sum of Squares	Mean Squares	Contribution (%)
CT	1	0.3067	0.3067	1.78
FL	2	12.7645	6.3822	73.96
LS	2	2.5603	1.2801	14.83
Residual error	12	1.6274	0.1356	9.43
Total	17	17.2588		100.00

Table 4- 9. ANOVA for Water absorption property

Source	Degree of freedom	Sum of Squares	Mean Squares	Contribution (%)
CT	1	0.267	0.2670	0.14
FL	2	186.355	93.1773	95.50
LS	2	4.348	2.1738	2.23
Residual error	12	4.171	0.3476	2.14
Total	17	195.140		100.00

4.12. Modeling of Governing Equations

In this study, linear regression analysis in Minitab 19.0 software tool has been used to develop the predictive mathematical models for the dependent variables of Tensile, Flexural, Compression, Impact strength, and water absorption properties as a function of Curing Temperature, Fiber Loading, and Layering sequence of fibers respectively. The predictive equations obtained from the regression analysis are shown in the Equations (4-8 to 4-12) respectively for Tensile, Flexural, Compression, and Impact strength and water absorption property.

Tensile Strength (MPa) = 24.03 - 0.695*CT + 4.398*FL- 0.847*LS, [R^2= 84.19%] (4-8)

Flexural Strength (MPa) = 78.31 - 4.40*CT+10.09*FL- 6.21*LS, [R^2= 76.62%] (4-9)

Compression Strength (MPa) = 14.89-0.712*CT+0.473*FL+1.968*LS, [R^2=81.62%] (4-10)

Impact Strength(kJ/m^2) = 33.93 - 0.761*CT-2.929*FL-0.748*LS, [R^2= 82.96%] (4-11)

Water Absorption (Mt%) = 20.34 + 0.314*CT- 5.227*FL+ 0.682*LS, [R^2= 91.52%] (4-12)

The capability of developed models was checked by using a coefficient of determination R^2 [82]. The coefficient of determination value varies from zero to one. If it is close to one it means that there is a good fit between the dependent and independent variables. If the value of R^2 is about 95% which means that new observations can be estimated with 95% variability. In this study, the developed regression models for Tensile, Flexural, Compression and Impact strength and Water absorption R^2 values are 84.19%, 76.62%, 81.62%, 82.96%, and 91.52% respectively. The residual plot was used to check the significance of the coefficients in the predicted model. If the residual plot is a straight line means that the residual errors in the model are normally distributed and coefficients in the model are significant. The residual plots obtained for Tensile, Flexural, Compression and Impact strength and Water absorption are shown in Figure 4-19 (a, b, c, d, e) respectively. As one can see from these figures, the residuals fall near the straight line for all response parameters which implies that the developed model coefficient models are significant.

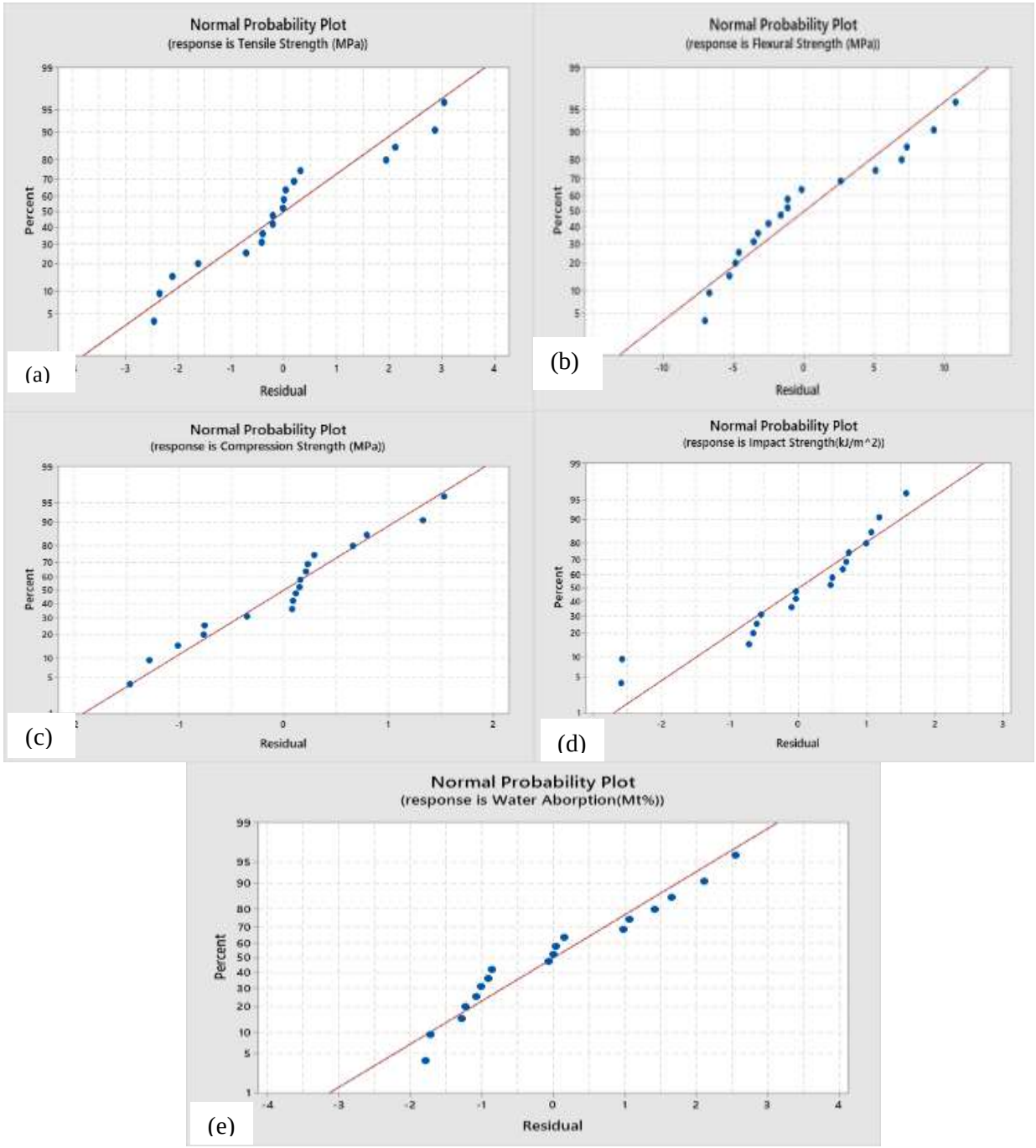

Figure 4- 19. Normal probability plot for (a) Tensile Strength (b) Flexural Strength (c) Compression Strength(d) Impact Strength (e) Water Absorption Test

4.13. Contour Plot

Contour plots examine the relation between the response variable and two control variables by viewing discrete contours of the predicted response variables. Figure 4-20 shows the contour plots explaining the relation between the manufacturing process parameters and Tensile and Flexural Strength. From Figure 4-20 (a), it was found to be a higher proportion of sisal fiber and a low level of curing temperature leads to maintain a higher value of tensile strength. But the high level of curing temperature and relatively lower proportion of sisal is responsible give the lower value of Tensile strength. Figure 4-20 (b) shows that Tensile strength is slightly affected by layering sequence and curing temperature in such a way SBS layering and lower curing temperature is better than the other combination. In Figure 4-20 (c), it was observed that the uniform mixing of the two fibers with 10B/20S produces a higher value of tensile strength. Similarly, Figure 4-20 (d-f) show that lower curing temperature, higher sisal fiber proportion than SCB fiber, and uniform mixing of the two fibers gives a higher Flexural Strength than other combinations. Contour plots explaining the relation between the Manufacturing process parameters and Compression and Impact Strength are shown in Figure 4-21. From Figure 4-21 (a-c), it was noticed that better compression strength was obtained at a low level of curing temperature, an equal proportion of the two fibers, and the SBS layering sequence. As figure 4-21 (d-f) depicted fact, the Impact strength is higher at the low curing temperature, a relatively higher proportion of SCB fiber than sisal fiber and BSB layering. Figure 4-22 (a-c) shows that curing temperature has no significant effect on water absorption properties. But increasing the proportion of sisal fiber to 20% and laying it up on the outer layer (SBS) of the composite can lower the water uptake property.

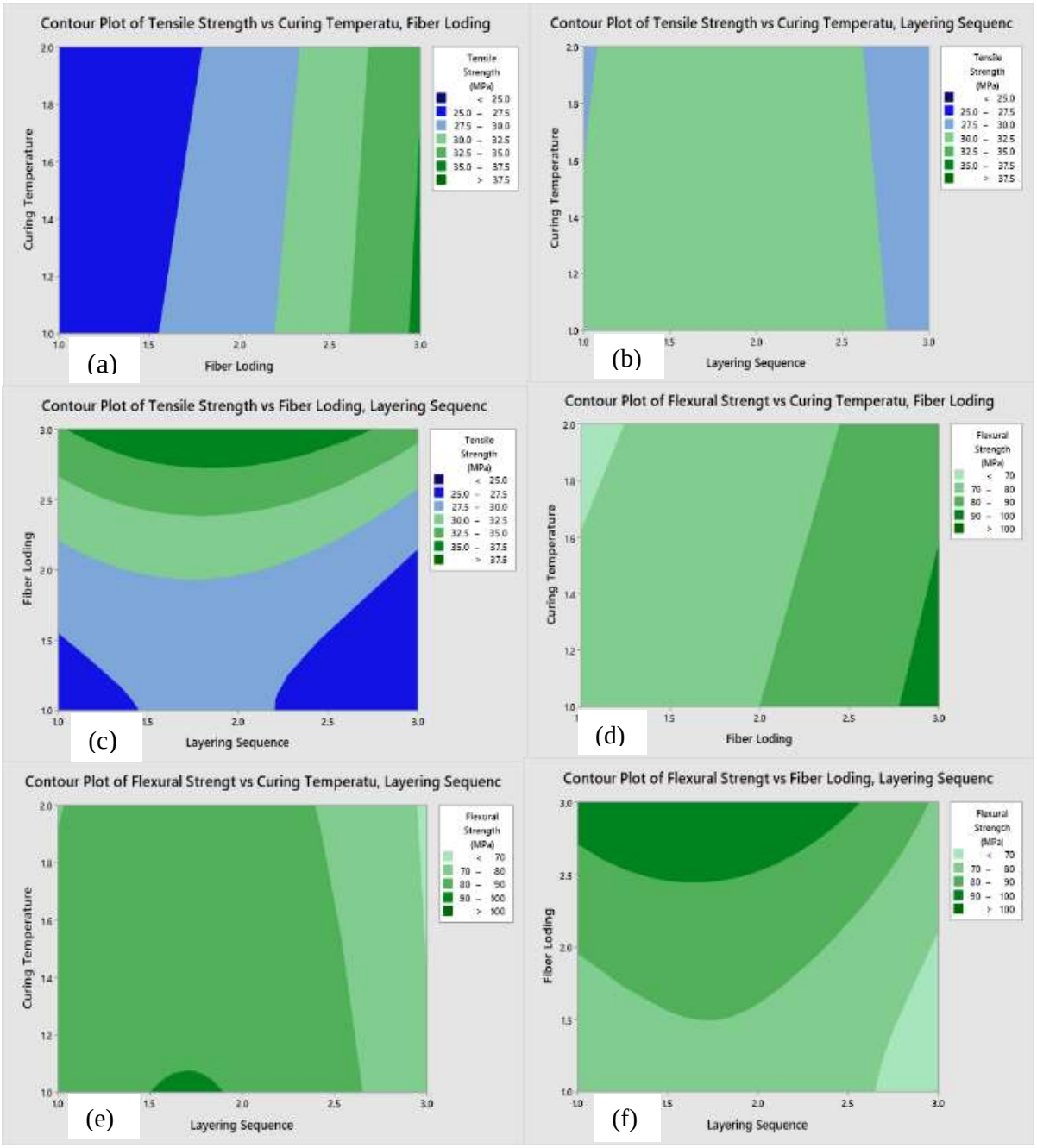

Figure 4- 20. Contour Plot for Tensile Strength vs (a) curing temp and fiber loading, (b) curing temp and layering sequence, (c) fiber loading and layering sequence: and Flexural strength vs (d) curing temp and fiber loading (e) curing temp and layering sequence (f) fiber loading and layering sequence

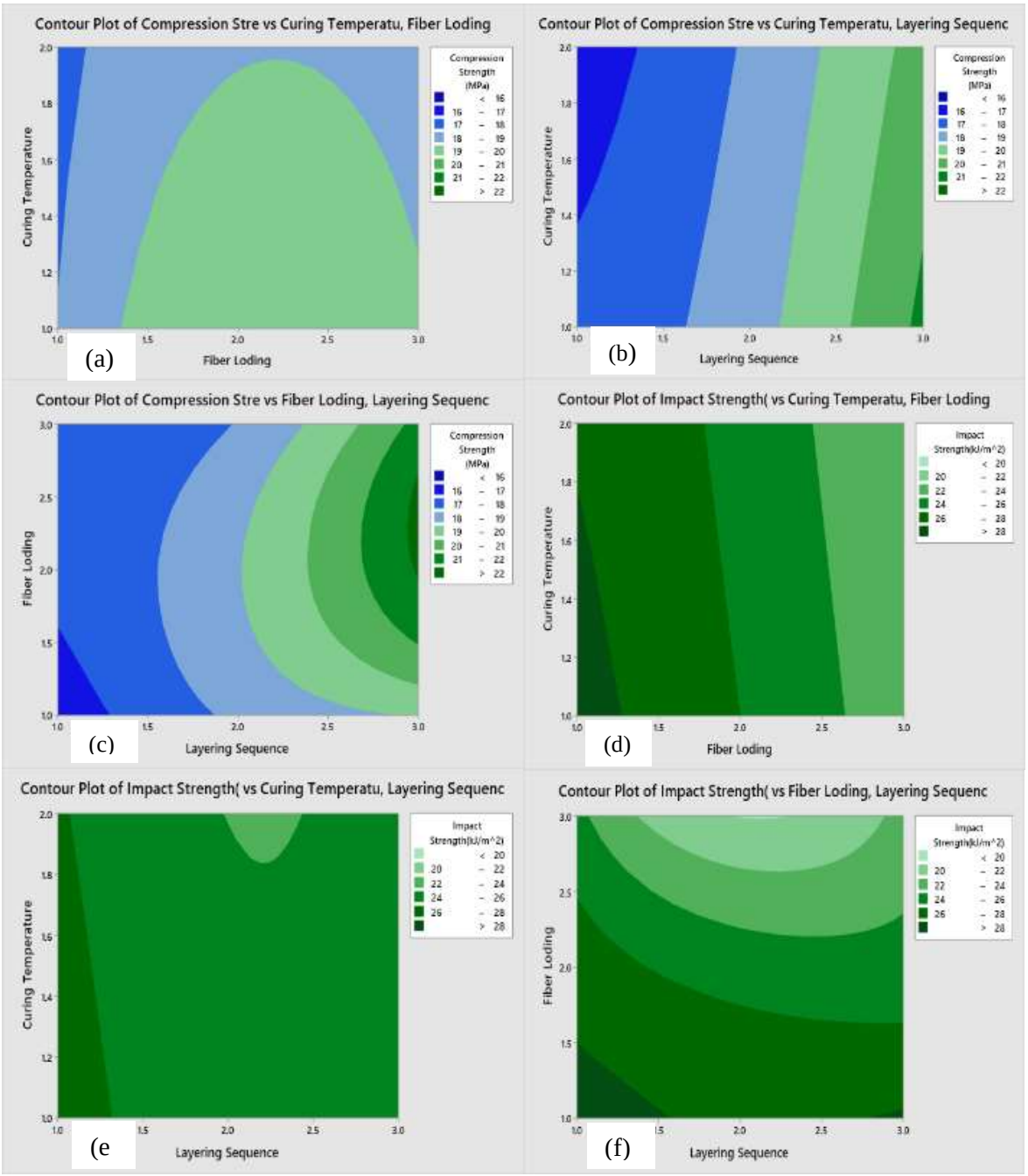

Figure 4- 21. Contour Plot for compression Strength vs (a) curing temp and fiber loading, (b) curing temp and layering sequence, (c) fiber loading and layering sequence: and Impact Strength vs (d) curing temp and fiber loading (e) curing temp and layering sequence (f) fiber loading and layering sequence

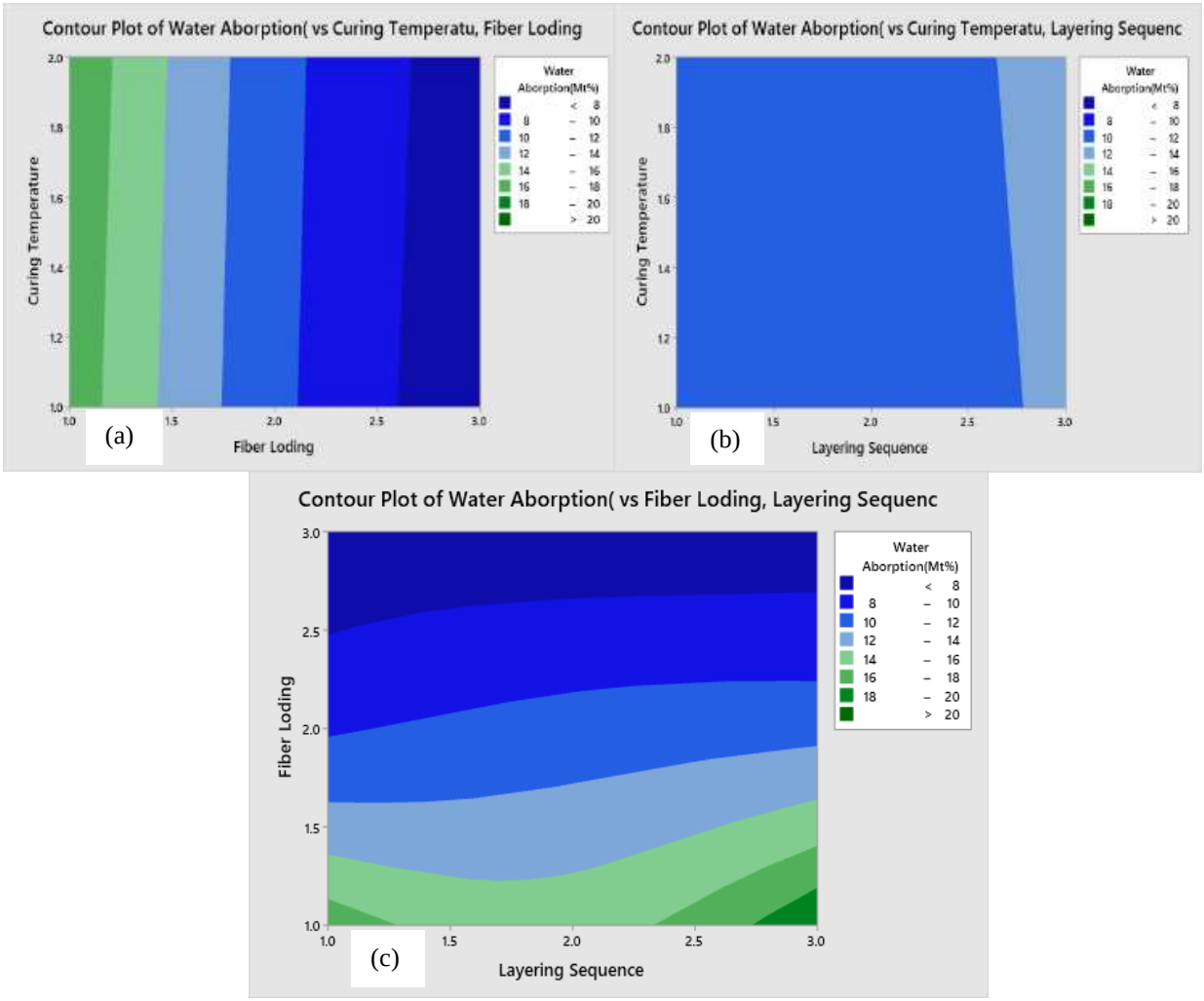

Figure 4- 22. Contour Plot for Water Uptake vs (a) curing temp and fiber loading, (b) curing temp and layering sequence, (c) fiber loading and layering sequence

4.14. Comparison with the Previous works

There are plenty of researches on sisal fiber reinforced composites and a few on the sugarcane bagasse fiber composites. But there are very few researches done on the hybrid composites of these two natural fibers. In order to compare the results of this research with previously worked researches some different papers are used in the following table 4-10 for different properties.

Table 4- 10. Comparison of test results with previous work

Hybrid Comp(Sisal/SCB + Resin)	Tensile strength (MPa)	Flexural strength (MPa)	Compress strength (MPa)	Impact strength (J/m^2)	Water up take (Ms %)	Reference
Sisal/SCB + epoxy	12.76-35.56	12.92-39.6	---	12.3-21.3	28.54-44.16	Prashant Dwivedi and Saurabh Kumar Shukla (2019) [48]
Sisal/SCB+ phenolic	---	---	---	14.9-21.5	2.7-12.1	SPS Tita et al. (2018) [83]
Sisal/SCB + epoxy	7.82-27.36	---	13.33-16.63	4.13-6.34	5.7-6.8 WA 1.6 -1.7 TS	Jafrey Daniel James D et al. (2019) [45]
Sisal/SCB +epoxy	16.6-44.4	---	---	---	2.5-11	Prashant Tripathi et al. (2019) [46]
Sisal/SCB+ polyester	24.81-37.89	60.83-102.55	16.0-22.56	19.56-22.46	6.37-20.34 WA 2.98-5.39 TS	Current Work

In the above table 10. the mechanical strength as well as water absorbing values are given as the range. Because these researches are conducted by changing different parameters (fiber proportion, fiber orientation, chemical treatment, and matrix) that affect the mechanical properties of the composite. As these parameters changed mechanical properties of the composites altered from minimum to maximum values as shown in the table above. The difference of mechanical properties between the current work and previous researches is because of the different matrix used, fiber proportion, and fiber incorporation methods. Up to the submission of this paper, there was not found exactly the same research with current work. But for the general validation, these researches are listed with slight difference in the mechanical properties and also in the water absorption properties. There is no value that goes out of the range of previous researches.

4.15. Ansys Simulation Results of door panel

The Ansys analysis results showed that the maximum and minimum values of equivalent stress total deformation, and strain energy. These values characterize the material property that helps to understand the suitability of these materials for the application area. The total deformation for each material is shown in the figure (4-23) below.

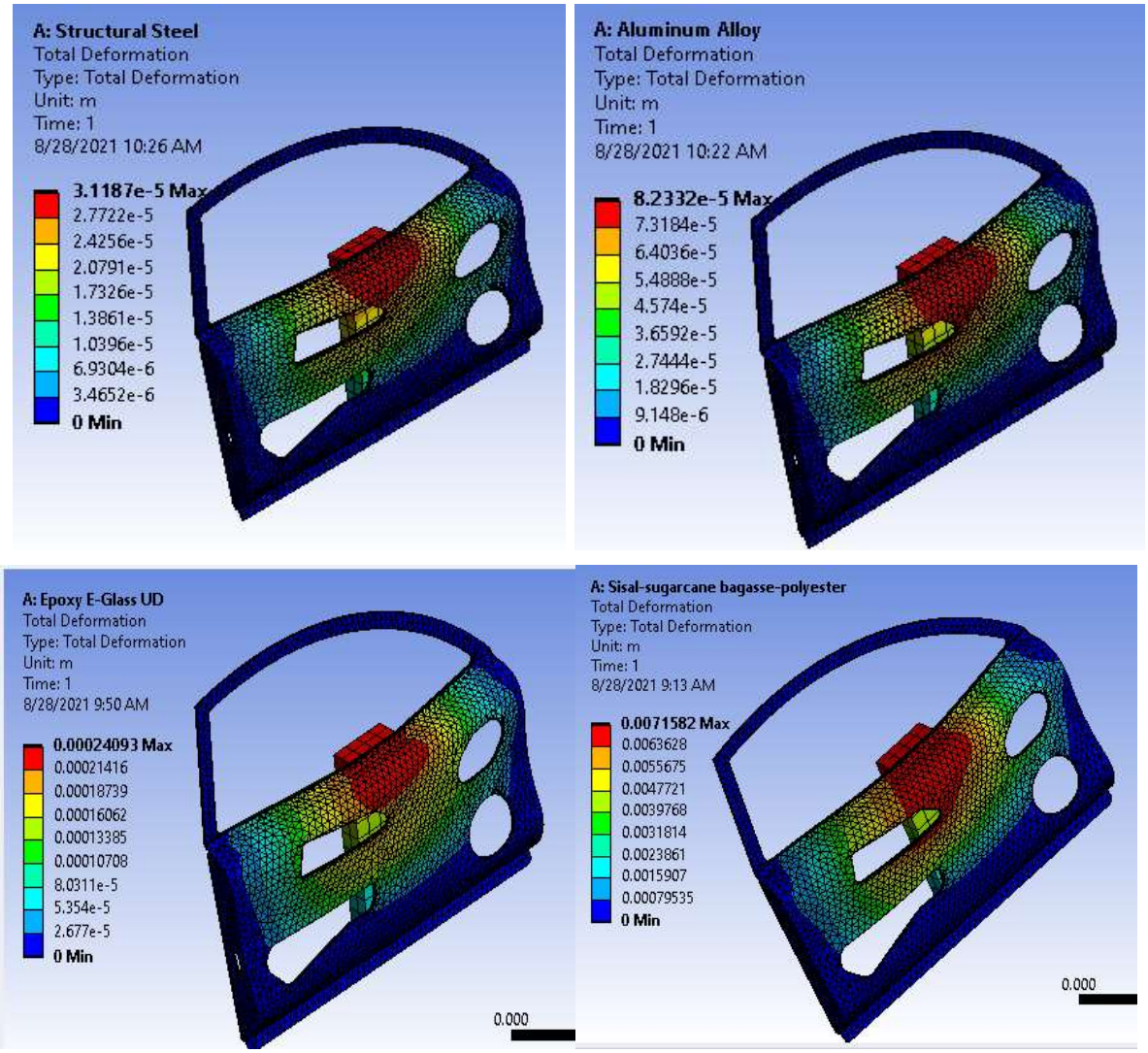

Figure 4- 23. Total deformation for all candidate materials

The equivalent stress of these three selected conventional materials for car door manufacturing and newly developed sisal and sugarcane bagasse hybrid fiber polyester composite is depicted in the following Figure (4-24).

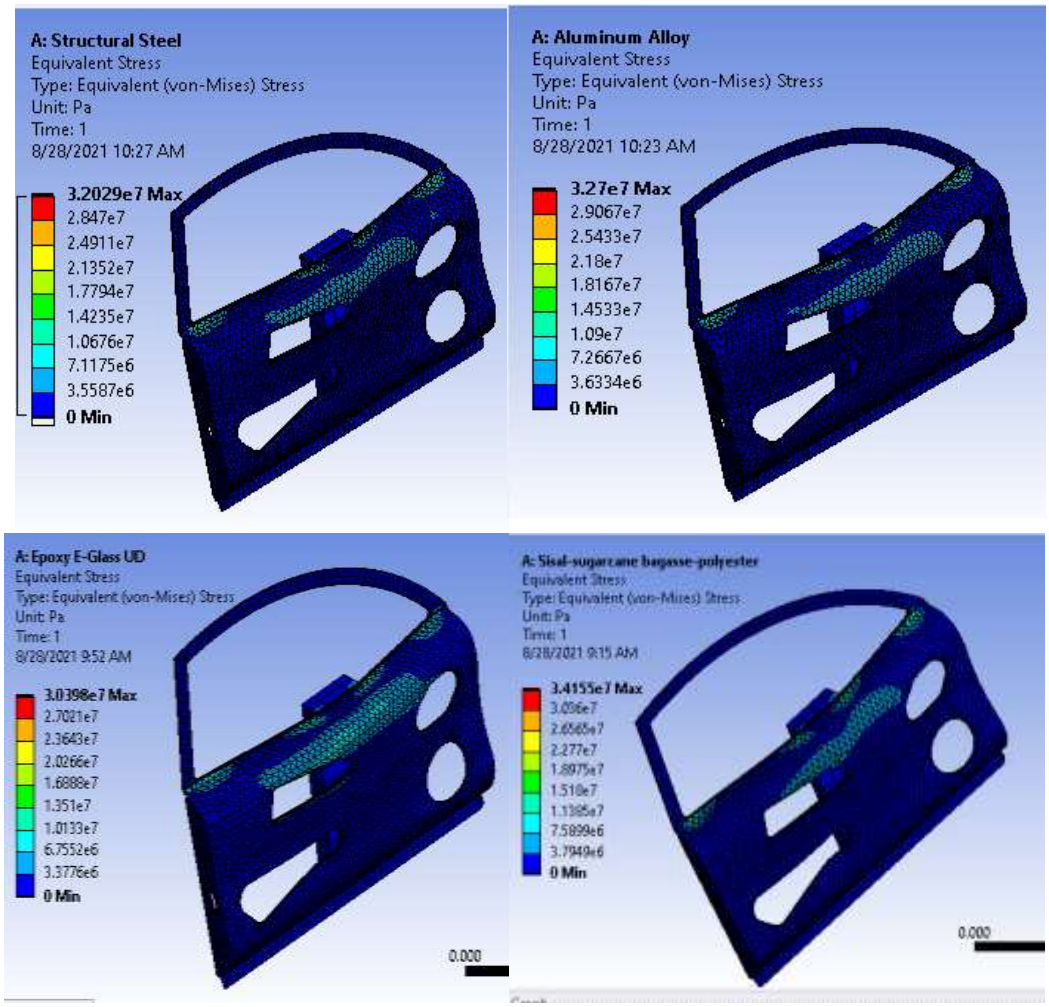

Figure 4- 24. Equivalent stress for all candidate materials

Strain Energy is a type of potential energy that is stored in the door panel as a result of elastic deformation. It can be calculated by the equation (4-13) below.

$$Strain\ Energy(U) = \frac{\sigma^2 V}{2E} \qquad (4\text{-}13)$$

Where: σ-stress, V- volume of deformed body, E- Young's Modulus

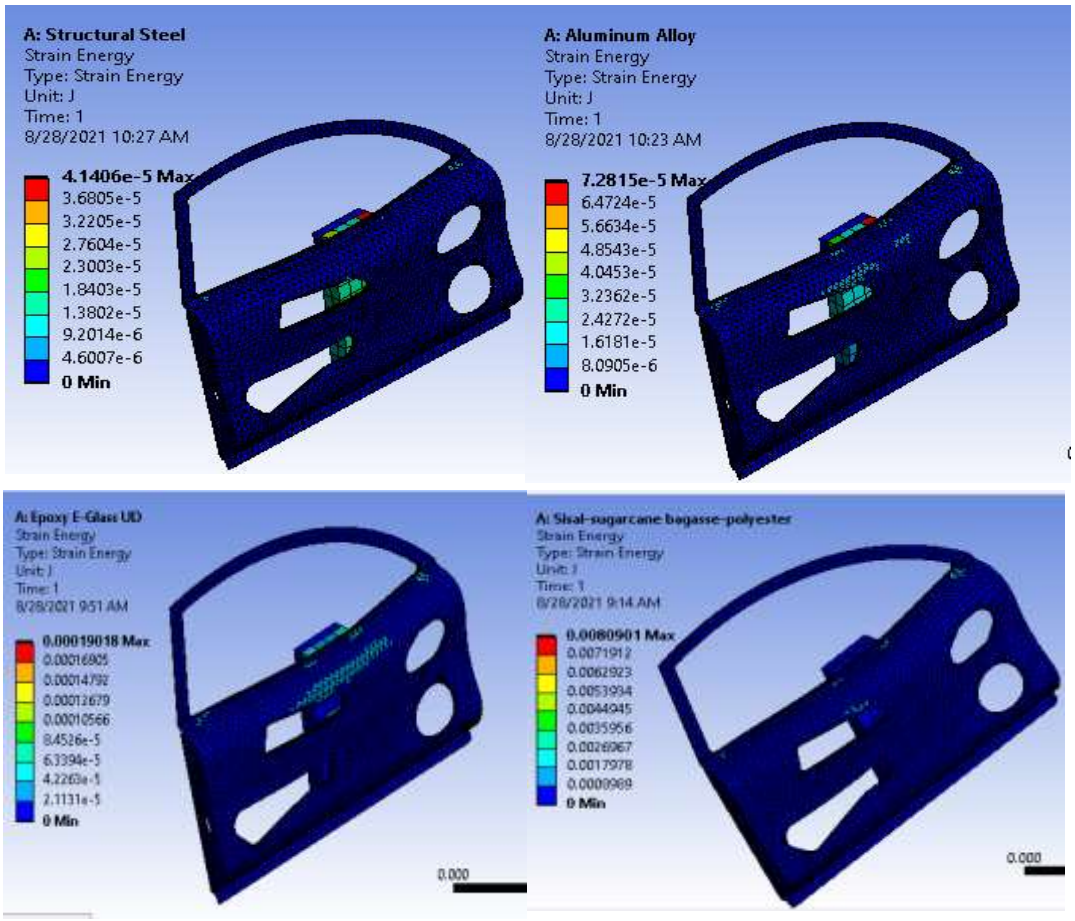

Figure 4- 25. Strain Energy for all candidate materials

The safety factor for each material

$$\text{Factor of Safety for Structural Steel (FoS)} = \frac{\text{Yield Point Stress}}{\text{Working Stress}} = \frac{2.5\text{E}8}{3.203\text{E}7} = 7.80$$

$$\text{Factor of Safety for Aluminum Alloy (FoS)} = \frac{\text{Yield Point Stress}}{\text{Working Stress}} = \frac{2.8\text{E}8}{3.27\text{E}7} = 8.56$$

$$\text{Factor of Safety for Epoxy E} - \text{Glass (FoS)} = \frac{\text{Ultimate stress}}{\text{Working Stress}} = \frac{3.5\text{E}7}{3.0398\text{E}7} = 1.15$$

$$\text{Factor of Safety for Sisal Bagasse polyester (FoS)} = \frac{\text{Ultimate stress}}{\text{Working Stress}} = \frac{3.79\text{E}7}{3.4155\text{E}7} = 1.11$$

The mass is calculated by the Ansys software from the model geometry and recorded as follow in the table 4-11.

The mass of sisal-bagasse hybrid fiber polyester composite is the minimum of the candidate materials.

Table 4- 11. Result Summary Table for Ansys Simulation

Candidate Materials	Maximum Total Deformation(m)	Maximum Equiva Stress (MPa)	Maximum Strain Energy(J)	Safety Factor	Mass (kg)
Structural Steel	3.12E-5	3.2E+7	4.14E-5	7.80	7.447
Aluminum alloy	8.23E-5	3.27E+7	7.28E-5	8.56	2.628
Epoxy E-Glass UD	2.41E-4	3.04E+7	1.90E-4	1.15	1.897
Sisal-SCB polyester	7.15E-3	3.42E+7	8.08E-3	1.11	0.798
Sisal-SCB polyester(3mm)	**4.14E-3**	**2.1E+7**	**7.75E-3**	**1.81**	**1.604**

From the summary table 4-11, it is noticeable the sisal-sugarcane bagasse hybrid fiber polyester composite has a minimum mass (0.798kg) with a 1.11 factor of safety. These results are recorded from the Ansys simulation with a door thickness of 1.5mm.

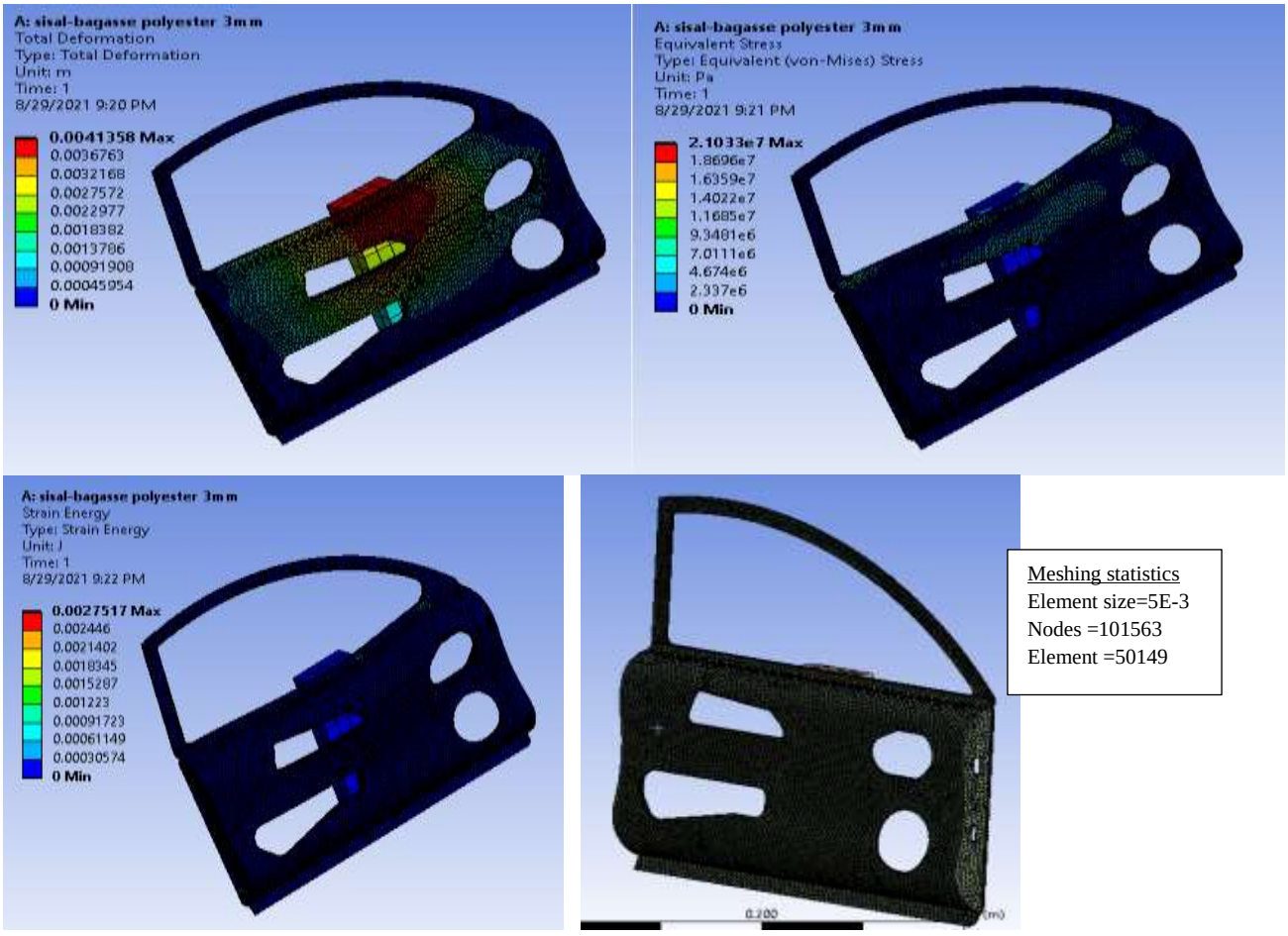

Figure 4- 26. sisal and bagasse hybrid fiber polyester composite door panel Ansys Simulation results for 3mm thickness

But by doubling the thickness of the sisal and sugarcane bagasse hybrid fiber polyester composite the factor of safety can be increased to 1.81 which is about 63% increment. The

total deformation was decreased by 42.1%, and the stress developed on the door panel was decreased by 38.6%. Here the mass of newly developed composite material is still the lowest compared to these three candidate materials.

4.15.1. Attaching mechanism of inner and outer door panels

Most of the time automotive body manufacturers use spot welding to join the two members which are made from similar material. For the attachment of dissimilar metallic materials, they use bolts and nuts, screws, and pins. But for the attachment of composite materials with metallic materials welding is impossible. Even bolts and pins joining not convenient to join them as cracking propagation happens due to fatigue and vibration. Therefore, the suitable attaching mechanism for dissimilar materials is adhesives like DELO MONOPOX and methacrylate. DELO MONOPOX products are heat-curing, single-component products. They are predominantly used in electronics, microelectronics, electrical engineering, precision engineering and sometimes in mechanical engineering for bonding and fixing. DELO MONOPOX VE403728 is the strongest adhesive which is recoded by Guinness Book of World record as it abled to lift 17.5 tons one meter high for one hour with 3gram adhesive in 2019. The other good adhesive called Methacrylate is a strong and fast curing at room temperature. It also does not affect the recyclability of composite. Therefore, by using these adhesives one can attach this natural composite made inner door panel with steel made outer door panel.

CHAPTER FIVE

5. CONCLUSION AND RECOMMENDATION

5.1. CONCLUSION

Investigation of mechanical properties of the hybrid composite of sisal and sugarcane fibers was the main objective and has been executed successfully. Hybridizing the two bio fibers made the composite enhance the synergetic properties of the two constituent fibers. By changing the proportion of fiber loading, layering sequence, and curing temperature during the manufacturing process, the effect on the mechanical properties and water absorption property was studied. Finally, the following conclusions can be drawn.

- Among the manufacturing process parameters (fiber loading, layering sequence, and curing temperature) fiber loading has the highest contribution on the tensile strength (86.27%), flexural strength (53.23%), and water absorption (95.5%) in favor of sisal fiber. But for the impact strength fiber loading has 73.96% contribution in favor of sugarcane bagasse fiber. For compression strength, the layering sequence has a 76% contribution at which BSB layering sequence recorded the highest value.
- As the proportion of sisal fiber increases the tensile strength and flexural strength regardless of layering sequence and curing temperature. For the compression strength, an equal proportion of sisal fiber and sugarcane bagasse fiber has a higher value (22.56MPa).
- As the proportion of SCB fiber increases from 10%Wt to 20%Wt the impact strength increases by about 25%.
- Curing temperature has a slight impact on all mechanical properties in such a way that elevating the curing temperature above room temperature has a negative effect. But it can lower curing time during manufacturing.
- The SBS layering gives a better tensile and flexural strength and low water absorbing tendency.
- Uniformly mixed composite of the sisal and SCB fibers has a relatively better impact strength.

- For tensile strength fiber loading has the highest contribution with 86.27% and flexural strength is highly influenced by fiber loading with 53.23% and secondly by layering sequence with 41.32%.
- Layering sequence has 76% contribution on compression strength and fiber loading has a contribution of 73.96% and 95.5% on impact strength and water absorption property respectively.
- In general, the combination of the manufacturing process parameters for better strength is given by the relation $CT_1 - FL_3 - LS_2$ for the tensile and flexural strength and lower water absorption property.
- $CT_1 - FL_2 - LS_3$ for compression strength and $CT_1 - FL_1 - LS_1$ for the impact strength.

From the Ansys Simulation results, the following conclusion can be drawn

- The sisal and sugarcane bagasse hybrid fiber polyester composite can withstand moderate loads with lightweight.
- Among the four-candidate materials sisal and sugarcane bagasse hybrid fiber polyester composite has the least mass 1.604kg with least equivalent stress developed on it.

5.2. RECOMMENDATION AND FUTURE WORK

This composite material made from hybridization of sisal and SCB fibers with polyester resin has moderately good mechanical strength with low weight and biodegradable properties. Therefore, the researchers want to recommend automotive body manufacturers to use this low-cost and eco-friendly material to manufacture their car interior bodies and low strength components like hoods, door panels, dashboards, and seatbacks.

For the future, the researchers want to point out the following research topics next to this work.

- Investigation of dynamic mechanical properties can be done for the same fibers.
- Combining other natural fibers with these fibers may be done.
- Hybridizing these fibers with synthetic fibers like carbon fiber and fiberglass can be done to increase mechanical strength and decrease water absorption properties.
- Examine the mechanical properties by changing the orientation of sisal fiber make to the cross-web form.
- Investigate the fatigue, shear, and hardness properties and morphological behavior.
- It is better to establish research center for natural fiber composite materials and fulfill convenient laboratory equipment in AASTU.

REFERENCE

[1] D. Verma and S. Sharma, “Green Biocomposites : A Prospective Utilization in Automobile Industry,” 2017, doi: 10.1007/978-3-319-49382-4.

[2] S. Singh, M. K. Gupta, and R. K. Srivastava, “ScienceDirect Effect of variation in frequencies on dynamic mechanical properties of short sisal fibre reinforced epoxy composite,” *Mater. Today Proc.*, vol. 4, no. 2, pp. 3387–3396, 2017, doi: 10.1016/j.matpr.2017.02.227.

[3] M. Jawaid, O. Y. Alothman, and M. S. Salit, “Preface,” *Green Energy Technol.*, vol. 0, no. 9783319493817, pp. vii–viii, 2017, doi: 10.1007/978-3-319-49382-4.

[4] M. T. H. S. and O. Y. A. N. Saba, Mohammad Jawaid, *Green Biocomposites for Structural Applications* .. Springer, 2017.

[5] G. Koronis, A. Silva, and M. Fontul, “Composites : Part B Green composites : A review of adequate materials for automotive applications,” *Compos. Part B*, vol. 44, no. 1, pp. 120–127, 2013, doi: 10.1016/j.compositesb.2012.07.004.

[6] N. Mazlan and Y. Ando, “Natural fiber for green technology in automotive industry : A brief review Related content Natural fiber for green technology in automotive industry : A brief review,” no. June, 2018, doi: 10.1088/1757-899X/368/1/012012.

[7] M. J. Mochane, T. C. Mokhena, T. H. Mokhothu, A. Mtibe, E. R. Sadiku, and S. S. Ray, “Recent progress on natural fiber hybrid composites for advanced applications : A review,” vol. 13, no. 2, pp. 159–198, 2019.

[8] A. Ticoalu, T. Aravinthan, and F. Cardona, “A review of current development in natural fiber composites for structural and infrastructure applications,” no. August 2015, 2010.

[9] A. N. N. and S. Chabba, “Composites get greener,” *Elsevier*, no. April, pp. 22–29, 2003, doi: ISSN:1369 7021 © Elsevier Science Ltd 2003.

[10] O. T. Adesina, “Mechanical evaluation of hybrid natural fibre – reinforced polymeric composites for automotive bumper beam : a review,” 2019.

[11] M. R. Sanjay, G. R. Arpitha, L. L. Naik, K. Gopalakrisha, and B. Yogesha, “Applications of Natural Fibers and Its Composites : An Overview,” 2016, doi: 10.4236/nr.2016.73011.

[12] J. Naveen and S. Satheeshkumar, “Journal of Reinforced Plastics and Composites,”

2014, doi: 10.1177/0731684413516393.

[13] Y. Li, Y. Mai, and L. Ye, “Sisal ® bre and its composites : a review of recent developments,” vol. 60, no. 2000, 2006.

[14] A. Al Faruque and K. Bilisik, “Plant-Based Natural Fibre Reinforced Composites : A Review on Fabrication , Properties and Applications,” pp. 1–34, 2020.

[15] L. Design and V. S. Door, “PhD Supervisor : PhD Coordinator :,” 2015, doi: 10.6092/polito/porto/2598565.

[16]. .. Srikanth Pilla Sai Aditya Pradeep, “Automotive Applications of Plastics: Past, Present, and Future Sai,” *Elsevier*, pp. 1–11, 2017, [Online]. Available: https://www.sciencedirect.com/science/article/pii/B9780323390408000316.

[17] T. P. Hovorun, K. V. Berladir, V. I. Pererva, S. G. Rudenko, and A. I. Martynov, “Modern materials for automotive industry,” *J. Eng. Sci.*, vol. 4, no. 2, pp. f8–f18, 2017, doi: 10.21272/jes.2017.4(2).f8.

[18] J. Naveen, M. Jawaid, P. Amuthakkannan, and M. Chandrasekar, *21 - Mechanical and physical properties of sisal and hybrid sisal fiber-reinforced polymer composites*, no. November. Elsevier Ltd, 2018.

[19] A. Balaji, B. Karthikeyan, and C. S. Raj, “Bagasse Fiber – The Future Biocomposite Material : A Review,” vol. 7, no. 01, pp. 223–233, 2015.

[20] D. Verma, P. C. Gope, M. K. Maheshwari, and R. K. Sharma, “Bagasse Fiber Composites-A Review,” vol. 3, no. 6, pp. 1079–1092, 2012.

[21] M. Davallo, H. Pasdar, and M. Mohseni, “Mechanical Properties of Unsaturated Polyester Resin,” no. October 2010, 2019.

[22] L. S. Nacher, J. E. C. Amoros, S. Moya, and J. L. Martinez, “of Polymer Analysis and Characterization Mechanical Properties of Polyester Resins in Saline Water Environments,” no. January 2015, pp. 37–41, doi: 10.1080/10236660701516557.

[23] D. A. chennakeshava R. S.sreenivasulu1, “Mechanical Properties Evalution of Bamboo Fiber Reinforced Composite Materials,” *Int. J. Eng. Res.*, vol. 3, no. 1, pp. 2–8, 2014, doi: ISSN:2319-6890, 2347-5013.

[24] S. K. Patel, M. E. Cad, C. A. M. Student, and V. V New, “Review on Manufacturing Techniques of Fibreglass Reinforced Composites,” vol. 3, no. 03, pp. 1687–1691, 2015.

[25] R. K. S. D. Verma1*, P.C. Gope2, M.K. Maheshwari1, “Bagasse fiber composites : A Review,” *Researchgate*, no. July 2012, 2015, doi: ISSN : 2028-2508 CODEN: JMESCN.

[26] B. Dhibar, S. V. Singh, S. Anwar, and A. Singh, “Sugarcane Bagasse Reinforced Polyester Composites,” *Int. Res. J. Eng. Technol.*, vol. 05, no. 05, 2018, doi: e-ISSN: 2395-0056 p-ISSN: 2395-0072.

[27] D. K. Rajak, D. D. Pagar, P. L. Menezes, and E. Linul, “Fiber-Reinforced Polymer Composites :,” 2019, doi: doi:10.3390/polym11101667.

[28] S. Mosisa and T. Batu, “Investigation of mechanical properties of bamboo / sisal fiber reinforced hybrid composite materials,” no. April, 2021.

[29] K. Lau, P. Hung, M. Zhu, and D. Hui, “Properties of natural fi bre composites for structural engineering applications,” *Compos. Part B*, vol. 136, no. September 2017, pp. 222–233, 2018, doi: 10.1016/j.compositesb.2017.10.038.

[30] H. Carvalho, H. Salman, and M. Leite, “Natural Fibre Composites and Their Applications : A Review,” pp. 1–20, 2018, doi: 10.3390/jcs2040066.

[31] L. Mohammed, M. N. M. Ansari, G. Pua, M. Jawaid, and M. S. Islam, “A Review on Natural Fiber Reinforced Polymer Composite and Its Applications,” vol. 2015, 2015.

[32] F. De Andrade, N. Chawla, R. Dias, and D. T. Filho, “Tensile behavior of high performance natural (sisal) fibers,” *Compos. Sci. Technol.*, vol. 68, no. 15–16, pp. 3438–3443, 2008, doi: 10.1016/j.compscitech.2008.10.001.

[33] M. P. Characterization, R. Epoxy, and R. Composite, “ADDIS ABABA INSTITUTE OF TECHNOLOGY SCHOOL OF GRADUATE STUDIES Fabrication and Mechanical Property Characterization of Sisal fiber Reinforced Epoxy Resin Composite Material for Automotive body Application Addis Ababa University Addis Ababa Institute of Te,” 2015.

[34] D. K. K. Cavalcanti, M. D. Banea, J. S. S. Neto, R. A. A. Lima, L. F. M. Silva, and R. J. C. Carbas, “Mechanical characterization of intralaminar natural fibre-reinforced hybrid composites,” *Compos. Part B*, vol. 175, no. May, p. 107149, 2019, doi: 10.1016/j.compositesb.2019.107149.

[35] M. K. Gupta and R. K. Srivastava, “Properties of sisal fibre reinforced epoxy

composite," vol. 41, no. September, pp. 235–241, 2016.

[36] Z. Alemayehu, R. Babu, M. Liben, and S. Kishan, "Materials Today : Proceedings Experimental investigation on characteristics of sisal fiber as composite material for light vehicle body applications," *Mater. Today Proc.*, no. xxxx, pp. 0–5, 2020, doi: 10.1016/j.matpr.2020.07.386.

[37] N. Uppal, A. Pappu, R. Patidar, and V. S. Gowri, "Synthesis and characterization of short sisal fibre polyester," *Bull. Mater. Sci.*, vol. 42, no. 3, pp. 1–8, 2019, doi: 10.1007/s12034-019-1792-6.

[38] D. G. Devadiga, K. S. Bhat, G. T. Mahesha, D. G. Devadiga, K. S. Bhat, and G. T. Mahesha, "Sugarcane bagasse fiber reinforced composites : Recent advances and applications MATERIALS ENGINEERING | REVIEW ARTICLE Sugarcane bagasse fiber reinforced composites : Recent advances and applications," *Cogent Eng.*, vol. 7, no. 1, 2020, doi: 10.1080/23311916.2020.1823159.

[39] Y. R. Loh, D. Sujan, M. E. Rahman, and C. A. Das, "Resources , Conservation and Recycling Sugarcane bagasse — The future composite material : A literature review," *"Resources, Conserv. Recycl.*, vol. 75, pp. 14–22, 2013, doi: 10.1016/j.resconrec.2013.03.002.

[40] S. Subramonian, A. Ali, and M. Amran, "Effect of fiber loading on the mechanical properties of bagasse fiber – reinforced polypropylene composites," vol. 8, no. 8, pp. 1–5, 2016, doi: 10.1177/1687814016664258.

[41] A. Athijayamani, B. Stalin, S. Sidhardhan, and C. Boopathi, "Parametric analysis of mechanical properties of bagasse fiber-reinforced vinyl ester composites," 2016, doi: 10.1177/0021998315576555.

[42] M. B. Hoque, S. Hossain, and R. A. Khan, "Study on Tensile , Bending and Water Uptake Properties of Sugarcane Bagasse Fiber Reinforced Polypropylene Based Composite," vol. 3, no. 1, pp. 18–23, 2019, doi: 10.11648/j.jb.20190301.13.

[43] M. K. Marichelvam, "A novel palm sheath and sugarcane bagasse fiber based hybrid composites for automotive applications : An experimental approach," no. September, pp. 1–10, 2020, doi: 10.1002/pc.25843.

[44] B. F. E. Bio-composites, "Physical and Mechanical Behaviour of Sugarcane Bagasse Fibre-Reinforced Epoxy Bio-Composites," pp. 1–13.

[45] J. D. J. D *et al.*, “Influence of Bagasse / Sisal Fibre Stacking Sequence on the Mechanical Characteristics of Hybrid-Epoxy Composites Influence of Bagasse / Sisal Fibre Stacking Sequence on the Mechanical Characteristics of Hybrid-Epoxy Composites,” *J. Nat. Fibers*, vol. 0, no. 0, pp. 1–11, 2019, doi: 10.1080/15440478.2019.1581119.

[46] P. Tripathi, V. K. Gupta, A. Dixit, and R. K. Mishra, “Development and characterization of low cost jute , bagasse and glass fiber reinforced advanced hybrid epoxy composites,” vol. 5, no. January, pp. 320–337, 2018, doi: 10.3934/matersci.2018.2.320.

[47] A. S. V. Vikram and S. Arivalagan, “Engineering Properties on the Sugar Cane Bagasse with Sisal Fibre Reinforced Concrete,” vol. 12, no. 24, pp. 15142–15146, 2017.

[48] P. Dwivedi and S. K. Shukla, “Study of Mechanical Behaviour & Water-Absorption Characteristics of Sisal-Bagasse Fibre Reinforced Hybrid Epoxy Composites,” no. June, 2019.

[49] D. Getu, R. Babu, M. Masresha, and S. Kishan, “Materials Today : Proceedings Production and characterization of bamboo and sisal fiber reinforced hybrid composite for interior automotive body application,” *Mater. Today Proc.*, no. xxxx, 2020, doi: 10.1016/j.matpr.2020.08.780.

[50] Lasikun, D. Ariawan, E. Surojo, and J. Triyono, “Effect of fiber orientation on tensile and impact properties of Zalacca Midrib fiber-HDPE composites by compression molding,” *AIP Conf. Proc.*, vol. 1931, pp. 5–9, 2018, doi: 10.1063/1.5024119.

[51] S. Candido, F. Santos, D. A. Luz, A. Clay, R. Da, and S. N. Monteiro, “Thermal Behavior of Polyester Composites Reinforced with Green Sugarcane Bagasse Fiber,” 2018, doi: 10.1007/s11837-018-3086-7.

[52] R. De Souza, L. Maria, S. De Souza, and F. De Andrade, “Special Issue 4th Brazilian Conference on Composite Materials (2018) Comparative study on the mechanical behavior and durability of polypropylene and sisal fiber reinforced concretes,” *Constr. Build. Mater.*, vol. 211, pp. 617–628, 2019, doi: 10.1016/j.conbuildmat.2019.03.282.

[53] A. Orue, A. Jauregi, U. Unsuain, J. Labidi, A. Eceiza, and A. Arbelaiz, "Composites : Part A The effect of alkaline and silane treatments on mechanical properties and breakage of sisal fibers and poly (lactic acid)/ sisal fiber composites," *Compos. PART A*, vol. 84, pp. 186–195, 2016, doi: 10.1016/j.compositesa.2016.01.021.

[54] M. K. Gupta, N. Choudhary, and V. Agrawal, "Static and dynamic mechanical analysis of hybrid composite reinforced with jute and sisal fibres," *J. Chinese Adv. Mater. Soc.*, vol. 0, no. 0, pp. 1–13, 2018, doi: 10.1080/22243682.2018.1539643.

[55] S. C. Das *et al.*, "Effect of stacking sequence on the performance of hybrid natural/synthetic fiber reinforced polymer composite laminates," *Compos. Struct.*, vol. 276, no. August, p. 114525, 2021, doi: 10.1016/j.compstruct.2021.114525.

[56] M. S. M. Jusoh, M. Y. Yahya, and N. I. S. Hussein, "The effect of fibre layering pattern in resisting bending loads of natural fibre-based hybrid composite materials," *MATEC Web Conf.*, vol. 39, no. January, 2016, doi: 10.1051/matecconf/20163901005.

[57] P. Sathyaseelan, P. Sellamuthu, and L. Palanimuthu, "Influence of Stacking Sequence on Mechanical Properties of Areca-kenaf Fiber-Reinforced Polymer Hybrid Composite," *J. Nat. Fibers*, vol. 00, no. 00, pp. 1–13, 2020, doi: 10.1080/15440478.2020.1745118.

[58] J. I. P. Singh, S. Singh, and V. Dhawan, "Effect of Curing Temperature on Mechanical Properties of Natural Fiber Reinforced Polymer Composites," *J. Nat. Fibers*, vol. 15, no. 5, pp. 687–696, 2018, doi: 10.1080/15440478.2017.1354744.

[59] C. Campana, R. Leger, R. Sonnier, L. Ferry, and P. Ienny, "Effect of post curing temperature on mechanical properties of a flax fiber reinforced epoxy composite," *Compos. Part A Appl. Sci. Manuf.*, vol. 107, pp. 171–179, 2018, doi: 10.1016/j.compositesa.2017.12.029.

[60] G. Slipher and A. Mechanics, *Mechanics of Composite and Multi-functional Materials , Volume 6*, vol. 6. 2017.

[61] N. Venkateshwaran, A. Elayaperumal, A. Alavudeen, and M. Thiruchitrambalam, "Mechanical and water absorption behaviour of banana / sisal reinforced hybrid composites," *Mater. Des.*, vol. 32, no. 7, pp. 4017–4021, 2011, doi:

10.1016/j.matdes.2011.03.002.

[62] S. Mishra, A. K. Mohanty, L. T. Drzal, M. Misra, and G. Hinrichsen, “A Review on Pineapple Leaf Fibers , Sisal Fibers and Their Biocomposites,” pp. 955–974, 2004, doi: 10.1002/mame.200400132.

[63] P. S. R. Kesavan and B. V. Ramnath, “Effect of Fiber Orientation and Stacking Sequence on Mechanical and Thermal Characteristics of Banana-Kenaf Hybrid Epoxy Composite,” *Silicon*, 2015, doi: 10.1007/s12633-015-9314-7.

[64] A. VRamesh, E. Paul, and S. K. Ali, “Comparitive Study of the Mechanical Properties of Alkali Treated and Untreated Sugarcane Bagasse Fiber Reinforced Composite Material,” *Int. Res. J. Eng. Technol.*, pp. 413–420, 2018, [Online]. Available: www.irjet.net.

[65] D. S. Bajwa and S. Bhattacharjee, “Current Progress, Trends and Challenges in the Application of Biofiber Composites by Automotive Industry,” *J. Nat. Fibers*, vol. 13, no. 6, pp. 660–669, 2016, doi: 10.1080/15440478.2015.1102790.

[66] M. Stevens, S. Modi, and M. Chess, “Mixed Materials Solutions : Alternative Materials for Door Assemblies Prepared In Conjunction With : Coalition for Automotive Lightweight Materials Prepared by :,” no. August, 2016, [Online]. Available: http://www.cargroup.org/wp-content/uploads/2017/02/Mixed-Materials-Solutions-Alternative-Materials-for-Door-Assemblies.pdf.

[67] V. Gheorghe, M. L. Scutaru, V. B. Ungureanu, E. Chircan, and M. Ulea, “SS symmetry Automotive Engineering,” 2021.

[68] S. Darwish, H. M. A. Hussein, and A. Gemeal, “Numerical study of automotive doors,” *Int. J. Eng. Technol.*, vol. 12, no. 04, pp. 82–92, 2012.

[69] J. L. T. MA, J D N Shaw, Roy J. Crawford, “Polyester Resin,” *Sciencedirect*, pp. 1–10, 2014, [Online]. Available: https://www.sciencedirect.com/science/article/pii/B9780750673280500112.

[70] C. Deo and S. K. Acharya, “Effect of moisture absorption on mechanical properties of chopped natural fiber reinforced epoxy composite,” *J. Reinf. Plast. Compos.*, vol. 29, no. 16, pp. 2513–2521, 2010, doi: 10.1177/0731684409353352.

[71] H. Muhsen, “TAGUCHI ’ S OPTIMIZATION METHOD AND ITS APPLICATION TO THE DESIGN APPLICATION TO THE DESIGN OF

ANTENNAS," no. August 2009, 2017, doi: 10.13140/RG.2.2.29610.93123.

[72] A. S. Fraley *et al.*, "14 . 1 : Design of Experiments via Taguchi Methods - Orthogonal Arrays," pp. 1–10, 2021.

[73] I. O. P. C. Series and M. Science, "Selection of Optimal Factor Level From Process Parameters in Palm Oil Industry Selection of Optimal Factor Level From Process Parameters in Palm Oil Industry," 2018, doi: 10.1088/1757-899X/288/1/012056.

[74] M. T. Bengisu and A. Akay, "Stick–slip oscillations: Dynamics of friction and surface roughness," *J. Acoust. Soc. Am.*, vol. 105, no. 1, pp. 194–205, 1999, doi: 10.1121/1.424580.

[75] C. Dong, L. Shi, L. Li, X. Bai, C. Yuan, and Y. Tian, "Stick-slip behaviours of water lubrication polymer materials under low speed conditions," *Tribol. Int.*, vol. 106, pp. 55–61, 2017, doi: 10.1016/j.triboint.2016.10.027.

[76] L. E. Roussel, "Experimental investigation of stick-slip behavior in granular materials," 2005.

[77] M. M. S. Dwaikat, C. Spitas, and V. Spitas, "Predicting nonlinear stress-strain curves of unidirectional fibrous composites in consideration of stick-slip," *Compos. Part B Eng.*, vol. 44, no. 1, pp. 501–507, 2013, doi: 10.1016/j.compositesb.2012.03.019.

[78] J. D. E. PhD, "Fick ' s Law of diffusion," *Sciencedirect*, pp. 1–20, 2018, [Online]. Available: https://www.sciencedirect.com/science/article/pii/B9780128169506000099.

[79] A. Paul, T. Laurila, V. Vuorinen, and S. V. Divinski, *Thermodynamics, diffusion and the kirkendall effect in solids*, vol. 9783319074. 2014.

[80] R. Wirawan, S. M. Sapuan, R. Yunus, and K. Abdan, "Density and water absorption of sugarcane bagasse-filled poly(vinyl chloride) composites," *Polym. Polym. Compos.*, vol. 20, no. 7, pp. 659–664, 2012, doi: 10.1177/096739111202000710.

[81] E. F. Cerqueira, C. A. R. P. Baptista, and D. R. Mulinari, "Mechanical behaviour of polypropylene reinforced sugarcane bagasse fibers composites," *Procedia Eng.*, vol. 10, pp. 2046–2051, 2011, doi: 10.1016/j.proeng.2011.04.339.

[82] P. Sivaiah and D. Chakradhar, "Modeling and optimization of sustainable manufacturing process in machining of 17-4 PH stainless steel," *Measurement*, vol.

134, pp. 142–152, 2019, doi: 10.1016/j.measurement.2018.10.067.

[83] S. P. S. Tita, R. Medeiros, J. R. Tarpani, E. Frollini, and V. Tita, “Chemical modification of sugarcane bagasse and sisal fibers using hydroxymethylated lignin : Influence on impact strength and water absorption of phenolic composites,” 2018, doi: 10.1177/0021998317753886.

APPENDIX

Appendix A. Charts for Tensile Strength

In this appendix, all the data have been collected during the laboratory specimens testing were provided.

Tensile Strength Test Charts which are close to the average of the three trial tests

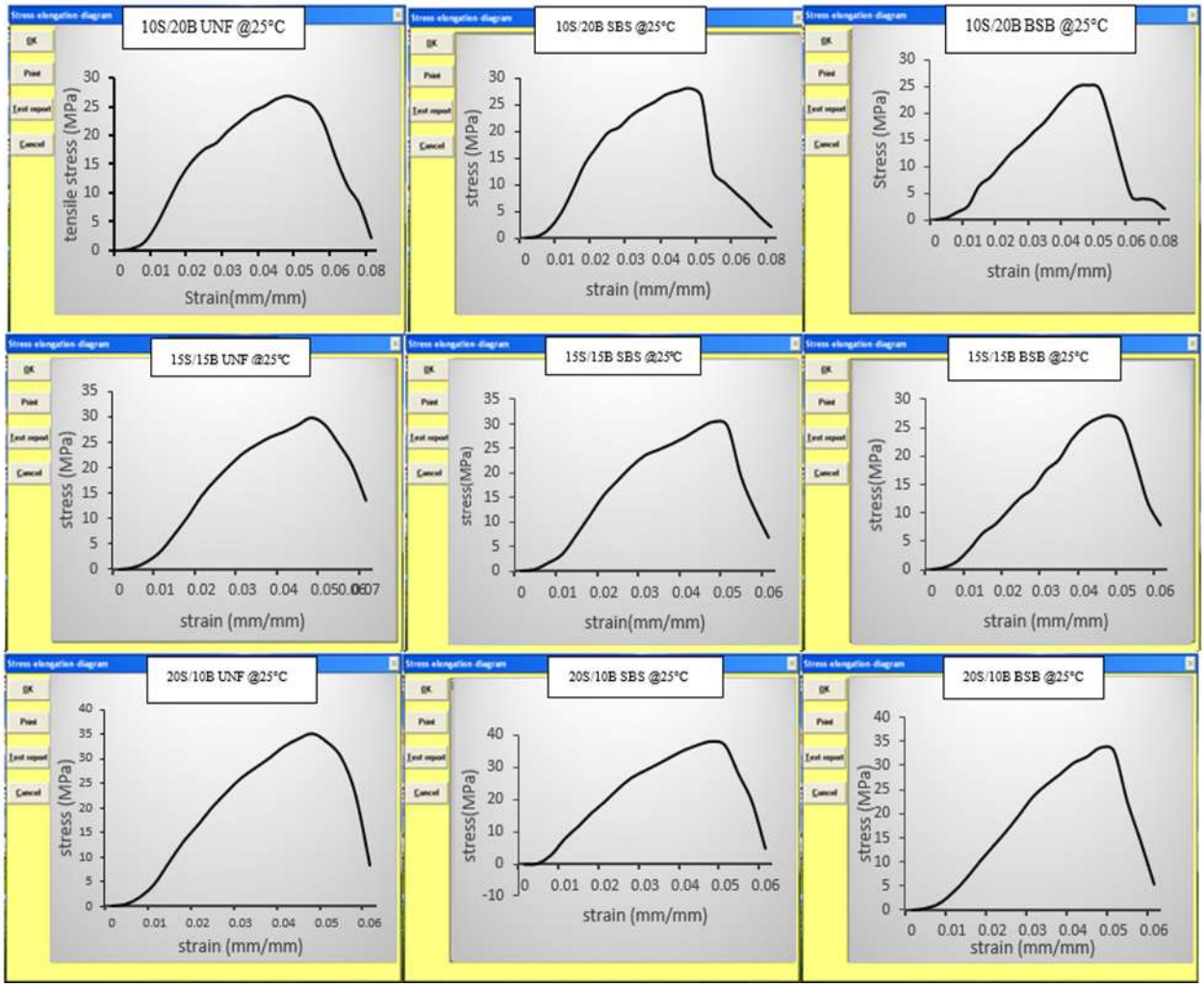

Appendix B. Data sheets collected during laboratory experimentation for Tensile strength

Trials	**Fiber Proportions or loadings for UNF mixing**			**Pressing**
	10S/20B(MPa)	15S/15B(MPa)	20S/10B(MPa)	**Temperature**
T1	27.585	29.305	30.502	25ºC
T2	27.891	29.444	37.812	
T3	25.146	30.252	36.554	
AV	26.874	29.667	34.963	
T1	25.062	24.760	35.345	60ºC
T2	29.856	28.658	35.356	
T3	24.485	32.025	33.021	
AV	25.976	28.481	34.574	
SBS layering				
Trials	10S/20B(MPa)	15S/15B(MPa)	20S/10B(MPa)	Cure Temp
T1	30.914	30.142	40.080	25ºC
T2	27.652	28.351	33.562	
T3	25.380	32.840	40.025	
AV	27.982	30.444	37.889	
T1	32.436	27.094	40.819	60ºC
T2	24.695	30.230	35.874	
T3	25.258	32.589	34.361	
AV	27.463	29.939	37.018	
BSB Layering				
Trials	10S/20B(MPa)	15S/15B(MPa)	20S/10B(MPa)	Cure Temp
T1	24.849	28.642	38.204	25ºC
T2	23.654	28.369	30.569	
T3	21.256	24.376	32.561	
AV	25.223	27.129	33.778	
T1	27.512	27.610	33.055	60ºC
T2	20.568	25.652	30.265	
T3	21.562	26.364	35.347	
AV	24.814	26.542	32.889	

Appendix C. Diagrams for selected Flexural Strength Test which are close to average value among the three trials

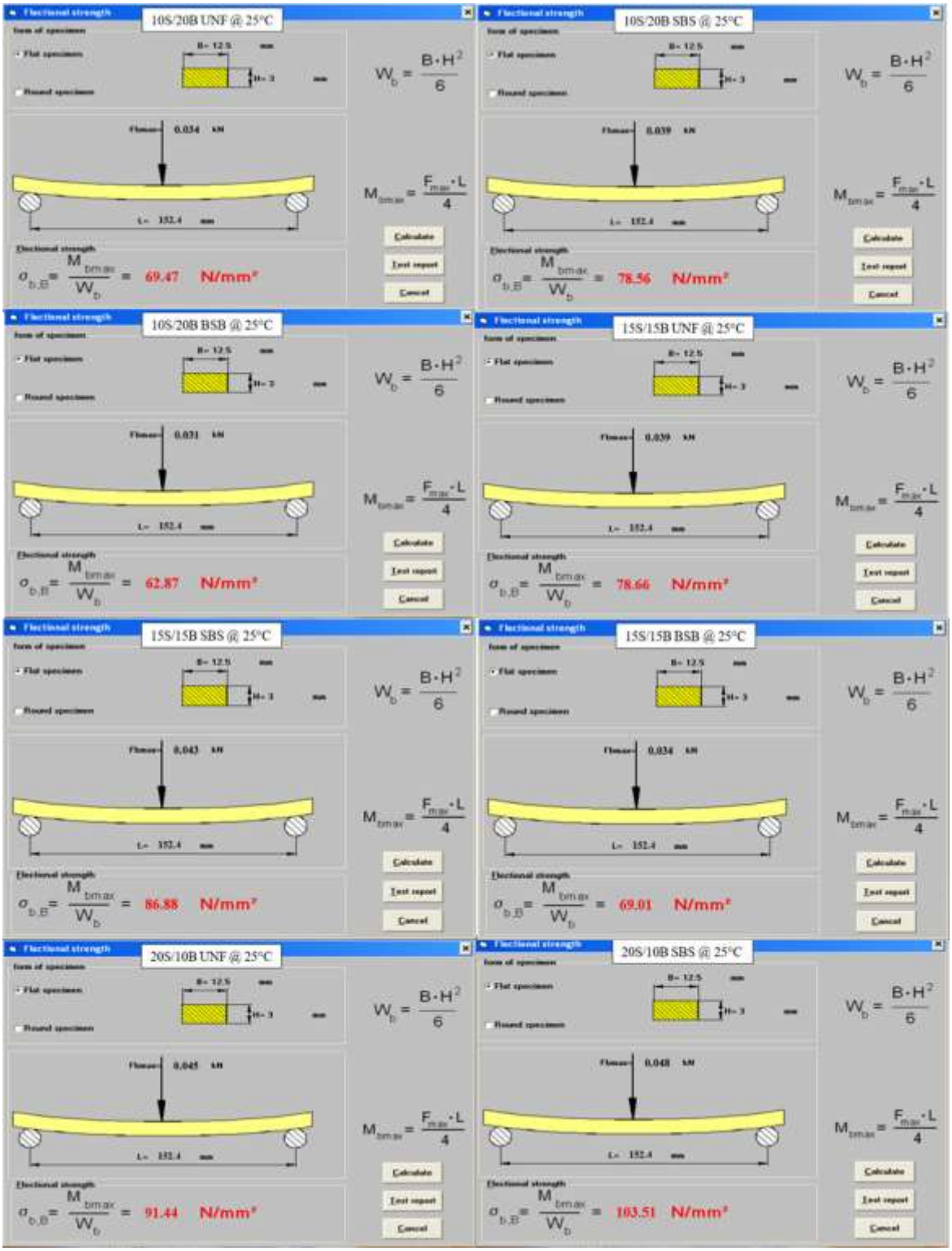

Appendix D. Data sheet for all trials of flexural strength test

Trials	**Fiber Proportions or loadings for UNF mixing**			**Pressing**
	10S/20B(MPa)	15S/15B(MPa)	20S/10B(MPa)	**Temperature**
T1	84.83	98.41	103.02	25ºC
T2	69.47	78.66	98.81	
T3	64.52	76.82	88.66	
AV	72.94	84.63	96.83	
T1	63.94	83.02	90.07	60ºC
T2	74.06	76.58	94.43	
T3	71.52	69.75	92.88	
AV	69.84	76.45	92.46	
SBS layering				
Trials	10S/20B(MPa)	15S/15B(MPa)	20S/10B(MPa)	Cure Temp
T1	78.56	86.88	105.66	25ºC
T2	79.94	89.31	98.48	
T3	77.12	84.06	103.51	
AV	78.53	86.76	102.55	
T1	71.95	83.64	99.37	60ºC
T2	80.26	81.63	93.82	
T3	77.17	74.52	89.86	
AV	76.46	79.93	94.35	
BSB Layering				
Trials	10S/20B(MPa)	15S/15B(MPa)	20S/10B(MPa)	Cure Temp
T1	60.27	65.89	79.47	25ºC
T2	62.87	71.29	78.68	
T3	65.38	69.01	84.67	
AV	62.84	68.73	80.94	
T1	56.42	66.84	70.79	60ºC
T2	64.54	68.91	77.22	
T3	61.56	72.51	79.57	
AV	60.83	69.42	75.86	

Appendix E. Diagrams for Compression strength test which are close to the average result

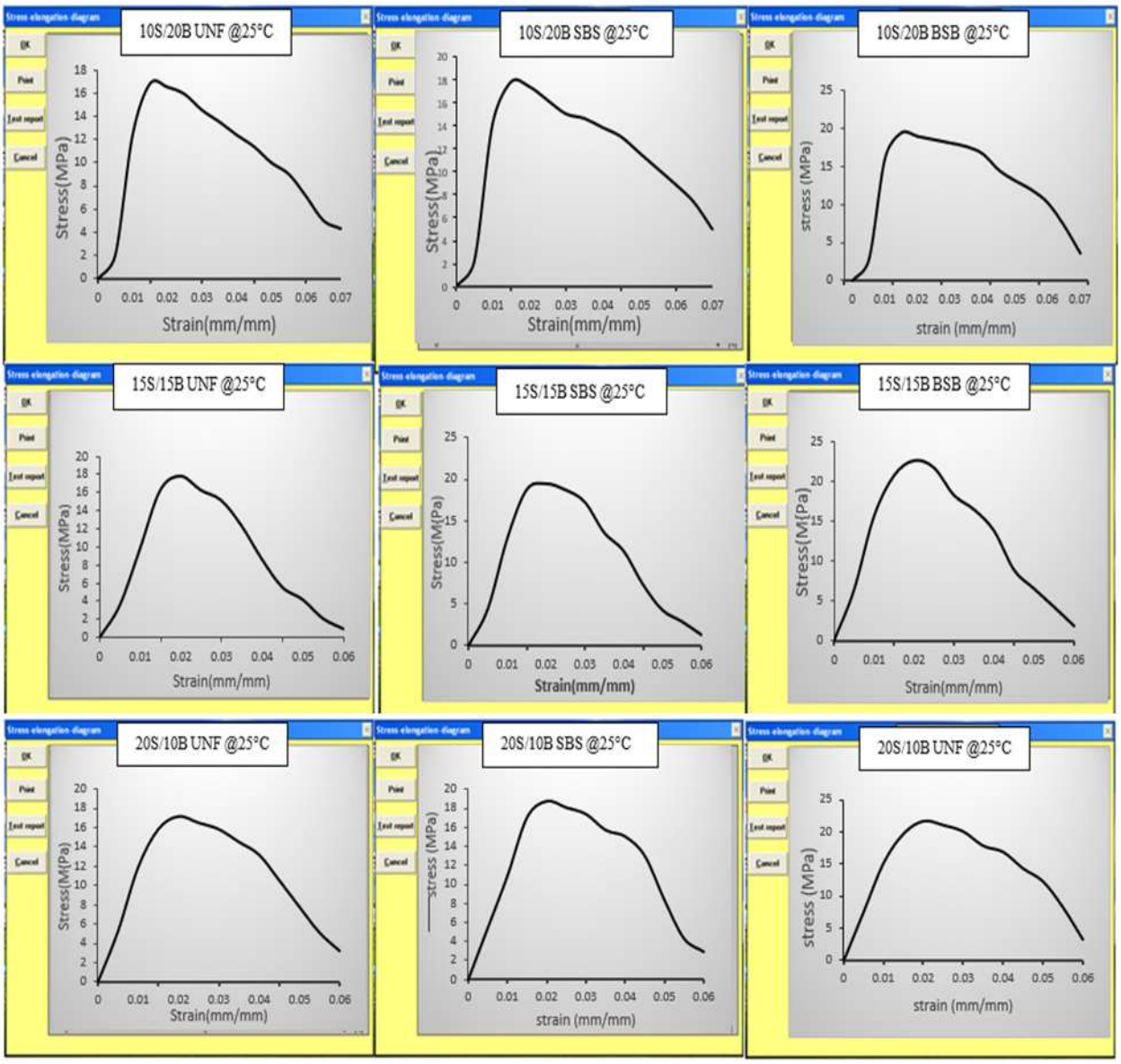

Appendix F. Data sheet for all trials of compression strength test

Trials	**Fiber Proportions or loadings for UNF mixing**			**Pressing**
	10S/20B(MPa)	15S/15B(MPa)	20S/10B(MPa)	**Temperature**
T1	14.491	18.974	17.106	25ºC
T2	18.289	16.451	17.256	
T3	17.561	18.239	17.274	
AV	16.780	17.888	17.212	
T1	15.438	17.182	15.682	60ºC
T2	14.848	15.847	15.539	
T3	16.512	16.561	19.571	
AV	15.998	16.530	16.931	
SBS layering				
Trials	10S/20B(MPa)	15S/15B(MPa)	20S/10B(MPa)	Cure Temp
T1	17.331	16.262	18.229	25ºC
T2	16.578	21.227	17.817	
T3	19.551	20.541	19.301	
AV	17.820	19.3503	18.779	
T1	20.471	21.269	17.852	60ºC
T2	15.604	14.843	16.043	
T3	19.554	19.571	18.248	
AV	18.540	18.561	17.351	
BSB Layering				
Trials	10S/20B(MPa)	15S/15B(MPa)	20S/10B(MPa)	Cure Temp
T1	19.452	23.649	22.184	25ºC
T2	18.582	19.582	20.536	
T3	20.592	24.446	22.149	
AV	19.542	22.559	21.619	
T1	22.229	16.772	23.217	60ºC
T2	17.549	23.658	25.52	
T3	15.896	24.522	23.538	
AV	18.558	21.651	21.021	

Appendix G. Data sheet for all trials of impact strength test

Trials	**Fiber Proportions or loadings for UNF mixing**			**Pressing**
	10S/20B(kJ/m^2)	15S/15B(kJ/m^2)	20S/10B(kJ/m^2)	**Temperature**
T1	28.25	27.11	24.12	25ºC
T2	29.45	27.98	22.85	
T3	30.68	26.57	28.69	
AV	29.46	27.22	25.22	
T1	27.01	26.32	23.23	60ºC
T2	29.51	27.21	23.44	
T3	27.51	27.11	24.94	
AV	28.01	26.88	23.87	
SBS layering				
Trials	10S/20B(kJ/m^2)	15S/15B(kJ/m^2)	20S/10B(kJ/m^2)	Cure Temp
T1	25.25	25.14	25.01	25ºC
T2	29.31	25.98	19.22	
T3	29.71	24.51	16.64	
AV	28.09	25.21	20.29	
T1	27.21	25.32	18.33	60ºC
T2	28.01	25.88	20.65	
T3	27.10	23.68	19.64	
AV	27.44	24.96	19.54	
BSB Layering				
Trials	10S/20B(kJ/m^2)	15S/15B(kJ/m^2)	20S/10B(kJ/m^2)	Cure Temp
T1	28.14	25.8	22.11	25ºC
T2	26.42	26.74	21.32	
T3	30.91	24.08	25.09	
AV	28.49	25.54	22.84	
T1	24.54	24.27	24.01	60ºC
T2	29.85	21.04	22.55	
T3	29.55	27.5	21.12	
AV	27.98	24.27	22.56	

Appendix H. Data sheet Water Absorption Test, Result Record at T=25°C, for 10S/20B from first day to 216 hours

Water Absorption Test, Result Record at T=25°C, for 10S/20B from first day to 216 hours													
Fiber Loading	Layering Sequence	Pressing Temp	Trials	Initial weight(g) Feb 15/2021	Weight (g) After 24 Hours Feb 16/2021	Weight (g) After 48 Hours Feb 17/2021	Weight (g) After 72 Hours Feb 18/2021	Weight (g) After 96 Hours Feb 19/2021	Weight (g) After 120 Hours Feb 20/2021	Weight (g) After 144 Hours Feb 21/2021	Weight (g) After 168 Hours Feb 22/2021	Weight (g) After 192 Hours Feb 23/2021	Weight (g) After 216 Hours Feb 24/2021
10S/20B	UNF Mixing	25C	T1	1.1681	1.2817	1.3033	1.3199	1.3484	1.3523	1.3554	1.3599	1.3607	1.3618
			T2	1.1871	1.2705	1.3102	1.3189	1.3376	1.3431	1.3482	1.3534	1.3542	1.3545
			T3	1.1821	1.2917	1.2928	1.3148	1.3166	1.3351	1.3491	1.3556	1.3564	1.3571
			AV	1.1791	1.2813	1.3021	1.3179	1.3342	1.3435	1.3509	1.3563	1.3571	1.3578
			Mt(%)		8.6676	10.4317	11.7717	13.1541	13.9428	14.5704	15.0284	15.0963	15.1556
		60C	T1	1.1688	1.2710	1.2898	1.3075	1.3238	1.3331	1.3405	1.3450	1.3461	1.3469
			T2	1.1787	1.2809	1.2997	1.3174	1.3337	1.3430	1.3504	1.3549	1.3560	1.3568
			T3	1.1598	1.2620	1.2808	1.2985	1.3148	1.3241	1.3315	1.3360	1.3371	1.3379
			AV	1.1691	1.2713	1.2901	1.3078	1.3241	1.3334	1.3408	1.3453	1.3464	1.3472
			Mt(%)		8.7418	10.3498	11.8638	13.2581	14.0535	14.6865	15.0714	15.1655	15.2339
	SBS Layering	25C	T1	1.1920	1.2930	1.3241	1.3341	1.3432	1.3497	1.3548	1.3591	1.3623	1.3648
			T2	1.1782	1.2792	1.3103	1.3203	1.3294	1.3359	1.3410	1.3453	1.3485	1.3510
			T3	1.1791	1.2801	1.3112	1.3212	1.3303	1.3368	1.3419	1.3462	1.3494	1.3519
			AV	1.1831	1.2841	1.3152	1.3252	1.3343	1.3408	1.3459	1.3502	1.3534	1.3559
			Mt(%)		8.5369	11.1656	12.0108	12.7800	13.3294	13.7605	14.1239	14.3944	14.6057
		60C	T1	1.1841	1.2578	1.2766	1.2943	1.3106	1.3163	1.3214	1.3249	1.3257	1.3264
			T2	1.1252	1.2438	1.2626	1.2803	1.2966	1.3023	1.3074	1.3109	1.3117	1.3124
			T3	1.1362	1.2526	1.2714	1.2891	1.3054	1.3111	1.3162	1.3197	1.3205	1.3212
			AV	1.1485	1.2514	1.2702	1.2879	1.3042	1.3099	1.3150	1.3185	1.3193	1.3200
			Mt(%)		8.9595	10.5964	12.1376	13.5568	14.0531	14.4972	14.8019	14.8716	14.9325
	BSB Layering	25C	T1	1.2183	1.3385	1.3528	1.3658	1.3740	1.3800	1.3857	1.3906	1.3948	1.3986
			T2	1.1984	1.3186	1.3329	1.3459	1.3541	1.3601	1.3658	1.3707	1.3749	1.3787
			T3	1.2094	1.3296	1.3439	1.3569	1.3651	1.3711	1.3768	1.3817	1.3859	1.3897
			AV	1.2087	1.3289	1.3432	1.3562	1.3644	1.3704	1.3761	1.3810	1.3852	1.3890
			Mt(%)		9.9446	11.1277	12.2032	12.8816	13.3780	13.8496	14.2550	14.6025	14.9169
		60C	T1	1.2045	1.3940	1.4260	1.4470	1.4570	1.4660	1.4684	1.4704	1.4714	1.4719
			T2	1.1965	1.3860	1.4180	1.4390	1.4490	1.4580	1.4604	1.4624	1.4634	1.4639
			T3	1.1964	1.3859	1.4179	1.4389	1.4489	1.4579	1.4603	1.4623	1.4633	1.4638
			AV	1.1991	1.3886	1.4206	1.4416	1.4516	1.4606	1.4630	1.4650	1.4660	1.4665
			Mt(%)		15.8035	18.4722	20.2235	21.0575	21.8080	22.0082	22.1775	22.2609	22.3001

Appendix I. Data sheet Water Absorption Test, Result Record at T=25°C, for 10S/20B from 216th hour to 432nd hours

							Water Absorption Test, Result Record at T=25°C, for 10S/20B from 216th hour to 432nd hours							
Fiber Loading	Layering Sequence	Pressing Temp	Trials	Weight (g) After 240 Hours Feb 25/2021	Weight (g) After 264 Hours Feb 26/2021	Weight (g) After 288 Hours Feb 27/2021	Weight (g) After 312 Hours Feb 28/2021	Weight (g) After 336 Hours Feb 29/2021	Weight (g) After 360 Hours Feb 30/2021	Weight (g) After 384 Hours Feb 31/2021	Weight (g) After 408 Hours Mar 01/2021	Weight (g) After 432 Hours Mar 02/2021	Weight gain (g) at Saturated (Ms%)
10S/20B	UNF Mixing	25C	T1	1.3622	1.3587	1.3592	1.3596	1.3599	1.3601	1.3602	1.3603	1.3603	16.4541
			T2	1.3551	1.3588	1.3593	1.3597	1.3600	1.3602	1.3603	1.3604	1.3604	14.5986
			T3	1.3576	1.3586	1.3591	1.3595	1.3598	1.3600	1.3601	1.3602	1.3602	15.0664
			AV	1.3583	1.3587	1.3592	1.3596	1.3599	1.3601	1.3602	1.3603	1.3603	15.3677
			Mt(%)	15.1980	15.2320	15.2744	15.3083	15.3337	15.3507	15.3592	15.3677	15.3677	15.3677
		60C	T1	1.3476	1.3482	1.3487	1.3491	1.3494	1.3496	1.3497	1.3498	1.3498	15.4860
			T2	1.3575	1.3581	1.3586	1.3590	1.3593	1.3595	1.3596	1.3597	1.3597	15.3559
			T3	1.3386	1.3392	1.3397	1.3401	1.3404	1.3406	1.3407	1.3408	1.3408	15.6061
			AV	1.3479	1.3485	1.3490	1.3494	1.3497	1.3499	1.3500	1.3501	1.3501	15.4820
			Mt(%)	15.2938	15.3451	15.3879	15.4221	15.4478	15.4649	15.4734	15.4820	15.4820	15.4820
	SBS Layering	25C	T1	1.3666	1.3680	1.3688	1.3693	1.3697	1.3700	1.3702	1.3703	1.3703	14.9581
			T2	1.3528	1.3542	1.3550	1.3555	1.3559	1.3562	1.3564	1.3565	1.3565	15.1333
			T3	1.3537	1.3551	1.3559	1.3564	1.3568	1.3571	1.3573	1.3574	1.3574	15.1217
			AV	1.3577	1.3591	1.3599	1.3604	1.3608	1.3611	1.3613	1.3614	1.3614	15.0706
			Mt(%)	14.7578	14.8762	14.9438	14.9861	15.0199	15.0452	15.0621	15.0706	15.0706	15.0706
		60C	T1	1.3269	1.3273	1.3277	1.3280	1.3283	1.3285	1.3286	1.3287	1.3287	12.2118
			T2	1.3129	1.3133	1.3137	1.3140	1.3143	1.3145	1.3146	1.3147	1.3147	16.8415
			T3	1.3217	1.3221	1.3225	1.3228	1.3231	1.3233	1.3234	1.3235	1.3235	16.4848
			AV	1.3205	1.3209	1.3213	1.3216	1.3219	1.3221	1.3222	1.3223	1.3223	15.1328
			Mt(%)	14.9761	15.0109	15.0457	15.0718	15.0980	15.1154	15.1241	15.1328	15.1328	15.1328
	BSB Layering	25C	T1	1.4016	1.4053	1.4089	1.4103	1.4108	1.4111	1.4113	1.4114	1.4114	15.8500
			T2	1.3817	1.3854	1.3890	1.3904	1.3909	1.3912	1.3914	1.3915	1.3915	16.1132
			T3	1.3927	1.3964	1.4000	1.4014	1.4019	1.4022	1.4024	1.4025	1.4025	15.9666
			AV	1.3920	1.3957	1.3993	1.4007	1.4012	1.4015	1.4017	1.4018	1.4018	15.9758
			Mt(%)	15.1651	15.4712	15.7690	15.8848	15.9262	15.9510	15.9676	15.9758	15.9758	15.9758
		60C	T1	1.4723	1.4726	1.4728	1.4730	1.4731	1.4732	1.4733	1.4734	1.4734	22.3246
			T2	1.4643	1.4646	1.4648	1.4650	1.4651	1.4652	1.4653	1.4654	1.4654	22.4739
			T3	1.4642	1.4645	1.4647	1.4649	1.4650	1.4651	1.4652	1.4653	1.4653	22.4758
			AV	1.4669	1.4672	1.4674	1.4676	1.4677	1.4678	1.4679	1.4680	1.4680	22.4252
			Mt(%)	22.3334	22.3584	22.3751	22.3918	22.4001	22.4085	22.4168	22.4252	22.4252	22.4252

Appendix J. Data sheet Water Absorption Test, Result Record at T=25°C, for 15S/15B from first day 216th hours

						Water Absorption Test, Result Record at T=25°C, for 15S/15B from the first day to 216th hour						
Fiber Loading	Layering Sequence	Pressing Temp	Trials	Initial weight(g) Feb 15/2021	Weight (g) After 24 Hours Feb 16/2021	Weight (g) After 48 Hours Feb 17/2021	Weight (g) After 72 Hours Feb 18/2021	Weight (g) After 96 Hours Feb 19/2021	Weight (g) After 120 Hours Feb 20/2021	Weight (g) After 144 Hours Feb 21/2021	Weight (g) After 168 Hours Feb 22/2021	Weight (g) After 192 Hours Feb 23/2021	Weight (g) After 216 Hours Feb 24/2021
15S/15B	UNF Mixing	25C	T1	1.4725	1.5479	1.5588	1.5676	1.5753	1.5818	1.5876	1.5925	1.5997	1.6018
			T2	1.4095	1.4849	1.4958	1.5046	1.5123	1.5188	1.5246	1.5295	1.5367	1.5388
			T3	1.4515	1.5269	1.5378	1.5466	1.5543	1.5608	1.5666	1.5715	1.5787	1.5808
			AV	1.4445	1.5199	1.5308	1.5396	1.5473	1.5538	1.5596	1.5645	1.5717	1.5738
			Mt(%)		5.2198	5.9744	6.5836	7.1166	7.5666	7.9682	8.3074	8.8058	8.9512
		60C	T1	1.4224	1.5304	1.5328	1.5346	1.5358	1.5458	1.5548	1.5628	1.5668	1.5703
			T2	1.4217	1.5297	1.5321	1.5339	1.5351	1.5451	1.5541	1.5621	1.5661	1.5696
			T3	1.3865	1.4945	1.4969	1.4987	1.4999	1.5099	1.5189	1.5269	1.5309	1.5344
			AV	1.4102	1.5182	1.5206	1.5224	1.5236	1.5336	1.5426	1.5506	1.5546	1.5581
			Mt(%)		7.6585	7.8287	7.9563	8.0414	8.7505	9.3887	9.9560	10.2397	10.4879
	SBS Layering	25C	T1	1.3992	1.4972	1.5096	1.5196	1.5284	1.5360	1.5425	1.5468	1.5511	1.5542
			T2	1.4182	1.5162	1.5286	1.5386	1.5474	1.5550	1.5615	1.5658	1.5701	1.5732
			T3	1.4045	1.5025	1.5149	1.5249	1.5337	1.5413	1.5478	1.5521	1.5564	1.5595
			AV	1.4073	1.5053	1.5177	1.5277	1.5365	1.5441	1.5506	1.5549	1.5592	1.5623
			Mt(%)		6.9637	7.8448	8.5554	9.1807	9.7207	10.1826	10.4882	10.7937	11.0140
		60C	T1	1.4174	1.5154	1.5278	1.5378	1.5466	1.5542	1.5607	1.5658	1.5701	1.5733
			T2	1.3840	1.4820	1.4944	1.5044	1.5132	1.5208	1.5273	1.5324	1.5367	1.5399
			T3	1.4232	1.5212	1.5336	1.5436	1.5524	1.5600	1.5665	1.5716	1.5759	1.5791
			AV	1.4082	1.5062	1.5186	1.5286	1.5374	1.5450	1.5515	1.5566	1.5609	1.5641
			Mt(%)		6.9592	7.8398	8.5499	9.1748	9.7145	10.1761	10.5383	10.8436	11.0709
	BSB Layering	25C	T1	1.4237	1.5217	1.5341	1.5441	1.5529	1.5605	1.5670	1.5721	1.5764	1.5795
			T2	1.3888	1.4868	1.4992	1.5092	1.5180	1.5256	1.5321	1.5372	1.5415	1.5446
			T3	1.4298	1.5278	1.5402	1.5502	1.5590	1.5666	1.5731	1.5782	1.5825	1.5856
			AV	1.4141	1.5121	1.5245	1.5345	1.5433	1.5509	1.5574	1.5625	1.5668	1.5699
			Mt(%)		6.9302	7.8071	8.5142	9.1366	9.6740	10.1337	10.4943	10.7984	11.0176
		60C	T1	1.3987	1.4997	1.5161	1.5297	1.5398	1.5484	1.5558	1.5603	1.5634	1.5642
			T2	1.4238	1.5248	1.5412	1.5548	1.5649	1.5735	1.5809	1.5854	1.5885	1.5893
			T3	1.4348	1.5358	1.5522	1.5658	1.5759	1.5845	1.5919	1.5964	1.5995	1.6003
			AV	1.4191	1.5201	1.5365	1.5501	1.5602	1.5688	1.5762	1.5807	1.5838	1.5846
			Mt(%)		7.1172	8.2728	9.2312	9.9429	10.5489	11.0704	11.3875	11.6059	11.6623

Appendix K. Data sheet Water Absorption Test, Result Record at T=25°C, for 15S/15B from 216th hour to 432nd hours

			Water Absorption Test, Result Record at T=25°C, for 15S/15B from 216th hour to 432nd hours									
Fiber Loading	Layering Sequence	Pressing Temp	Trials	Weight (g) After 240 Hours Feb 25/2021	Weight (g) After 264 Hours Feb 26/2021	Weight (g) After 288 Hours Feb 27/2021	Weight (g) After 312 Hours Feb 28/2021	Weight (g) After 336 Hours Feb 29/2021	Weight (g) After 360 Hours Feb 30/2021	Weight (g) After 384 Hours Feb 31/2021	Weight (g) After 408 Hours Mar 01/2021	Weight (g) After 432 Hours Mar 02/2021	Weight gain (g) at Saturated (Ms%)
15S/15B	UNF Mixing	25C	T1	1.4016	1.4053	1.4089	1.4103	1.4108	1.4111	1.4113	1.4114	1.4114	15.8500
			T2	1.3817	1.3854	1.3890	1.3904	1.3909	1.3912	1.3914	1.3915	1.3915	16.1132
			T3	1.3927	1.3964	1.4000	1.4014	1.4019	1.4022	1.4024	1.4025	1.4025	15.9666
			AV	1.3920	1.3957	1.3993	1.4007	1.4012	1.4015	1.4017	1.4018	1.4018	15.9758
			Mt(%)	15.1651	15.4712	15.7690	15.8848	15.9262	15.9510	15.9676	15.9758	15.9758	15.9758
		60C	T1	1.4723	1.4726	1.4728	1.4730	1.4731	1.4732	1.4733	1.4734	1.4734	22.3246
			T2	1.4643	1.4646	1.4648	1.4650	1.4651	1.4652	1.4653	1.4654	1.4654	22.4739
			T3	1.4642	1.4645	1.4647	1.4649	1.4650	1.4651	1.4652	1.4653	1.4653	22.4758
			AV	1.4669	1.4672	1.4674	1.4676	1.4677	1.4678	1.4679	1.4680	1.4680	22.4252
			Mt(%)	22.3334	22.3584	22.3751	22.3918	22.4001	22.4085	22.4168	22.4252	22.4252	22.4252
	SBS Layering	25C	T1	1.5564	1.5576	1.5584	1.5590	1.5594	1.5597	1.5599	1.5600	1.5600	11.4923
			T2	1.5754	1.5766	1.5774	1.5780	1.5784	1.5787	1.5789	1.5790	1.5790	11.3383
			T3	1.5617	1.5629	1.5637	1.5643	1.5647	1.5650	1.5652	1.5653	1.5653	11.4489
			AV	1.5645	1.5657	1.5665	1.5671	1.5675	1.5678	1.5680	1.5681	1.5681	11.4261
			Mt(%)	11.1703	11.2556	11.3124	11.3551	11.3835	11.4048	11.4190	11.4261	11.4261	11.4261
		60C	T1	1.5754	1.5766	1.5774	1.5780	1.5784	1.5787	1.5789	1.5790	1.5790	11.4012
			T2	1.5420	1.5432	1.5440	1.5446	1.5450	1.5453	1.5455	1.5456	1.5456	11.6763
			T3	1.5812	1.5824	1.5832	1.5838	1.5842	1.5845	1.5847	1.5848	1.5848	11.3547
			AV	1.5662	1.5674	1.5682	1.5688	1.5692	1.5695	1.5697	1.5698	1.5698	11.4756
			Mt(%)	11.2200	11.3052	11.3620	11.4046	11.4330	11.4543	11.4685	11.4756	11.4756	11.4756
	BSB Layering	25C	T1	1.5817	1.5829	1.5837	1.5843	1.5847	1.5850	1.5852	1.5853	1.5853	11.3507
			T2	1.5468	1.5480	1.5488	1.5494	1.5498	1.5501	1.5503	1.5504	1.5504	11.6359
			T3	1.5878	1.5890	1.5898	1.5904	1.5908	1.5911	1.5913	1.5914	1.5914	11.3023
			AV	1.5721	1.5733	1.5741	1.5747	1.5751	1.5754	1.5756	1.5757	1.5757	11.4278
			Mt(%)	11.1732	11.2580	11.3146	11.3570	11.3853	11.4065	11.4207	11.4278	11.4278	11.4278
		60C	T1	1.5649	1.5654	1.5658	1.5662	1.5665	1.5667	1.5668	1.5669	1.5669	12.0255
			T2	1.5900	1.5905	1.5909	1.5913	1.5916	1.5918	1.5919	1.5920	1.5920	11.8135
			T3	1.6010	1.6015	1.6019	1.6023	1.6026	1.6028	1.6029	1.6030	1.6030	11.7229
			AV	1.5853	1.5858	1.5862	1.5866	1.5869	1.5871	1.5872	1.5873	1.5873	11.8526
			Mt(%)	11.7116	11.7469	11.7751	11.8033	11.8244	11.8385	11.8455	11.8526	11.8526	11.8526

Appendix L. Data sheet Water Absorption Test, Result Record at T=25°C, for 20S/10B from first da to 216th hours

													Water Absorption Test, Result Record at T=25°C, for 20S/10B from the first day to 216th hour				
Fiber Loading	Layering Sequence	Pressing Temp	Trials	Initial weight(g) Feb 15/2021	Weight (g) After 24 Hours Feb 16/2021	Weight (g) After 48 Hours Feb 17/2021	Weight (g) After 72 Hours Feb 18/2021	Weight (g) After 96 Hours Feb 19/2021	Weight (g) After 120 Hours Feb 20/2021	Weight (g) After 144 Hours Feb 21/2021	Weight (g) After 168 Hours Feb 22/2021	Weight (g) After 192 Hours Feb 23/2021	Weight (g) After 216 Hours Feb 24/2021
20S/10B	UNF Mixing	25C	T1	1.4452	1.4574	1.4676	1.4826	1.4924	1.4965	1.5039	1.5084	1.5096	1.5104
			T2	1.4544	1.4666	1.4768	1.4918	1.5016	1.5057	1.5131	1.5176	1.5188	1.5196
			T3	1.4465	1.4587	1.4689	1.4839	1.4937	1.4978	1.5052	1.5097	1.5109	1.5117
			AV	1.4487	1.4609	1.4711	1.4861	1.4959	1.5000	1.5074	1.5119	1.5131	1.5139
			Mt(%)		0.8421	1.5462	2.5816	3.2581	3.5411	4.0519	4.3625	4.4454	4.5006
		60C	T1	1.4607	1.5161	1.5304	1.5404	1.5481	1.5540	1.5568	1.5594	1.5620	1.5648
			T2	1.4321	1.4875	1.5018	1.5118	1.5195	1.5254	1.5282	1.5308	1.5334	1.5362
			T3	1.4506	1.5060	1.5203	1.5303	1.5380	1.5439	1.5467	1.5493	1.5519	1.5547
			AV	1.4478	1.5032	1.5175	1.5275	1.5352	1.5411	1.5439	1.5465	1.5491	1.5519
			Mt(%)		3.8265	4.8142	5.5049	6.0367	6.4443	6.6377	6.8172	6.9968	7.1902
	SBS Layering	25C	T1	1.4573	1.5014	1.5116	1.5193	1.5263	1.5321	1.5371	1.5411	1.5441	1.5461
			T2	1.4575	1.5016	1.5118	1.5195	1.5265	1.5323	1.5373	1.5413	1.5443	1.5463
			T3	1.4586	1.5027	1.5129	1.5206	1.5276	1.5334	1.5384	1.5424	1.5454	1.5474
			AV	1.4578	1.5019	1.5121	1.5198	1.5268	1.5326	1.5376	1.5416	1.5446	1.5466
			Mt(%)		3.0251	3.7248	4.2530	4.7332	5.1310	5.4740	5.7484	5.9542	6.0914
		60C	T1	1.4747	1.5190	1.5397	1.5486	1.5549	1.5587	1.5606	1.5625	1.5644	1.5663
			T2	1.4648	1.5091	1.5298	1.5387	1.5450	1.5488	1.5507	1.5526	1.5545	1.5564
			T3	1.4621	1.5064	1.5271	1.5360	1.5423	1.5461	1.5480	1.5499	1.5518	1.5537
			AV	1.4672	1.5115	1.5322	1.5411	1.5474	1.5512	1.5531	1.5550	1.5569	1.5588
			Mt(%)		3.0194	4.4302	5.0368	5.4662	5.7252	5.8547	5.9842	6.1137	6.2432
	BSB Layering	25C	T1	1.4855	1.5309	1.5432	1.5532	1.5622	1.5688	1.5720	1.5748	1.5766	1.5782
			T2	1.4674	1.5128	1.5251	1.5351	1.5441	1.5507	1.5539	1.5567	1.5585	1.5601
			T3	1.4688	1.5142	1.5265	1.5365	1.5455	1.5521	1.5553	1.5581	1.5599	1.5615
			AV	1.4739	1.5193	1.5316	1.5416	1.5506	1.5572	1.5604	1.5632	1.5650	1.5666
			Mt(%)		3.0803	3.9148	4.5933	5.2039	5.6517	5.8688	6.0588	6.1809	6.2894
		60C	T1	1.4573	1.5250	1.5440	1.5498	1.5534	1.5555	1.5573	1.5583	1.5592	1.5599
			T2	1.4674	1.5351	1.5541	1.5599	1.5635	1.5656	1.5674	1.5684	1.5693	1.5700
			T3	1.4289	1.4966	1.5156	1.5214	1.5250	1.5271	1.5289	1.5299	1.5308	1.5315
			AV	1.4512	1.5189	1.5379	1.5437	1.5473	1.5494	1.5512	1.5522	1.5531	1.5538
			Mt(%)		4.6651	5.9744	6.3740	6.6221	6.7668	6.8908	6.9598	7.0218	7.0700

Appendix M. Data sheet Water Absorption Test, Result Record at T=25°C, for 20S/10B from 216th hour to 432nd hours

			Water Absorption Test, Result Record at T=25°C, for 20S/10B from 216th hour to 432nd hours								
Fiber Loading			Weight (g) After 240 Hours Feb 25/2021	Weight (g) After 264 Hours Feb 26/2021	Weight (g) After 288 Hours Feb 27/2021	Weight (g) After 312 Hours Feb 28/2021	Weight (g) After 336 Hours Feb 29/2021	Weight (g) After 360 Hours Feb 30/2021	Weight (g) After 384 Hours Feb 31/2021	Weight (g) After 408 Hours Mar 01/2021	Weight (g) After 432 Hours Mar 02/2021	Weight gain (g) at Saturated (Ms%)
20S/10B	UNF Mixing	25C	T1	1.5111	1.5117	1.5122	1.5126	1.5129	1.5131	1.5133	1.5134	1.5134	4.7191
			T2	1.5203	1.5209	1.5214	1.5218	1.5221	1.5223	1.5225	1.5226	1.5226	4.6892
			T3	1.5124	1.5130	1.5135	1.5139	1.5142	1.5144	1.5146	1.5147	1.5147	4.7148
			AV	1.5146	1.5152	1.5157	1.5161	1.5164	1.5166	1.5168	1.5169	1.5169	4.7077
			Mt(%)	4.5489	4.5903	4.6248	4.6524	4.6732	4.6870	4.7008	4.7077	4.7077	4.7077
		60C	T1	1.5658	1.5666	1.5673	1.5678	1.5682	1.5684	1.5686	1.5687	1.5687	7.3937
			T2	1.5372	1.5380	1.5387	1.5392	1.5396	1.5398	1.5400	1.5401	1.5401	7.5414
			T3	1.5557	1.5565	1.5572	1.5577	1.5581	1.5583	1.5585	1.5586	1.5586	7.4452
			AV	1.5529	1.5537	1.5544	1.5549	1.5553	1.5555	1.5557	1.5558	1.5558	7.4596
			Mt(%)	7.2593	7.3145	7.3629	7.3974	7.4251	7.4389	7.4527	7.4596	7.4596	7.4596
	SBS Layering	25C	T1	1.5471	1.5479	1.5486	1.5491	1.5495	1.5498	1.5500	1.5501	1.5501	6.3679
			T2	1.5473	1.5481	1.5488	1.5493	1.5497	1.5500	1.5502	1.5503	1.5503	6.3671
			T3	1.5484	1.5492	1.5499	1.5504	1.5508	1.5511	1.5513	1.5514	1.5514	6.3623
			AV	1.5476	1.5484	1.5491	1.5496	1.5500	1.5503	1.5505	1.5506	1.5506	6.3658
			Mt(%)	6.1600	6.2148	6.2629	6.2972	6.3246	6.3452	6.3589	6.3658	6.3658	6.3658
		60C	T1	1.5682	1.5700	1.5720	1.5735	1.5739	1.5744	1.5746	1.5746	1.5746	6.7743
			T2	1.5583	1.5601	1.5621	1.5636	1.5640	1.5645	1.5647	1.5647	1.5647	6.8200
			T3	1.5556	1.5574	1.5594	1.5609	1.5613	1.5618	1.5620	1.5620	1.5620	6.8326
			AV	1.5607	1.5625	1.5645	1.5660	1.5664	1.5667	1.5669	1.5671	1.5671	6.8089
			Mt(%)	6.3727	6.4954	6.6317	6.7339	6.7612	6.7816	6.7953	6.8089	6.8089	6.8089
	BSB Layering	25C	T1	1.5794	1.5804	1.5810	1.5815	1.5819	1.5821	1.5822	1.5822	1.5822	6.5096
			T2	1.5613	1.5623	1.5629	1.5634	1.5638	1.5640	1.5641	1.5641	1.5641	6.5899
			T3	1.5627	1.5637	1.5643	1.5648	1.5652	1.5654	1.5655	1.5655	1.5655	6.5836
			AV	1.5678	1.5688	1.5694	1.5699	1.5703	1.5705	1.5706	1.5706	1.5706	6.5608
			Mt(%)	6.3709	6.4387	6.4794	6.5133	6.5405	6.5540	6.5608	6.5608	6.5608	6.5608
		60C	T1	1.5605	1.5610	1.5615	1.5619	1.5622	1.5624	1.5625	1.5626	1.5626	7.2257
			T2	1.5706	1.5711	1.5716	1.5720	1.5723	1.5725	1.5726	1.5727	1.5727	7.1760
			T3	1.5321	1.5326	1.5331	1.5335	1.5338	1.5340	1.5341	1.5342	1.5342	7.3693
			AV	1.5544	1.5549	1.5554	1.5558	1.5561	1.5563	1.5564	1.5565	1.5565	7.2561
			Mt(%)	7.1114	7.1458	7.1803	7.2078	7.2285	7.2423	7.2492	7.2561	7.2561	7.2561

Appendix N. Taguchi Method analysis Minitab 19.0 software results

Taguchi Analysis: Tensile Strength (MPa) versus Curing Temperature, Fiber Loading, Layering Sequence

Linear Model Analysis: SN ratios versus Curing Temperature, Fiber Loading, Layering Sequence

Estimated Model Coefficients for SN ratios

Term	Coef	SE Coef	T	P
Constant	29.4944	0.02217	1330.331	0.000
Curing T 25	0.1011	0.02217	4.561	0.001
Fiber Lo 10S/20B	-1.0743	0.03135	-34.263	0.000
Fiber Lo 15S/15B	-0.3479	0.03135	-11.096	0.000
Layering UNF	0.0159	0.03135	0.508	0.620
Layering SBS	0.4799	0.03135	15.307	0.000

Model Summary

S	R-Sq	R-Sq(adj)
0.0941	99.54%	99.34%

Analysis of Variance for SN ratios

Source	DF	Seq SS	Adj SS	Adj MS	F	P
Curing Temperature	1	0.1841	0.1841	0.18409	20.81	0.001
Fiber Loading	2	19.7866	19.7866	9.89332	1118.18	0.000
Layering Sequence	2	2.8590	2.8590	1.42948	161.57	0.000
Residual Error	12	0.1062	0.1062	0.00885		
Total	17	22.9359				

R denotes an observation with a large standardized residual.

Response Table for Signal to Noise Ratios

Larger is better

Level	Curing Temperature	Fiber Loading	Layering Sequence
1	29.60	28.42	29.51
2	29.39	29.15	29.97
3		30.92	29.00
Delta	0.20	2.50	0.98
Rank	3	1	2

Response Table for Means

Source	DF	Seq SS	Adj SS	Adj MS	F	P
Curing Temperature	1	0.9491	0.9491	0.94909	21.10	0.001
Fiber Loading	2	14.5318	14.5318	7.26590	161.54	0.000
Layering Sequence	2	11.2807	11.2807	5.64035	125.40	0.000
Residual Error	12	0.5398	0.5398	0.04498		
Total	17	27.3014				

Level	Curing Temperature	Fiber Loading	Layering Sequence
1	30.44	26.39	30.09
2	29.74	28.70	31.79
3		35.19	28.40
Delta	0.69	8.80	3.39
Rank	3	1	2

Taguchi Analysis: Flexural Strength (MPa) versus Curing Temperature, Fiber Loading, Layering Sequence

Linear Model Analysis: SN ratios versus Curing Temperature, Fiber Loading, Layering Sequence

Estimated Model Coefficients for SN ratios

Term	Coef	SE Coef	T	P
Constant	37.9184	0.04999	758.534	0.000
Curing T 25	0.2296	0.04999	4.593	0.001
Fiber Lo 10S/20B	-1.0179	0.07070	-14.398	0.000
Fiber Lo 15S/15B	-0.1498	0.07070	-2.119	0.056
Layering UNF	0.3147	0.07070	4.452	0.001
Layering SBS	0.7731	0.07070	10.936	0.000

Model Summary

S	R-Sq	R-Sq(adj)
0.2121	98.02%	97.20%

Analysis of Variance for SN ratios

Unusual Observations for SN ratios

Observation	SN ratios	Fit	SE Fit	Residual	St Resid	
15	36.830	36.451	0.122	0.379	2.19	R

R denotes an observation with a large standardized residual.

Response Table for Signal to Noise Ratios

Larger is better

Level	Curing Temperature	Fiber Loading	Layering Sequence
1	38.15	36.90	38.23
2	37.69	37.77	38.69
3		39.09	36.83
Delta	0.46	2.19	1.86
Rank	3	1	2

Response Table for Means

Level	Curing Temperature	Fiber Loading	Layering Sequence
1	81.68	70.31	82.19
2	77.29	77.65	86.50
3		90.50	69.77
Delta	4.40	20.19	16.73
Rank	3	1	2

Taguchi Analysis: Compression Strength (MPa) versus Curing Temperature, Fiber Loading, Layering Sequence

Linear Model Analysis: SN ratios versus Curing Temperature, Fiber Loading, Layering Sequence

Estimated Model Coefficients for SN ratios

Model Summary

Term	Coef	SE Coef	T	P
Constant	25.3970	0.07328	346.569	0.000
Curing T 25	0.1665	0.07328	2.272	0.042
Fiber Lo 10S/20B	-0.3724	0.10364	-3.593	0.004
Fiber Lo 15S/15B	0.3194	0.10364	3.082	0.010
Layering UNF	-0.8496	0.10364	-8.198	0.000
Layering SBS	-0.1060	0.10364	-1.023	0.327

S	R-Sq	R-Sq(adj)
0.3109	91.08%	87.36%

Analysis of Variance for SN ratios

Source	DF	Seq SS	Adj SS	Adj MS	F	P
Curing Temperature	1	0.4991	0.4991	0.49905	5.16	0.042
Fiber Loading	2	1.4611	1.4611	0.73057	7.56	0.008
Layering Sequence	2	9.8781	9.8781	4.93904	51.10	0.000
Residual Error	12	1.1600	1.1600	0.09666		
Total	17	12.9982				

Unusual Observations for SN ratios

Observation	SN ratios	Fit	SE Fit	Residual	St Resid	
11	25.362	24.752	0.180	0.610	2.40	R

R denotes an observation with a large standardized residual.

Response Table for Signal to Noise Ratios

Larger is better

Level	Curing Temperature	Fiber Loading	Layering Sequence
1	25.56	25.02	24.55
2	25.23	25.72	25.29
3		25.45	26.35
Delta	0.33	0.69	1.81
Rank	3	2	1

Response Table for Means

Taguchi Analysis: Impact Strength(kJ/m^2) versus Curing Temperature, Fiber Loading, Layering Sequence

Linear Model Analysis: SN ratios versus Curing

Level	Curing Temperature	Fiber Loading	Layering Sequence
1	19.06	17.87	16.89
2	18.35	19.42	18.40
3		18.82	20.82
Delta	0.71	1.55	3.94
Rank	3	2	1

Temperature, Fiber Loading, Layering Sequence Estimated Model Coefficients for SN ratios

Term	Coef	SE Coef	T	P
Constant	28.0559	0.08680	323.227	0.000
Curing T 25	0.1305	0.08680	1.504	0.158
Fiber Lo 10S/20B	0.9609	0.12275	7.828	0.000
Fiber Lo 15S/15B	0.1289	0.12275	1.050	0.314
Layering UNF	0.4790	0.12275	3.902	0.002
Layering SBS	-0.4427	0.12275	-3.606	0.004

Model Summary

S	R-Sq	R-Sq(adj)
0.3683	90.57%	86.64%

Analysis of Variance for SN ratios

Level	Curing Temperature	Fiber Loading	Layering Sequence
1	28.19	29.02	28.53
2	27.93	28.18	27.61
3		26.97	28.02
Delta	0.26	2.05	0.92
Rank	3	1	2

Response Table for Signal to Noise Ratios

Larger is better

Source	DF	Seq SS	Adj SS	Adj MS	F	P
Curing Temperature	1	0.3067	0.3067	0.3067	2.26	0.158
Fiber Loading	2	12.7645	12.7645	6.3822	47.06	0.000
Layering Sequence	2	2.5603	2.5603	1.2801	9.44	0.003
Residual Error	12	1.6274	1.6274	0.1356		
Total	17	17.2588				

Response Table for Means

Level	Curing Temperature	Fiber Loading	Layering Sequence
1	25.82	28.25	26.78
2	25.06	25.68	24.25
3		22.39	25.28
Delta	0.76	5.86	2.52
Rank	3	1	2

Taguchi Analysis: Water Absorption (Mt%) versus Curing Temperature, Fiber Loading, Layering Sequence

Linear Model Analysis: SN ratios versus Curing Temperature, Fiber Loading, Layering Sequence

Estimated Model Coefficients for SN ratios

Term	Coef	SE Coef	T	P
Constant	-20.7515	0.1390	-149.337	0.000
Curing T 25	0.1218	0.1390	0.877	0.398
Fiber Lo 10S/20B	-4.0448	0.1965	-20.583	0.000
Fiber Lo 15S/15B	0.2171	0.1965	1.105	0.291
Layering UNF	0.1236	0.1965	0.629	0.541
Layering SBS	0.5305	0.1965	2.700	0.019

Model Summary

S	R-Sq	R-Sq(adj)
0.5895	97.86%	96.97%

Analysis of Variance for SN ratios

Source	DF	Seq SS	Adj SS	Adj MS	F	P
Curing Temperature	1	0.267	0.267	0.2670	0.77	0.398
Fiber Loading	2	186.355	186.355	93.1773	268.08	0.000
Layering Sequence	2	4.348	4.348	2.1738	6.25	0.014
Residual Error	12	4.171	4.171	0.3476		
Total	17	195.140				

Response Table for Signal to Noise Ratios

Smaller is better

Level	Curing Temperature	Fiber Loading	Layering Sequence
1	-20.63	-24.80	-20.63
2	-20.87	-20.53	-20.22
3		-16.92	-21.41
Delta	0.24	7.87	1.18
Rank	3	1	2

Response Table for Means

Level	Curing Temperature	Fiber Loading	Layering Sequence
1	11.564	17.480	11.472
2	11.878	10.657	10.857
3		7.027	12.836
Delta	0.314	10.454	1.979
Rank	3	1	2

Regression Analysis: Tensile Strength (MPa) versus Curing Temp, Fiber Loading, Layering Seq

Regression Equation

Tensile Strength (MPa) = 24.03 - 0.695 Curing Temp + 4.398 Fiber Loading - 0.847 Layering Seq

Coefficients

Term	Coef	SE Coef	T-Value	P-Value	VIF
Constant	24.03	2.00	12.04	0.000	
Curing Temp	-0.695	0.851	-0.82	0.428	1.00
Fiber Loading	4.398	0.521	8.44	0.000	1.00
Layering Seq	-0.847	0.521	-1.62	0.126	1.00

Model Summary

S	R-sq	R-sq(adj)	R-sq(pred)
1.80492	84.19%	80.80%	75.51%

Analysis of Variance

Source	DF	Adj SS	Adj MS	F-Value	P-Value
Regression	3	242.910	80.970	24.85	0.000
Curing Temp	1	2.172	2.172	0.67	0.428
Fiber Loading	1	232.135	232.135	71.26	0.000
Layering Seq	1	8.602	8.602	2.64	0.126
Error	14	45.608	3.258		
Total	17	288.518			

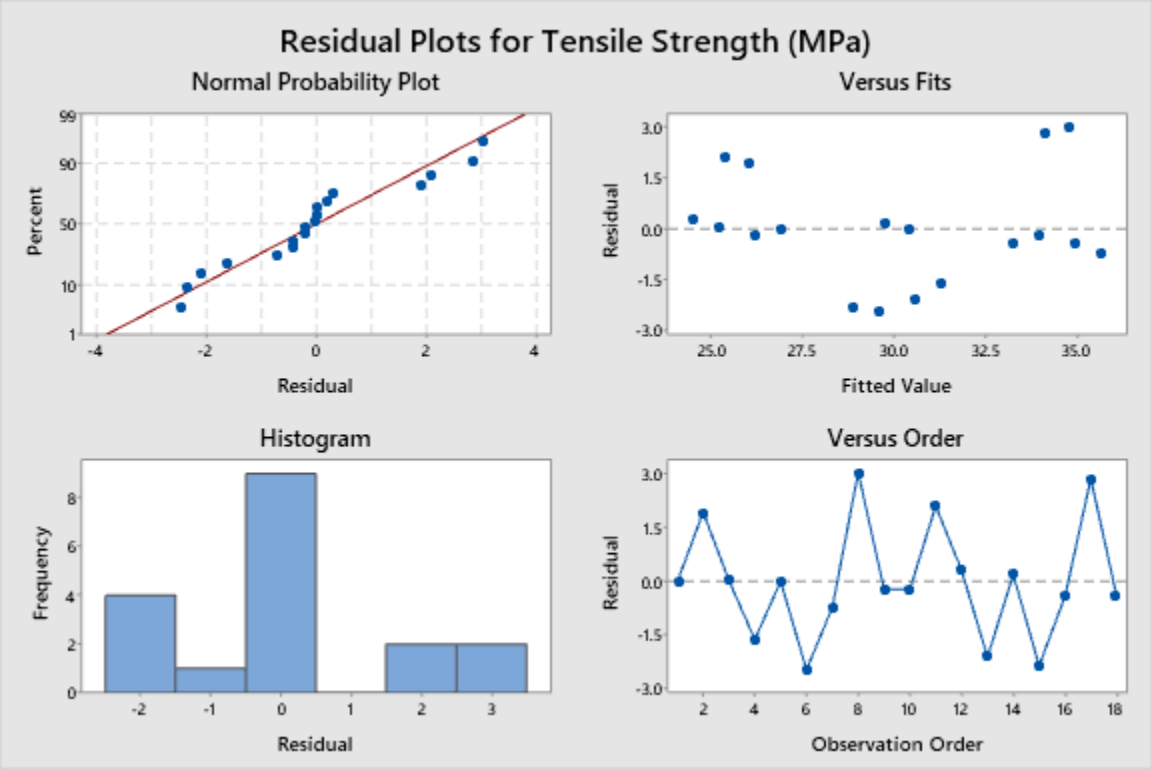

Regression Analysis: Flexural Strength (MPa) versus Curing Temp, Fiber Loading, Layering Seq

Regression Equation

Flexural Strength (MPa) = 78.31 - 4.40 Curing Temp + 10.09 Fiber Loading - 6.21 Layering Seq

Coefficients

Term	Coef	SE Coef	T-Value	P-Value	VIF
Constant	78.31	6.87	11.40	0.000	
Curing Temp	-4.40	2.93	-1.50	0.156	1.00
Fiber Loading	10.09	1.79	5.63	0.000	1.00
Layering Seq	-6.21	1.79	-3.46	0.004	1.00

Model Summary

S	R-sq	R-sq(adj)	R-sq(pred)
6.21536	76.62%	71.61%	62.82%

Analysis of Variance

Source	DF	Adj SS	Adj MS	F-Value	P-Value
Regression	3	1772.75	590.92	15.30	0.000
Curing Temp	1	86.94	86.94	2.25	0.156
Fiber Loading	1	1222.91	1222.91	31.66	0.000
Layering Seq	1	462.89	462.89	11.98	0.004
Error	14	540.83	38.63		
Total	17	2313.58			

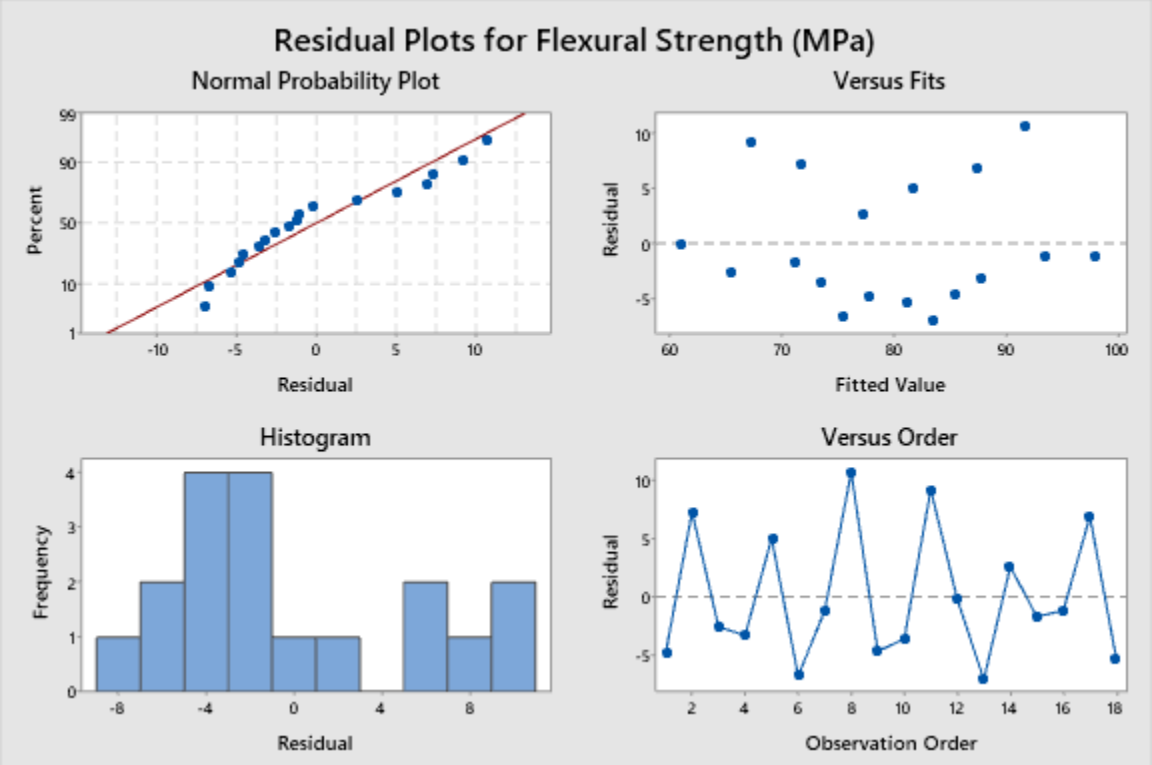

Regression Analysis: Compression Strength (MPa) versus Curing Temp, Fiber Loading, Layering Seq

Regression Equation

Compression Strength (MPa) = 14.89 - 0.712 Curing Temp + 0.473 Fiber Loading + 1.968 Layering Seq

Coefficients

Term	Coef	SE Coef	T-Value	P-Value	VIF
Constant	14.89	1.01	14.81	0.000	
Curing Temp	-0.712	0.429	-1.66	0.119	1.00
Fiber Loading	0.473	0.263	1.80	0.093	1.00
Layering Seq	1.968	0.263	7.49	0.000	1.00

Model Summary

S	R-sq	R-sq(adj)	R-sq(pred)
0.909548	81.62%	77.68%	69.99%

Analysis of Variance

Source	DF	Adj SS	Adj MS	F-Value	P-Value
Regression	3	51.422	17.1406	20.72	0.000
Curing Temp	1	2.281	2.2815	2.76	0.119
Fiber Loading	1	2.684	2.6838	3.24	0.093
Layering Seq	1	46.457	46.4566	56.16	0.000
Error	14	11.582	0.8273		
Total	17	63.004			

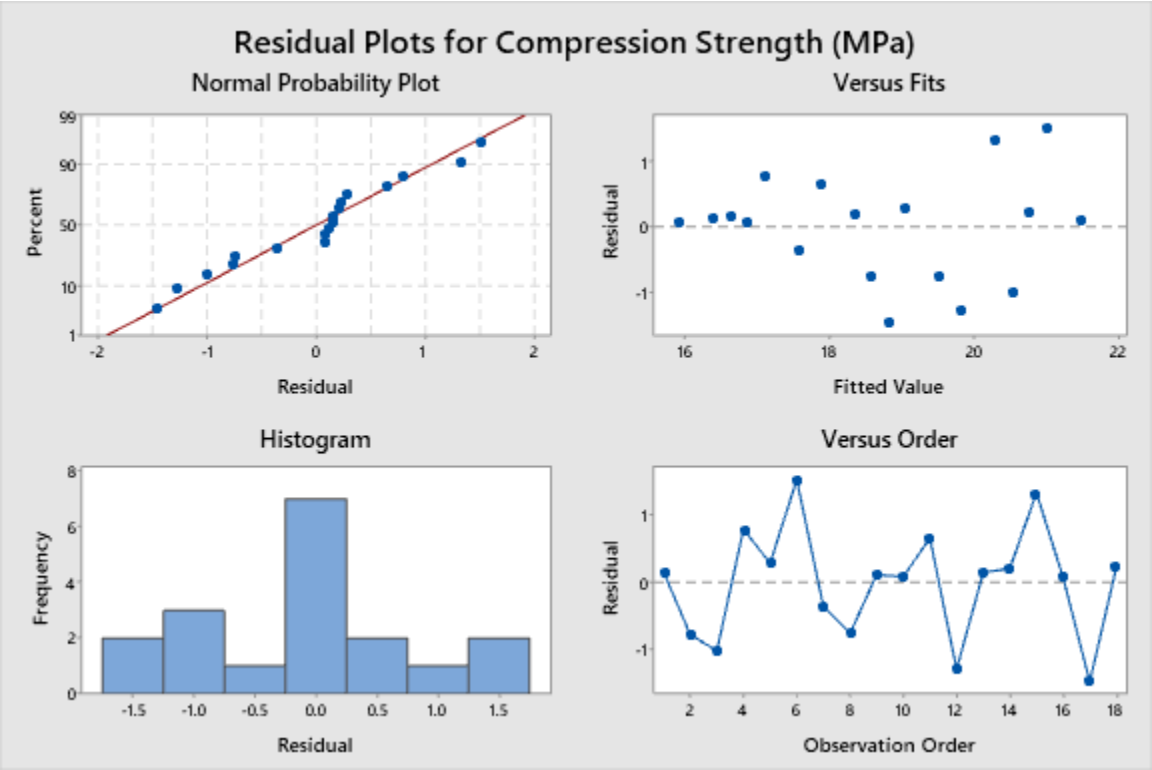

Regression Analysis: Impact Strength(kJ/m^2) versus Curing Temp, Fiber Loading, Layering Seq

Regression Equation

Impact Strength(kJ/m^2) = 33.93 - 0.761 Curing Temp
- 2.929 Fiber Loading
- 0.748 Layering Seq

Coefficients

Term	Coef	SE Coef	T-Value	P-Value	VIF
Constant	33.93	1.42	23.92	0.000	
Curing Temp	-0.761	0.605	-1.26	0.229	1.00
Fiber Loading	-2.929	0.370	-7.91	0.000	1.00
Layering Seq	-0.748	0.370	-2.02	0.063	1.00

Model Summary

S	R-sq	R-sq(adj)	R-sq(pred)
1.28339	82.96%	79.31%	71.96%

Analysis of Variance

Source	DF	Adj SS	Adj MS	F-Value	P-Value
Regression	3	112.287	37.429	22.72	0.000
Curing Temp	1	2.607	2.607	1.58	0.229
Fiber Loading	1	102.960	102.960	62.51	0.000
Layering Seq	1	6.720	6.720	4.08	0.063
Error	14	23.059	1.647		
Total	17	135.346			

Fits and Diagnostics for Unusual Observations

Obs	Impact Strength (kJ/m^2)	Fit	Resid	Std Resid	
8	20.290	22.889	-2.599	-2.26	R
17	19.540	22.127	-2.587	-2.25	R

R Large residual

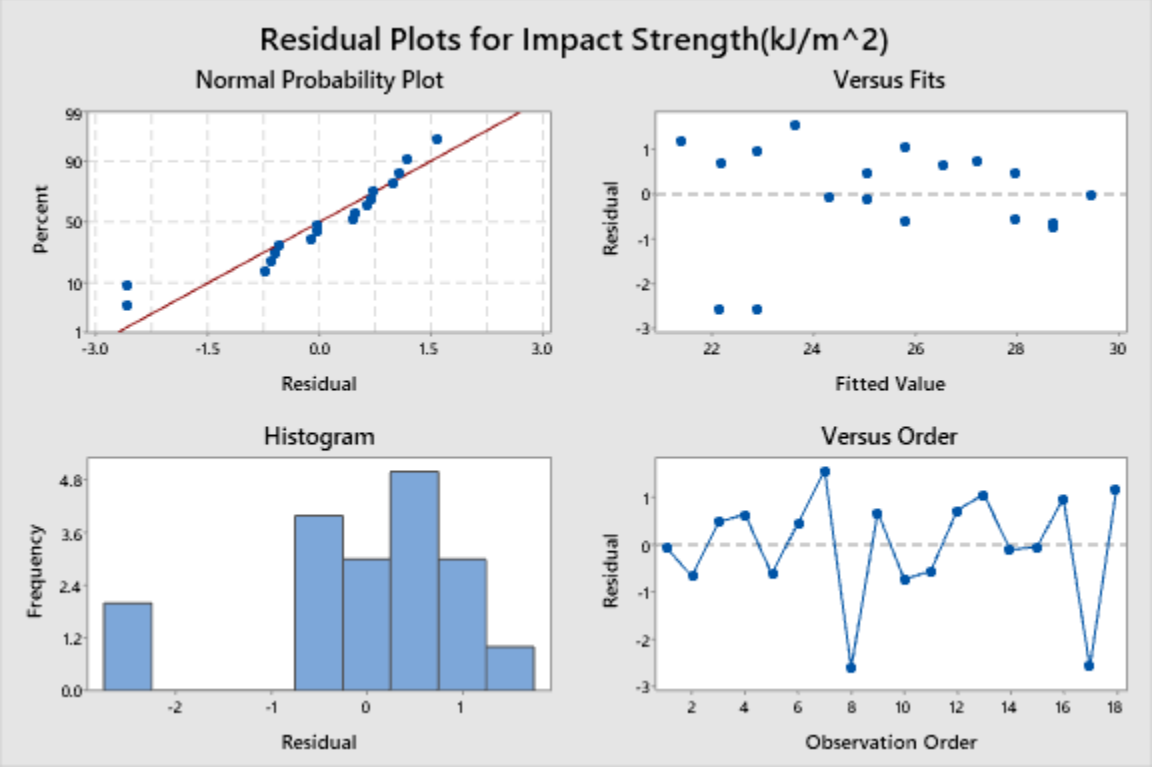

Regression Analysis: Water Absorption (Mt%) versus Curing Temp, Fiber Loading, Layering Seq

Regression Equation

Water Absorption (Mt%) = 20.34 + 0.314 Curing Temp - 5.227 Fiber Loading + 0.682 Layering Seq

Coefficients

Term	Coef	SE Coef	T-Value	P-Value	VIF
Constant	20.34	1.64	12.38	0.000	
Curing Temp	0.314	0.701	0.45	0.661	1.00
Fiber Loading	-5.227	0.429	-12.18	0.000	1.00
Layering Seq	0.682	0.429	1.59	0.134	1.00

Model Summary

S	R-sq	R-sq(adj)	R-sq(pred)
1.48643	91.52%	89.70%	85.23%

Analysis of Variance

Source	DF	Adj SS	Adj MS	F-Value	P-Value
Regression	3	333.871	111.290	50.37	0.000
Curing Temp	1	0.443	0.443	0.20	0.661
Fiber Loading	1	327.848	327.848	148.38	0.000
Layering Seq	1	5.580	5.580	2.53	0.134
Error	14	30.933	2.209		
Total	17	364.803			

Fits and Diagnostics for Unusual Observations

Obs	Water Absorption (Mt%)	Fit	Resid	Std Resid	
12	20.343	17.787	2.556	2.02	R

R Large residual

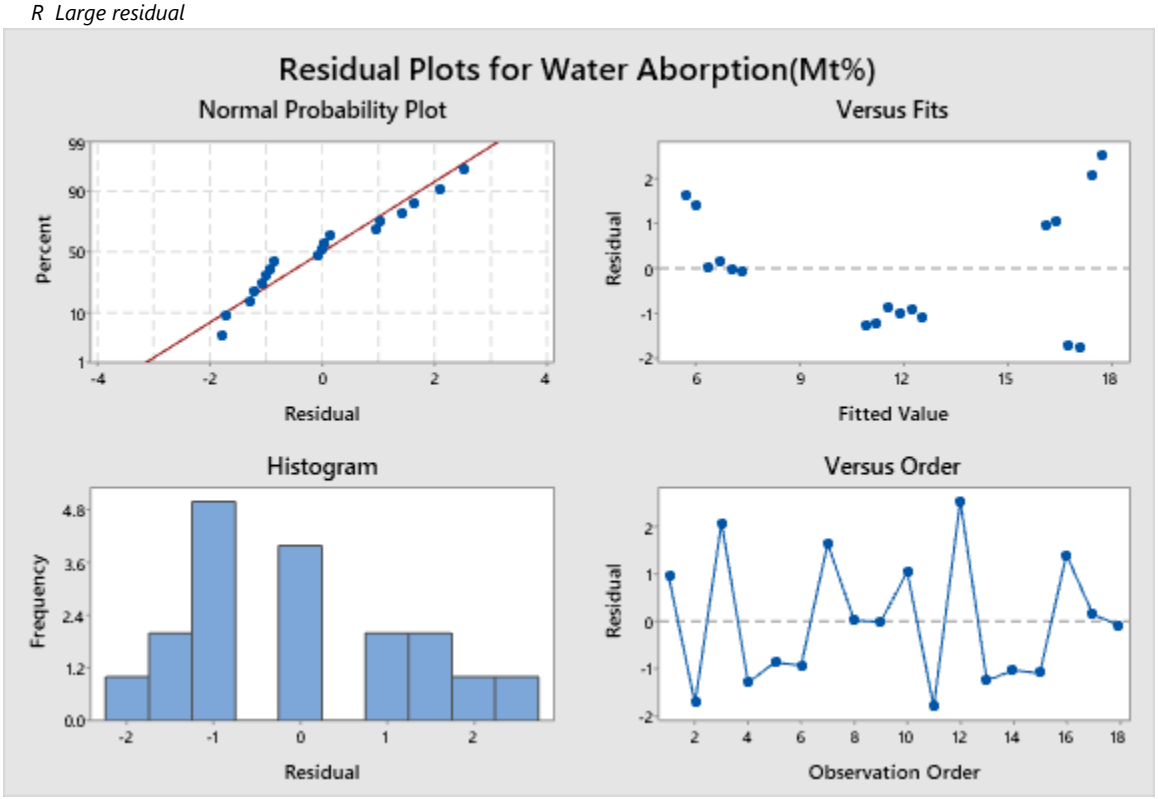

Ansys Workbench structural analysis Simulation for sisal and sugarcane bagasse hybrid fiber polyester composite with 3mm thickness

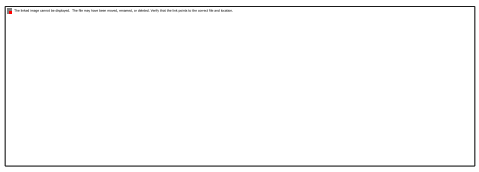

Project*

First Saved	24 August, 2021
Last Saved	29 August, 2021
Product Version	2020 R1

Object Name	*B3|Cut-Extrude7*	*B31|Boss-Extrude1*
Material		
Assignment	Sisal-Bagasse Polyester	Structural Steel
Properties		
Volume	6.5202e-004 m³	6.048e-004 m³
Mass	0.80198 kg	4.7477 kg
Statistics		
Nodes	101563	713
Elements	50149	104

Mesh **Statistics**	
Nodes	102276
Elements	50253
Element Size	5.e-003 m

Force		
Z Component	600. N (ramped)	

Definition						
Type	Total Deformation	Equivalent (von-Mises) Stress	Directional Deformation	Shear Stress	Strain Energy	Equivalent Elastic Strain
Results						
Minimum	0. m	0. Pa	-4.9993e-004 m	-5.3434e+006 Pa	0. J	1.5379e-033 m/m
Maximum	4.1358e-003 m	2.1033e+007 Pa	4.5257e-004 m	5.7748e+006 Pa	2.7517e-003 J	3.2207e-002 m/m
Average	9.7871e-004 m	7.8883e+005 Pa	2.3258e-006 m	4212.8 Pa		1.1235e-003 m/m